THE UNIVERSITY OF MICHIGAN

INDUSTRY PROGRAM OF THE COLLEGE OF ENGINEERING

CONTROL OF THE COMBUSTION OF COMPRESSION IGNITION ENGINES

Abdel R. A. F. Ibrahim

A dissertation submitted in partial fulfillment
of the requirements for the degree of
Doctor of Philosophy in the
University of Michigan
1960

June, 1960

IP-436

ACKNOWLEDGEMENTS

I wish to express my gratitude and appreciation to all those who have offered assistance, encouragement and guidance during the course of this investigation.

The author gratefully acknowledges Professor E. T. Vincent, the Co-chairman of the Doctoral Committee, for his continued active interest and suggestions which were a major factor in the completion of this work. Professor J. A. Bolt, the co-chairman of the committee, for his suggestions and help with the experimental parts and William Mirsky was of great help with the instrumentation portion of the work. The author wishes to thank Professor R. A. Wolfe of the Physics Department, Professor J. L. York of the Chemical Engineering Department, and Mr. I. Bishop of the Ford Motor Company.

Help in preparation of this report by the Industry Program of the College of Engineering, The University of Michigan is gratefully acknowledged. Acknowledgment is also due to the men of the Automotive Laboratory, who in spite of their duties, were of help in building the experimental equipment.

Many thanks to the Nordburg Manufacturing Company and American Basch Arma Corporation for providing some of the material and parts for building the apparatus.

TABLE OF CONTENTS

TABLE OF CONTENTS CONT'D

LIST OF FIGURES

LIST OF FIGURES CONT'D

NOMENCLATURE

A	Area
a	Number of molecules per unit volume
c	Specific heat
d	Diameter
E	Activation energy
e	Natural base of logarithm
f	Steric factor or volumetric fraction of residualsof combustion
K, k	Specific reaction rate coefficient = $fz\ e^{-E/RT}$
M	Molecular weight
N	Engine speed R.P.M.
N_a	Avogadro's Number = 6×10^{23}
n_o	Rate of initiation reaction
n	Order of reaction
P, p	Pressure
Q,	Heat of reation per gram - mol.
q	Quantity of heat or energy per unit time
R	Gas constant
s	Surface area
T	Absolute temperature
t	Time
V	Volume
W	Rate of reaction
z	Frequency of collision

λ	Thermal conductivity
η	Parameter as defined by Equation (2) page 93.
ξ	Parameter as defined by Equation (1) page 93.
θ	Angles, deg. crankangle
τ	Time characteristics as defined on page 43.
μ	Time lag in milliseconds or degrees crank angle
[ ]	Concentration

Subscripts

p,v	Refers to pressure and volume respectively
o	Refers to initial conditions
i	Refers to ignition
C.W.	Cooling water
m	Main
p	Primary

Abbreviations

b.s.f.c. B.S.F.C.	Brake specific fuel consumption
b.h.p. B.H.P.	Brake horsepower
b.m.e.p. B.M.E.P.	Brake mean effective pressure
B.T.C. A.T.C.	Before and after top dead center respectively
B.B.C. A.B.C.	Before and after bottom dead center respectively
F/A	Fuel to air ratio (weight ratio)
E. C.	Energy cell

P.F.	Primary fuel
M.F.	Main fuel
T.F.	Total fuel
V_s	Piston displacement
R.P.M. r.p.m.	Revolutions per minute
deg.	Degrees crank angles
exh.	Exhaust
max.	Maximum
comp.	Compression
suc.	Suction
k.cal	Kilo calory
H.V.	Heating value

I. INTRODUCTION

In the dual cycle, a charge of air is compressed in the engine and then the fuel is injected. The air is so hot, because of the approximately adiabatic compression, that the fuel spray ignites.

The word ignition as used here, covers a multitude of unknowns about how soon and how much vaporization occurs, and how fast some undefined chemical reactions take place after the injection of the fuel into the hot swirling air.

The mixture in the diesel combustion chamber is far from homogeneous since it consists of air and exhaust residuals from the previous cycle, and into this mixture liquid fuel is injected. It is easy to imagine droplets of fuel enveloped by a vapor-air mixture with a large variety of ratios and fairly large pockets where there is no fuel.

The photographs of Rothrock and Waldron[1] show that ignition starts in the small zones near the boundary of individual sprays where the temperature is somewhat lower than the air-compression temperature owing to heat absorption by the spray. According to F. Schmidt[2], the physicochemical delay is of the range 0.7 to 3 milliseconds for usual diesel fuels.

Lewis[3], Granger[4], Mason[5], and many other investigators observed the relation between the formation of formaldehyde and the tendency to knock in spark ignition engines. With increasing knock intensity, the formaldehyde absorption bands increase in intensity. Formaldehyde also appears under nonknocking conditions, but under conditions where formaldehyde is not detectable, knock is never observed.

Although formaldehyde is a reaction product rather than a promoter, it is an indication of the progress of the attack on the fuel by the oxygen.

Granger[4], and others, believe that a hot flame must always be preceded by a cool flame. They also observed that these cool preflames are accompanied by high concentrations of aldehydes. Their results show also that the peroxides are present in the combustion chamber during the preflame period. They also found that there is no correlation between cetane number and intermediate compounds, but there is a correlation between cetane number and the time elapsing between injection and peroxide concentration.

Granger[6] in an earlier paper showed the effect of some additives to the air stream on the delay period. Of these additives some were peroxides. The most sensitive fuels to additives are the most parafinic

Recent investigations by Lyn[7], Royle[8], Schweitzer[9,10] showed that the delay period was shortened by introducing part of the fuel with the intake air. Lyn's curves showed higher fuel consumption at part loads. Schweitzer showed the effect of droplet size on the smoke limit.

Corzilius[11] observed that in a hydrocarbon-air mixture, no detectable chemical reactions occur until certain temperature and pressure conditions were reached.

A report on Bi-fuel combustion systems[12] indicated that low cetane value fuels can be used, in engines whose compression ratio would not be normally high enough to cause ignition, by injecting auxiliary fuels into the cylinder 60° to 120° before the main injection.

The maximum output of compression ignition engines is limited by its smoke limit, the knock of the engine due to the long delay period of the fuel, and its relatively low rotating speed. All of these are handicaps in utilizing such engines in many fields particulary the automotive.

The above mentioned situation indicated a need to investigate the factors affecting the combustion and devise a reliable technique to control it.

It was thought that by injecting part of the fuel early in the cycle directly into the energy cell, sufficient concentration of active radicals, mainly hydroperoxides, could be prepared immediately before the main injection in order to trigger the hot flame reaction and shorten the delay period. By controlling the beginning of the ignition as well as the rate of reaction, the rate of heat addition and the point of the maximum pressure rise could be controlled.

Because of the numerous number of factors to be controlled, it was decided to investigate, individually, the effect of different variables in a certain order on the engine performance. These factors and their order are given on page 33 .

II. EXPERIMENTAL APPARATUS

A vertical single-cylinder, four-stroke cycle, liquid-cooled Nordberg Diesel engine was used in the experimental work. The engine had a bore of 4 1/2 inches, a stroke of 5 1/4 inches, and a compression ratio of 14 1/2. Other engine specifications are given in Appendix II. The general test setup is shown in Figure 1. The various systems and the methods of measurements (instrumentation) are described in the following paragraphs.

A. Fuel System

The engine was equipped with a second injection valve placed to inject the primary fuel into the energy cell as shown in Figures 4 and 5. An additional injection pump was used to supply the primary fuel. This pump was driven by the engine by means of a chain and sprockets (Figure 3). The timing and the quantity of the primary fuel could be easily altered and controlled or maintained constant during any run. Two separate fuel weighing units were used to measure the fuel rate which was injected through each valve individually. The fuel rate was determined by measuring the time required for consuming a predetermined weight of fuel.

The fuel weighing unit consists of a fuel container mounted on a balance, timer and electronic revolutions counter. With the engine operating at test trial conditions, and drawing fuel from the container only, the scale weight is adjusted so that the scales are almost ready to pass through balance. At a particular point during the balancing movement, the timer and the revolution counter start;

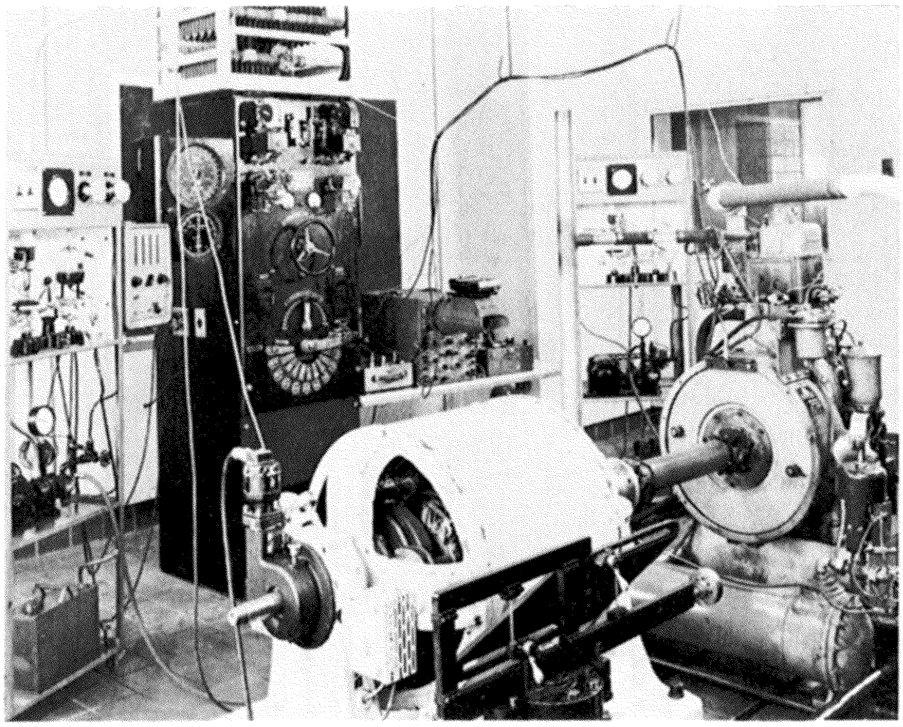

Figure 1. General Layout of the Experimental Setup.

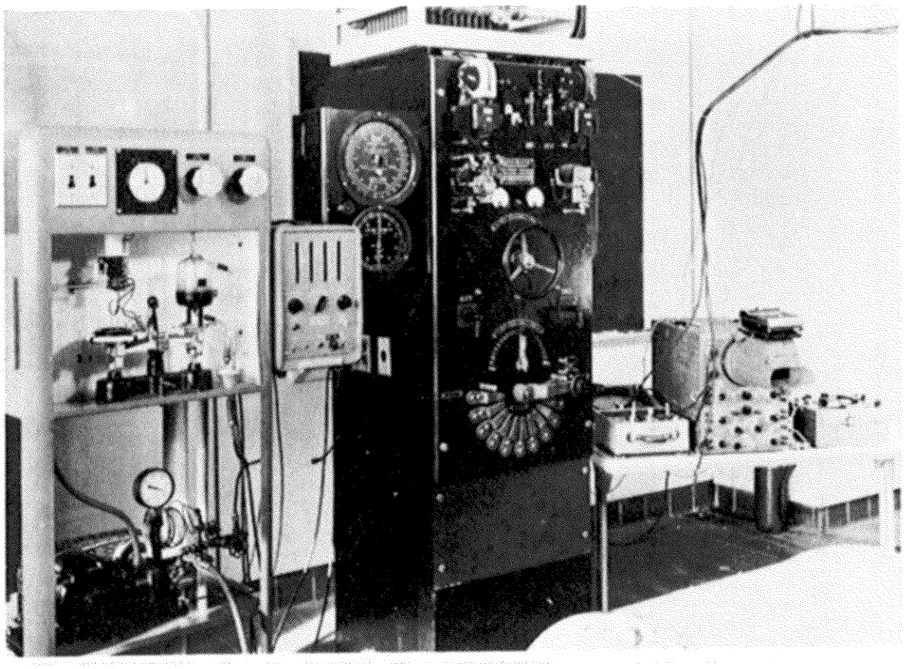

Figure 2. Fuel Weighing System, Control Panel, Amplifier and Oscilloscope, and Potentiometer.

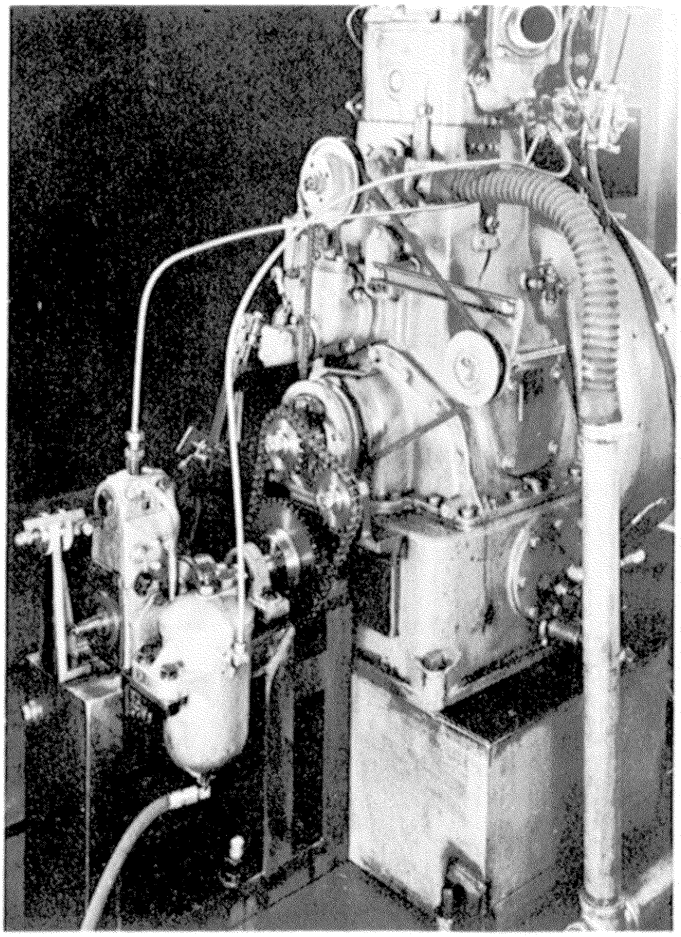

Figure 3. The Primary Fuel Injection Pump, its Drive and Control.

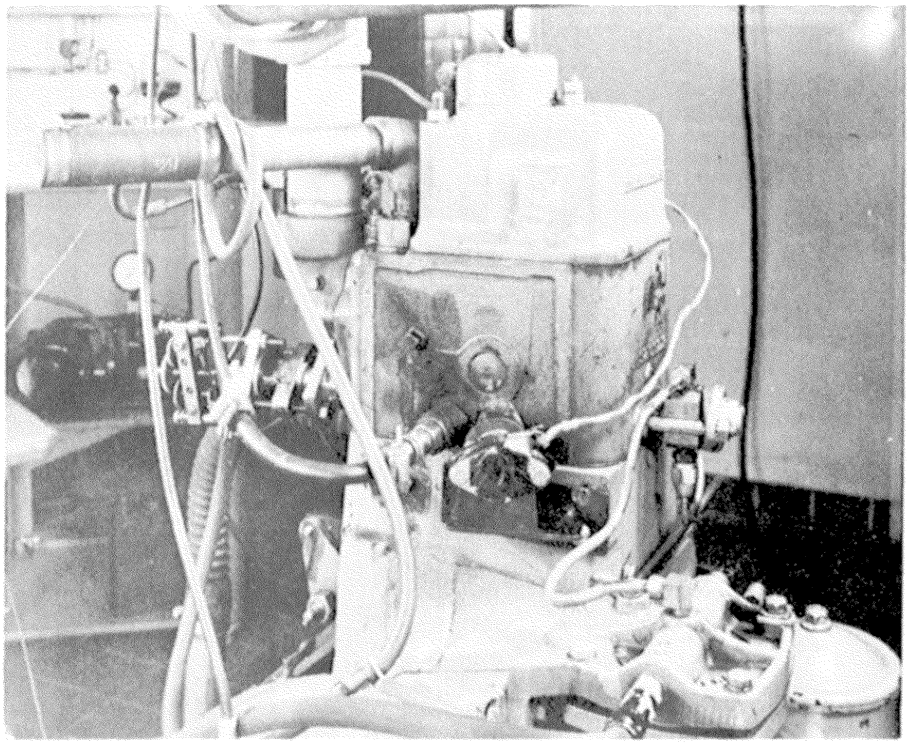

Figure 4. Cylinder Head View, Showing the Two Injection Valves, Pressure Pick-up and Photoelectric Cell.

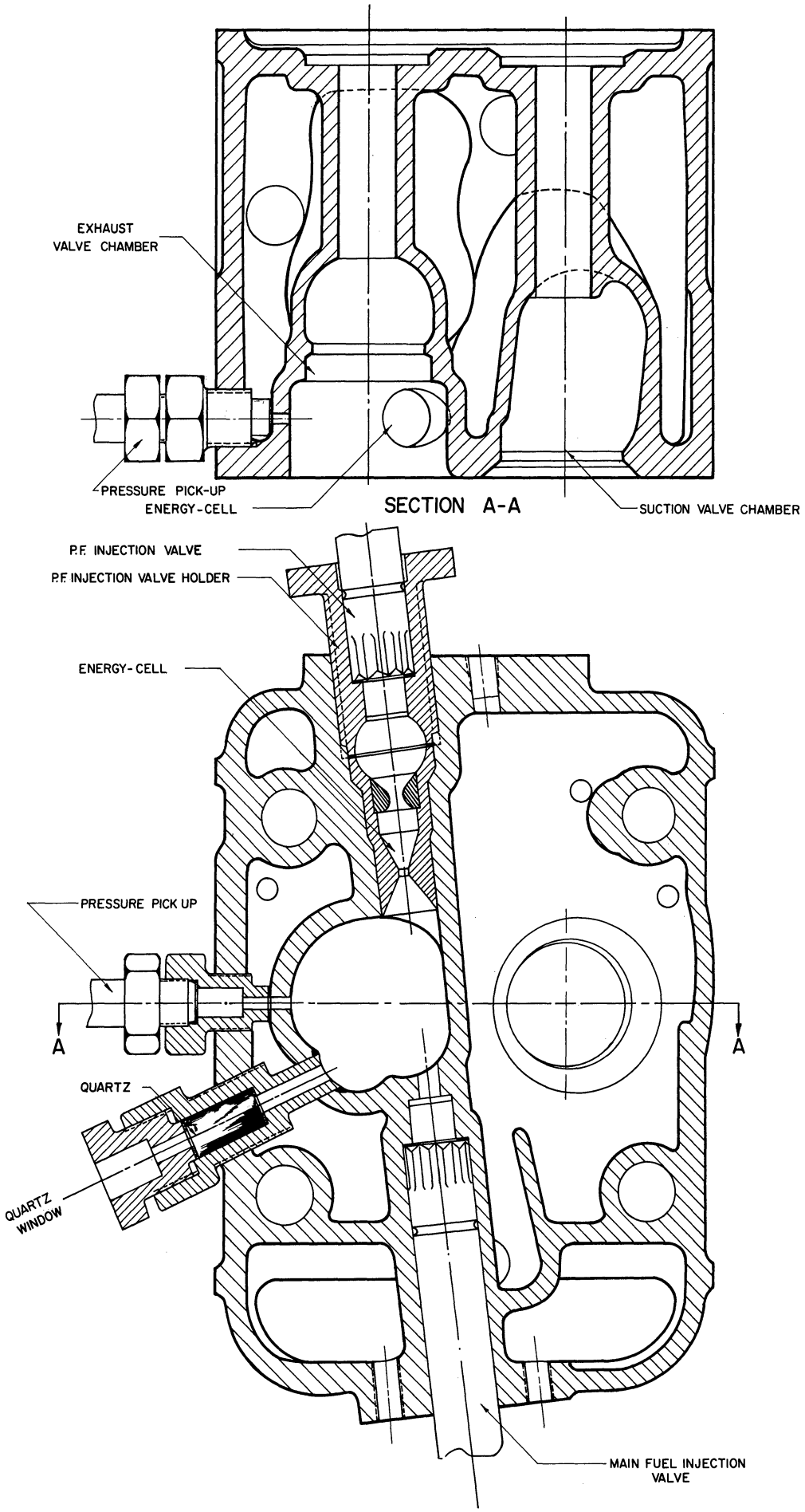

Figure 5. Cylinder Head After Modification.

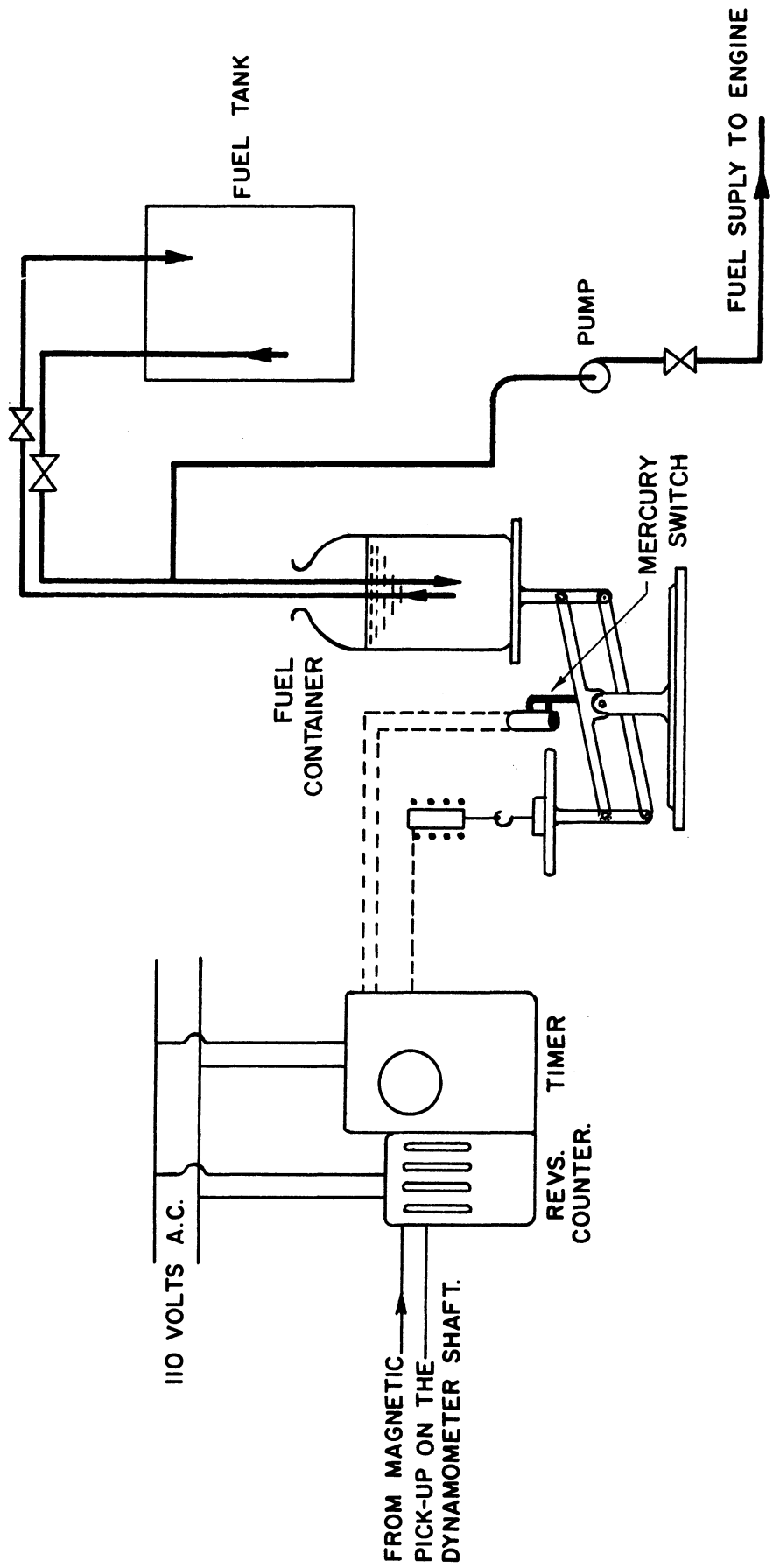

Figure 6. Schematic Diagram for Automatic Fuel Weighing System.

then the scale weight is immediately raised off the scale so that the fuel container side of the scale is heavy by an amount equal to the weight of the fuel to be consumed during the trial. As the scales again pass through balance, the timer is stopped at exactly the same point in the balancing movement. The timer and the revolution counter are simultaneously engaged and disengaged and the scale weight raised automatically through relays actuated by a mercury switch mounted on the scale beam (Figures 2 and 6).

B. Cooling Water System

Figure 7 shows diagrammatically the cooling water system. It is of the closed type, consisting of a water pump and a heat exchanger. The water pump is of centrifugal type, built in and driven by the engine. The heat exchanger is of the shell and tube type, and is equipped with an automatic thermostatic control to maintain the cooling water temperature constant at the water pump inlet. The automatic regulator could be set manually to maintain the water temperature at any desired level within two degrees Fahrenheit. A rust inhibitor was added to the cooling water.

C. Exhaust System

The engine exhaust manifold was connected to the main exhaust underground conduit by a two inch pipe. The exhaust gas temperature was measured by an iron-constantan thermocouple placed in the exhaust pipe just after it leaves the cylinder head block. The temperature was read directly on a calibrated potentiometer indicator (Leeds and Northrup) in degrees Fahrenheit.

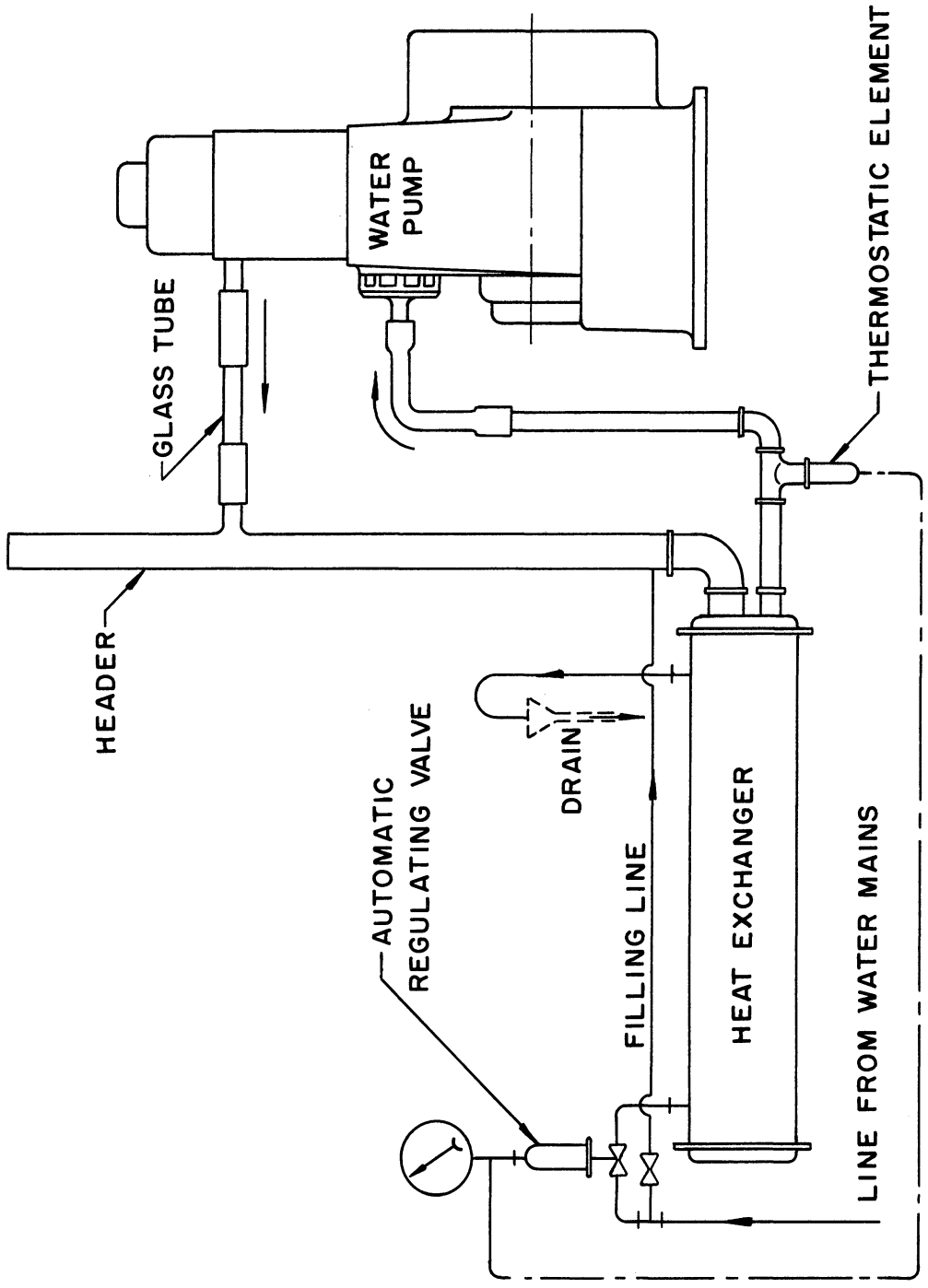

Figure 7. Schematic Diagram of Cooling Water System.

D. Power Absorbing Unit

A D-C cradle dynamometer, type TLC, was used to start the engine and absorb the power output. The power output of the engine (B.H.P.) is converted to electrical energy in the dynamometer (generator) and this energy was absorbed as heat in the loading air cooled resistance grids. The dynamometer was equipped with an electric tachometer to measure the speed and a Link Unibeam to measure the torque applied on the dynamometer. The torque was read directly in foot-pounds on a Wallace and Tiernan gage. The average speed for accurate power determination was measured by means of a stop watch and revolution counter which was explained under fuel system.

E. Lubricating Oil System

The engine parts were lubricated under pressure. The lubricating oil temperature, in the engine sump, was kept constant during the course of test. Figure 8 shows the lubricating oil cooling system. The oil was drawn from the engine sump, put under pressure and divided into two parts. One part was passed through a shell and tube heat exchanger to be cooled and then mixed with uncooled oil. An automatic thermostatic regulating valve regulated the proportion of the two parts to maintain the oil mixture at the required temperature. To measure the lubricating oil temperature in the sump, an iron-constantan thermocouple was used with calibrated potentiometer indicator.

F. Gas Pressure Indicator

Channel A of a dual-beam cathode-ray oscilloscope was used to trace the pressure-time diagram of the gas in the cylinder. The indicator was composed of:

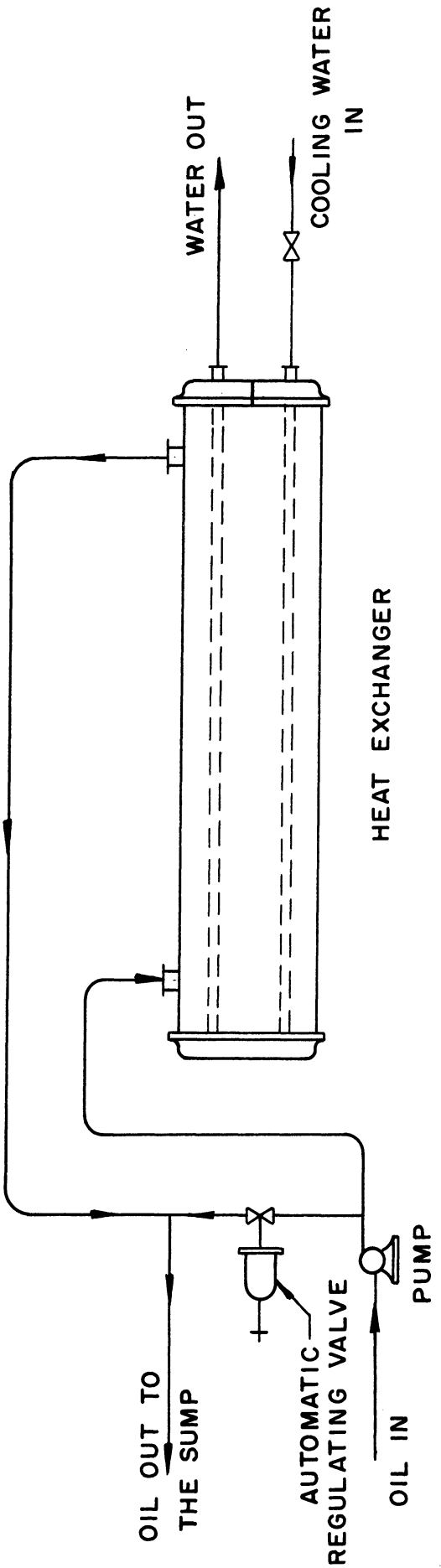

Figure 8. Schematic Diagram of Lubricating Oil Cooling System.

a. Pressure pick-up type P-701-1, Control Engrg. Corp.

b. Magnetic pick-up type 3010-A, Electro Products Lab.

a. Pressure Pick-Up

It consists of a thin diaphragm with two catenary-shaped depressions. Resting in the circular groove formed by the intersection of the two catenaries, is one end of a thin-wall steel tube, the upper end of which is developed into a heavy flange, clamped securely to the main body. This is the strain tube on which are cemented two 1000 ohms, single layer, strain gage windings. One winding is wound longitudinally and the other circumferentially. When pressure is applied, the strain tube is compressed along its axis and expanded around its circumference. The two windings form two legs of a Wheatstone Bridge circuit. The variation in the winding resistances, due to pressure application, changes the balancing condition across the bridge. The resulting difference in voltage is amplified and fed to channel A of the oscilloscope.

b. Magnetic Pick-Up

The magnetic pick-up was mounted on the fly wheel casing, with its pole close to the tip of a heavy iron pointer which was oriented to the bottom dead center. The voltage pulse generated by the rotation of the pointer was applied to the external synchronization terminals of channel A of the oscilloscope (Figures 2 and 9).

G. Primary Injection Valve Opening Indicator

The primary injection valve was equipped with an adjustable bouncing pin used as an electric switch. The circuit was supplied with 1.5 volts D.C. The electric signal, from the valve opening, was supplied to channel B of the oscilloscope. Figure 9 shows the circuit

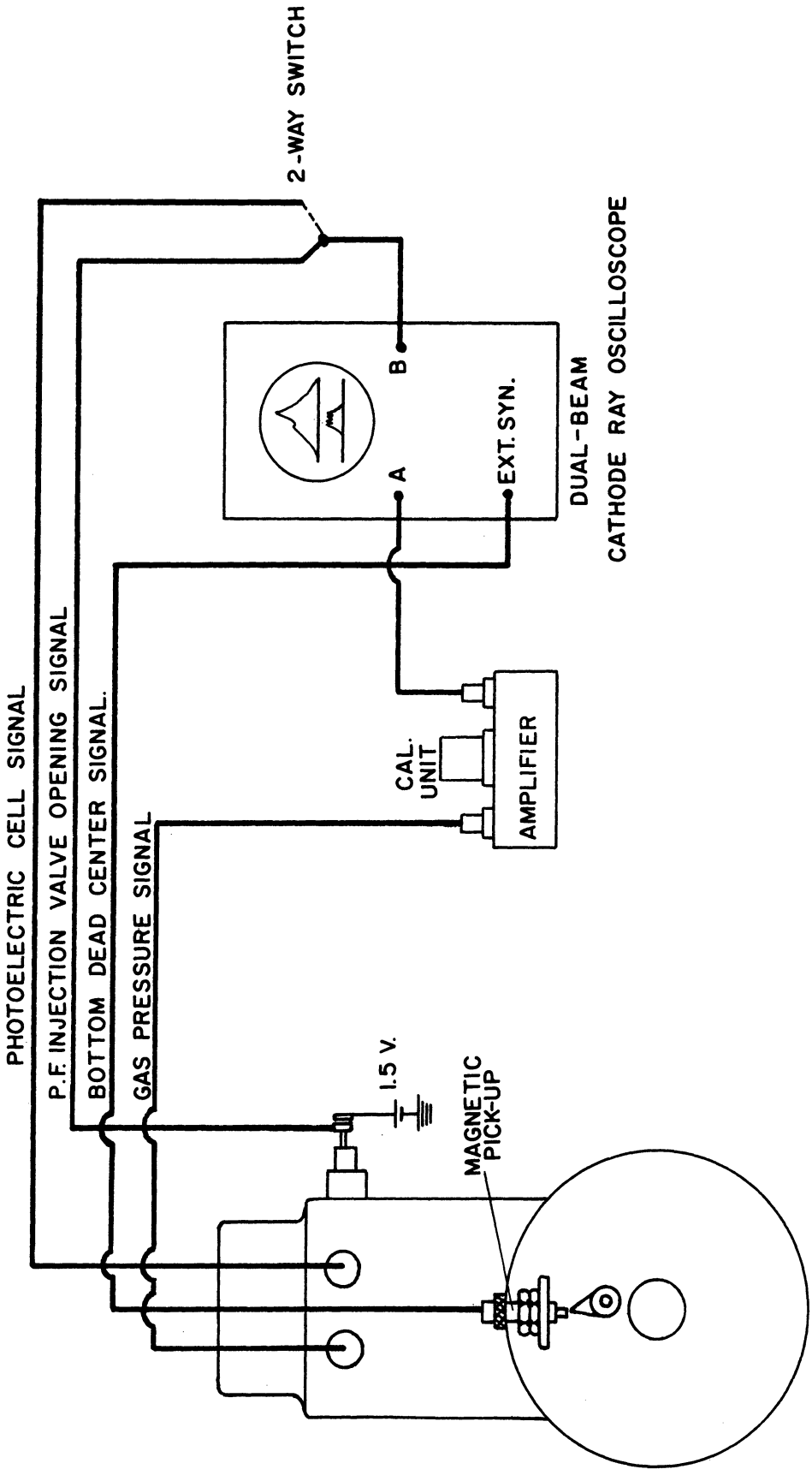

Figure 9. Schematic Wiring Diagram of the Oscilloscope.

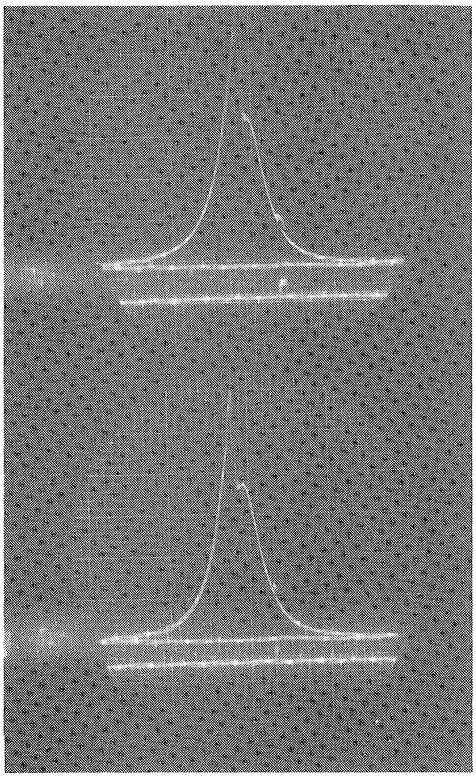

Figure 10. Primary Injection Valve Opening Signal as Indicated on the Oscilloscope (the lower trace).

and Figure 10 (the bottom trace) shows the signal of the valve opening on the oscilloscope screen.

H. Ignition Indicator

A quartz window was built in the cylinder head (Figure 5), through which the light from the ignition was transmitted and fell on the selenium face of a self-generating photoelectric cell. The electric current from the cell was applied to the B channel of the oscilloscope. Figures 5, 9, 11 and 15 show the quartz window, the oscilloscope circuit, the photocell housing, and the ignition trace respectively.

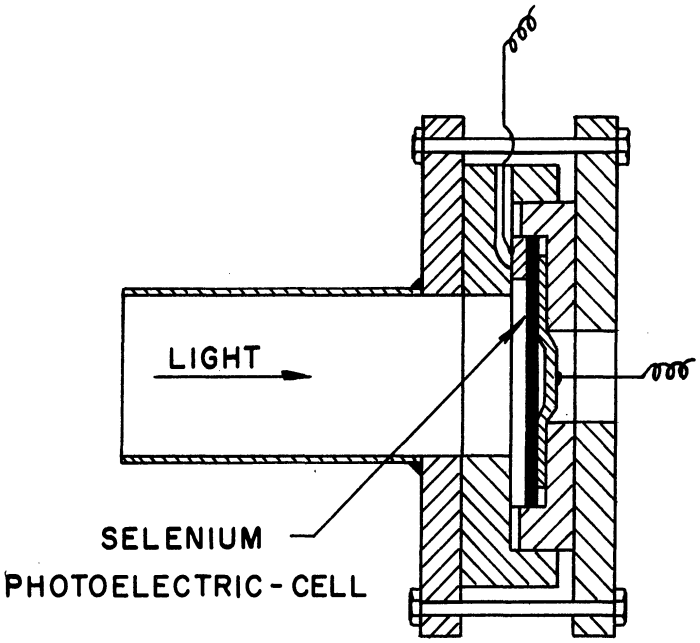

Figure 11. Photoelectric Cell Mounting.

III. THE COMBUSTION PROCESS

Knowledge of the stages through which a heterogeneous mixture of air and fuel passes before ignition starts is necessary for the rational design of any heat engine in general, and of high speed compression ignition engines in particular, where the small fraction of a second can seriously affect the performance of the engine. For discussion purposes, the time elapsed before ignition (delay period) is often divided into two components: physical and chemical. The physical component is the time during which atomization, mixing and vaporization take place, and the chemical component is that time for chemical reactions. Although the actual relative magnitudes of these two components are not known, yet, Boerlage and Broeze[13] have stated that for fuels of normal volatility, the chemical character governs the total ignition period, showing that the physical delay is short.

Fuel injected through a nozzle into a combustion chamber is believed[14] to pass through the following stages:

The fuel leaves the nozzle orifices as a ligament or sheet then breaks down into different size droplets. Appreciable heat transfer from the air present in the combustion chamber to the fuel occurs only after the ligament has broken up into droplets. This is due to the appreciable increase of surface area of the fuel that is exposed to the air. As heat transfer takes place, the droplets heat up (or possibly cool down, depending upon ambient air conditions and initial fuel temperature) and at the same time lose part of their mass by vaporization and diffusion into the air, with both heat and

mass transfer being markedly affected by droplet size and velocity relative to the air. At the same time, the droplets are being slowed down relative to the air by aerodynamic drag forces. After a certain time has elapsed, each droplet tends to approach the equilibrium temperature equal to the wet-bulb temperature corresponding to the conditions present at that moment.

The larger droplets are slower in attaining equilibrium conditions; but, although they have essentially the same initial speed as the smaller ones, they are slowed down relative to the air at a lesser rate, due to its larger momentum, and they move along with the air ahead of the smaller ones that were injected at the same instant. The smaller drops, however, give away their mass and completely vaporize faster and travel a shorter distance through the combustion chamber than the larger droplets.

A cloud of vapor due to the smaller droplets is thus rapidly formed and moves along with the air. The mass of vapor given away by the incoming larger droplets is added to this vapor cloud. Somewhere in the combustion chamber a combustible mixture of air and fuel vapor is formed and is ready for ignition at that point.

In the absence of outside means of ignition, two kinds of reactions may take place simultaneously, a simple molecular reaction[15] and a chain process. The rate of molecular reaction is much larger than that of the chain reactions in some cases, and vice versa in other cases. For fuels of interest, high hydrocarbons, it is believed that the reaction is of the kind suggested by Semenov[15] "degenerate branching."

Since some reactions may take place during the liquid phase of the fuel the chemical portion of the ignition delay period probably overlaps the physical portion. The determination of the chemical delay depends upon understanding the mechanism of oxidation of hydrocarbons which will be discussed in the following chapter.

IV. CHEMICAL KINETICS OF OXIDATION OF HYDROCARBONS

The work on the chemical kinetics of reactions shows overwhelming evidence that most of the chemical reactions of combustion occur in a series of steps involving highly unstable species, such as free atoms and radicals. The oxidation of hydrocarbons and other organic combustibles is not completely understood, but it is known to be a chain reaction.

Already the earliest theory of simultaneous explosion assumed that heat should be transfered until the unburnt layer reaches its spontaneous ignition temperature. Attractive though this theory is, its falseness is shown easily by the fact that according to it, combustion velocity should tend toward infinity with rising pre-flame temperature. But then, even for actual self-ignition processes occurring under condition of short induction periods (ignition in Diesel engines), the original static conception of a spontaneous ignition temperature had proven to be inadequate; no wonder it falls even shorter of being useful in this more complicated and highly dynamic process.

The oxidation of hydrocarbons frequently show an induction period, followed by very rapid reaction. In the case of methane it has been found[16] that traces of formaldehyde are formed in the induction period and the addition of formaldehyde shortens or eliminates the period.

Thus a more dynamic concept of hypothetical character, very simplified, might start from the active particles.

Todes[17] has demonstrated that the rate of energy release, on a purely thermal basis, rises sharply with time after the first few per cent of the reaction have taken place.

With all paraffins and olefins from propylene upward, cool flames occur followed by hot flames. This type of two-stage ignition is characterized with its two separate induction periods τ_1 and τ_2. The induction period τ_1 is from the beginning of the reaction to the appearance of cool flames; and τ_2 is the period from the appearance of the cool flames to the onset of violent explosion. The cool flames usually reveal peroxides and aldehydes on analysis. The emitter in these flames has been found to[18] be electronically excited formaldehydes.

The temperature and pressure limits for the occurrence of cool flames, and of explosions, have been studied carefully by Townend and his co-workers[19]; for all of the hydrocarbons the temperature limits for the cool flames are about 280 to 410°C (536 to 770°F).

Some of the usual features of this kind of reaction are explained by Semenov's[15] hypothesis of "degenerate branching chains," which was put forward primarily to interpret the long induction periods found in the reaction. The chain branching actually occurs and is indicated by the fact that the reactions accelerate without any rise in temperature.

Because of the complexity and hetrogeneity of the reactants in compression ignition engines the plausible mechanism, by Walsh[20], for the oxidation of a straight-chain hydrocarbon RCH_2CH_3 will be considered to explain the chemical kinetics of the combustion. The mechanism may be represented by the following scheme:

$$RCH_2CH_3 + O_2 \longrightarrow RCHCH_3 + HO_2^{*} \qquad (4\text{-}1)$$

$$RCHCH_3 + O_2 \longrightarrow R(CH_3)CHOO \qquad (4\text{-}2)$$

$$R(CH_3)CHOO + RCH_2CH_3 \rightarrow R(CH_3)CHOOH + RCHCH_3 \qquad (4\text{-}3)$$

$$R(CH_3)CHOOH \longrightarrow R(CH_3)CO + H_2O \qquad (4\text{-}4)$$

$$R(CH_3)CHOOH \longrightarrow R + CH_3CHO + OH^{**} \qquad (4\text{-}5)$$

$$R'CH_2 + O_2 \longrightarrow R'CH_2OO \qquad [R'CH_2 = R] \qquad (4\text{-}6)$$

$$R'CH_2OO \longrightarrow R'CHO + OH \qquad (4\text{-}7)$$

$$R'CHO \longrightarrow R'H + CO \qquad (4\text{-}8)$$

According to this mechanism, the hydroperoxide $R(CH_3)CHOOH$ is an important intermediate, and is responsible for the formation of the aldehydes (CH_3CHO). The radical R produced in reaction (4-5) can undergo a further series of reactions (4-6), (4-7) and (4-8), similar to (4-2) to (4-5), until all the C-C bonds are severed. Several features of this reaction scheme may now be discussed.

According to the reaction (4-1), the oxygen attacks the hydrocarbon $RCH_2\underset{|}{CH_3}$ not at the end of the chain but at the tertiary carbon atom $(-\underset{|}{CH})$[7]. In a straight-chain hydrocarbon the oxygen will therefore avoid the hydrogen atoms attached to the end carbon atoms.***

At temperatures between 300 to 400°C [572 to 752°F] it is supposed that the decomposition of the secondary radical, $R(CH_3)CHOO$,

---

* This event is rare due to high energy required.

** This step may be regarded as degenerate branching.

*** The most probable point of attack is at a tertiary carbon atom ($-\dot{C}H$), and a secondary carbon atom ($-\dot{C}H_2$) is preferred over a primary carbon atom ($-CH_3$); the probabilities of attack are 33:3:1 respectively at low temperatures corresponding to cool flame range [ref. 3, p. 172].

is unimportant, the decomposition via the hydroperoxide, $R(CH_3)CHOOH$ being dominant and the induction period is shorter the higher the temperature. As the temperature is raised the decomposition of the secondary radical becomes relatively more important, and that of the hydroperoxide molecule less. The fact that the decomposition of the molecule can be a branching chain process (reaction 4-5) explains the fact that the temperature coefficient of the rate is often found to be negative* in the range from 400 to 450°C [752 to 842°F]. At still higher temperatures the rate of the radical decomposition may have increased so much that the thermal explosions can take place. This scheme of reactions therefore represents a specific mechanism for the degenerate branching postulated by Semenov; the role of the intermediate is played by $R(CH_3)CHOOH$, which can give rise to branching (reaction 4-5) but which can also decompose without the occurrence of branching (reaction 4-4).

A. Rates of Chain Propagation and Termination

In the liquid phase, the diffusion of free radicals is difficult and linear termination of chains at the wall, as in the gas reactions, is not expected. The most natural termination is by recombination of radicals $R(CH_3)CHOO$ and $RCHCH_3$.[15] The chain termination in oxidation is of quadratic nature. When the oxygen pressure is high enough, termination occurs practically exclusively by recombination of the $R(CH_3)CHOO$ radicals. Let n_o be the rate of initiation, k_2, k_3 the rate constants of steps (4-2) and (4-3), k_3' the rate constant for recombination of $R(CH_3)CHOO$ radicals. With the steady state assumption, the rate W of oxidation is:

* At this range the time of reaction increases as the temperature increases.

$$W = \frac{k_3}{\sqrt{k_3'}} [RCH_2CH_3] \sqrt{n_o}$$

The ratio $\frac{k_3}{\sqrt{k_3'}}$ depends on the nature of the hydrocarbons. The striking feature that the pre-exponential factors, of k's, are 5 to 7 orders of magnitude smaller than the collision factors.

B. Chain Initiation and Degenerate Branching

The characteristic feature of both gas and liquid phase oxidation of hydrocarbons is the auto-acceleration of the reaction. This is quite natural since hydroperoxides accumulate during the liquid phase oxidation of hydrocarbons. But peroxide compounds have the ability to initiate the process. In this sense, liquid phase oxidation of hydrocarbons is a process with degenerate chain branching and the branching agents are the hydroperoxides.

In the general case, the expression for the oxidation rate has the form:[15]

$$W = \frac{k_3}{\sqrt{k_3'}} [RCH_2CH_3] \sqrt{k'[R(CH_3)CHOOH] + k''[R(CH_3)CHOOH]^2}$$

k' may be an effective constant containing a constant solvent concentration.

Bateman[21] has shown that this relation represents adequately the variation of W with $[R(CH_3)CHOOH]$ for a number of hydrocarbons, in a very wide range of hydroperoxide concentrations. Bateman has also measured the bimolecular rate constants for hydroperoxide decomposition in a variety of cases. In the case of ethyllinoleate

$$k'' = 1.6 \times 10^{-10} \exp(-26000/RT) \quad cm^3/sec.$$

The most likely chain initiation step in the absence of peroxides (i.e., in the very early stages of the process) is the reaction (4-1). The reaction rate can be written as

$$W_o = k_1[RCH_2CH_3][O_2] = f \times 10^{-10} \exp[-(q_{C-H}-47000)/RT][RCH_2CH_3][O_2]$$

where f is a steric factor.

for olefin q_{C-H} = 77 k.cal.

for branched paraffin q_{C-H} = 89 k.cal. tertiary C-H bond

for straight chain paraffin q_{C-H} = 94 k.cal. secondary C-H bond.

C. The Induction Period

The rate W_o largely determines the length of the induction period. In order to determine the latter, it is necessary to know the kinetic equation of the oxidation process.

The systems of differential equations describing the kinetics of the initial stages of the oxidation process, as long as the decomposition of hydrocarbons can be neglected, can be written as follows:

$$\frac{d[RCHCH_3]}{dt} = W_o - k_2[RCHCH_3][O_2] + k_3[R(CH_3)CHOO][RCH_2CH_3] + k_1[R(CH_3)CHOOH] \quad (4\text{-}9)$$

$$\frac{d[R(CH_3)CHOO]}{dt} = k_2[RCHCH_3][O_2] - k_3[R(CH_3)CHOO][RCH_2CH_3] - k_3'[R(CH_3)CHOO]^2 \quad (4\text{-}10)$$

$$\frac{d[R(CH_3)CHOOH]}{dt} = k_3[R(CH_3)CHOO][RCH_2CH_3] \quad (4\text{-}11)$$

This system can be reduced to (Appendix IV):

$$\tau = \int_0^{\eta} \frac{d\eta}{\sqrt{\eta + (1/2 - W_o')(1 - e^{-2\eta})}} \quad (4\text{-}12)$$

The induction period will be defined as the time required to build up a concentration of hydroperoxide equal to 10^{-4}% (the threshold of analytical

detection) which is equivalent to $\eta = 0.1$ and[15]

$$\tau = \int_0^{0.1} \frac{d\eta}{\sqrt{\eta + (1/2 - W_o')(1 - e^{-2\eta})}} = \left[\cosh^{-1} \frac{W_o}{\eta}\right]_0^{0.1}$$

$$\tau_r = \int_{0.1}^{1000} \frac{d\eta}{\sqrt{\eta + (1/2 - W_o')(1 - e^{-2\eta})}}$$

For branched paraffins Semenov gave the following values

$W_o = 10^{-8}$

$\tau = 16.8$ for induction period

$\tau_r = 64.4$ for reaction period

$\frac{\tau_r}{\tau} = 3.8$

Emperical equations by Rögener[27] for n-heptane are:

$$\tau_1 = 8.1 \times 10^{-12}\, p^{-0.66}\, e^{15100/T}$$

$$\tau_2 = 0.5\, p^{-1.82}\, e^{-1400/T}$$

τ_1, τ_2 are induction periods of cool and hot flames respectively and p and T are in atmospheres and °K of the conditions at the end of compression.

D. Effect of Vitiation

The term vitiation here will be applied to the air which contains additional gas that is neither fuel nor oxygen. For example, air containing a diluent such as nitrogen, argon or contaminated by the products of a previous combustion process within it is vitiated.

The presence of diluent gases frequently plays a very important role in the nature and course of the chemical reactions involved.

Dixon[22] found in his early work that within the range of delays 0.5 to 3 seconds that:

$$\tau \times p_o = \text{constant}$$

where p_o is the partial pressure of oxygen and τ is the delay period.

Mullins[23] found in the case of kerosene the relation:

$$\tau\, a^2 = 10^{-10} \exp \frac{24000}{T}$$

where a is an oxygen index and T is °K. The effect of vitiation on the adiabatic flame temperature of a stoichiometric kerosene-air mixture is very great; it falls by approximately 70°C[23] for each one per cent reduction in the oxygen concentration of the air.

At temperatures below 500°C and particularly at sub-atmospheric pressures vitiation influences largely the course of homogeneous reactions. At higher pressures and temperatures (above 800°C) the reaction rates are usually reduced.

These effects are due to:

a. The change in the thermal properties of the mixture.

b. Inhibition action of some of the components at certain temperatures and pressures.

c. Change in the chemical reaction course, simply the rate of reaction constant.

d. Change in the reaction mechanism.

R. E. Miller[24] gave the following equation:

$$\frac{\tau\, a}{(8.5\, C' + 1)} = 4.88 \times 10^{-13} \exp \frac{32400}{T}$$

C' is the fractional concentration by volume of water vapor and carbon dioxide.

a is an oxygen index equal to oxygen/air ratio by volume.

For pure air

$$\tau\, a^{1.02} = 4.88 \times 10^{-12} \exp \frac{32400}{T}$$

That means that with vitiation the delay period increases to (8.5 C'+1) fold which is equal to two fold approximately under conditions of interest.

It is believed that this increase in the delay period occurs mostly in the preflame reaction period i.e., τ_1.

V. APPLICATION OF THE THEORY

It was shown from the theoretical analysis that if it is desired to burn hydrocarbon fuel quickly it is necessary to establish at least the minimum possible quantity of radicals that suffices to bring about quick reaction. This necessitates introducing some of the fuel, to form a suitable F/A, into the engine cylinder at a certain spot and time to allow the fuel to undergo a chain process which leads to cool flame reaction where the radical concentration is sufficient to accelerate the main combustion. The formation of this concentration should occur just before the main fuel is injected at such a time as to maintain the point of the maximum pressure rise inside the cylinder at about 15° A.T.C. in order to realize the maximum availability of the chemical energy of the fuel.

An energy cell combustion chamber engine was chosen. The primary part of the fuel was injected into the energy cell at low pressure to form, locally, a rich mixture of fuel and air. Since the energy cell is at a temperature, on the average, corresponding to the cool flame range, thus the formation of the radicals can be secured. Should part of the fuel diffuse into the main combustion chamber, it will help in raising the combustion chamber efficiency and improve the air utilization and increase the maximum output of the engine i.e., decreased the specific weight of the engine.

VI. OPERATING CONDITIONS AND TEST PROCEDURE

The engine was started and run for a period of time to warm up to a predetermined condition as expressed by cooling water and lubricating oil sump temperatures.

The points on the b.s.f.c. versus P.F./T.F.% curves were deliberately obtained at P.F./T.F.% in a random order and this scatter of adjacent points about the mean curves gives some indication of the reproducibility.

The following series of experiments were carried out:

Series I. The purpose of which was to determine the performance of the engine after modification without P.F.*

Series II. To determine the most favorable time of injecting the primary fuel into the energy cell covering the range from 45° A.T.C. during the suction stroke to 60° B.T.C. during the compression stroke. This range was limited by those timings at which excessive brake specific fuel consumption occurred. These series were conducted at a constant engine speed of 1600 r.p.m. and 54.3 lb/in^2 b.m.e.p. for safety consideration which will be mentioned later.

Series III. Its purpose was to investigate the effect of injection pressure of the primary fuel on the engine performance. The range of pressure was from 600 to 1400 lb/in^2 in 200 lb/in^2 increments. The test was carried out for the above chosen load and speed at the optimum primary fuel injection timing.

The pressure range was limited by those pressures at which excessive brake specific fuel consumption occurred.

---

* This modification includes provision for pressure pick-up installation, the quartz window, modifying the energy cell as shown in Figure 5 and driving the primary injection pump.

Series IV. To show the effect of cooling water temperature on the engine performance and to determine the optimum operating temperature.

The test was carried out at constant speed for the optimum performance as determined by series I to III and at constant rack position of primary fuel injection pump to supply the P.F./T.F.% of about 5% which produce an economical b.s.f.c. The range of temperature was from 115° to 180°F limited by the occurrance of excessive b.s.f.c.

Series V. To determine the physicochemical delay of the combustion at variable speeds. This series covered the range from 800 r.p.m., the idling speed, to 2000 r.p.m. The maximum speed of 2000 r.p.m. was asigned for safety consideration. The P.F./T.F.% was determined as the minimum quantity that the primary injection pump could supply and still produce ignition at idling speed. This amounted to about 15.8of the total charge.

Series VI. With the primary injection timing, and pressure, and cooling water temperature set at the optimum conditions (maximum economy), the effect of changing the main fuel injection timing was investigated. Timing was altered by changing the clearance between the cam and the injection pump plunger follower. Injection at 9° B.T.C. and 14° B.T.C. were tested and compared with the standard 19° and a series of runs carried out for each timing.

Series VII. To show the effect of adding cumene hydroperoxide to both primary and main fuel individually and simultaneously. A mixture of 1% by volume of cumene hydroperoxide in diesel fuel was used.

Series VIII. To find the effect of the energy cell throat cross sectional area on the performance. Two throat diameters were investigated. The original diameter was 0.1495 in.($A = 0.017554$ in^2) and the second

alternative was 0.196 in. ($A = 0.030171$ in^2). No larger diameter needed to be examined because of the resulting increase in b.s.f.c. Smaller sizes have yet to be investigated.

The following readings were taken for each run:

1. Lubricating oil temperature in the crank case sump = T_{oil} °F.
2. Cooling water temperature at the water pump inlet = $T_{C.W.}$ °F.
3. Exhaust gas temperature after it leaves the cylinder head = $T_{exh.}$ °F.
4. Time for consumption of 1/8 lb of main fuel in minutes = t_m minute.
5. Time for consumption of 1/16 lb of primary fuel in minutes = t_p minute.
6. Number of revolutions of the crank shaft during the time recorded under 4 = N_m.
7. Brake torque F lb.ft.
8. Primary fuel injection timing in degrees before or after T.D.C. = θ_p deg.
9. Beginning of combustion as indicated by the start of sudden pressure rise = θ_i deg.
10. Point of maximum pressure = θ_{max} deg.
11. The ratio of sudden pressure rise to compression pressure.
12. Pictorial records of representative runs showing the following traces:
    a. Pressure-time diagram for the cycle.
    b. Primary injection valve opening time.
    c. Optical intensity of flame in the cylinder.

The test results are given in the appendix in Tables I to XLIII.

Since the engine was designed to run under normal conditions, and to avoid undue damage, the following limits were employed:

Exhaust temperature not to exceed 1100°F.

Maximum pressure inside the cylinder not to exceed 1200 lb/in^2.

According to these limitations the following engine conditions were chosen for the majority of runs:

Load (b.m.e.p.)	= 54.3 lb/in^2
Speed	= 1600 r.p.m. $\pm$ 3%
Cooling water temperature	= 140°F $\pm$ 2°
Lubricating oil temperature in the engine sump	= 160°F $\pm$ 2°

The engine was inspected at the end of the tests and found in satisfactory condition.

VII. DISCUSSION OF EXPERIMENTAL RESULTS

Series I. Performance Test of the Engine After Modification

This series of runs was carried out to determine the performance of the engine after modification and duplicate runs were made from time to time to assure the consistency of the engine conditions. This test was carried out at a constant engine speed of 1600 r.p.m. and covered the load range together with the maximum over-load employed.

These results are shown in Table I and Figure 12 which are typical of such engines. Figure 13 shows the P-t diagrams of this test.

Series II. Runs at Variable Primary Injection Timing

Under constant engine conditions, series of runs were carried out at each timing. The primary fuel consumption to the total fuel consumption was changed from zero to about forty per cent. The chosen load and speed for this series were 54.3 lb/in^2 b.m.e.p. and 1600 r.p.m. respectively. The P.F. injection pressure was 800 lb/in^2.

Figure 14 shows the relation between P.F./T.F.% and brake specific fuel consumption, delay period in degrees crank angles, τ, and exhaust gas temperature for P.F. injection occurred at 45° B.T.C. during the compression stroke, 5° B.T.C. and 60° B.T.C. during the exhaust stroke.

The brake specific fuel consumption decreases to a minimum as the P.F./T.F.% increases, then it begins to increase to a maximum value, usually higher than the value corresponding to non-primary

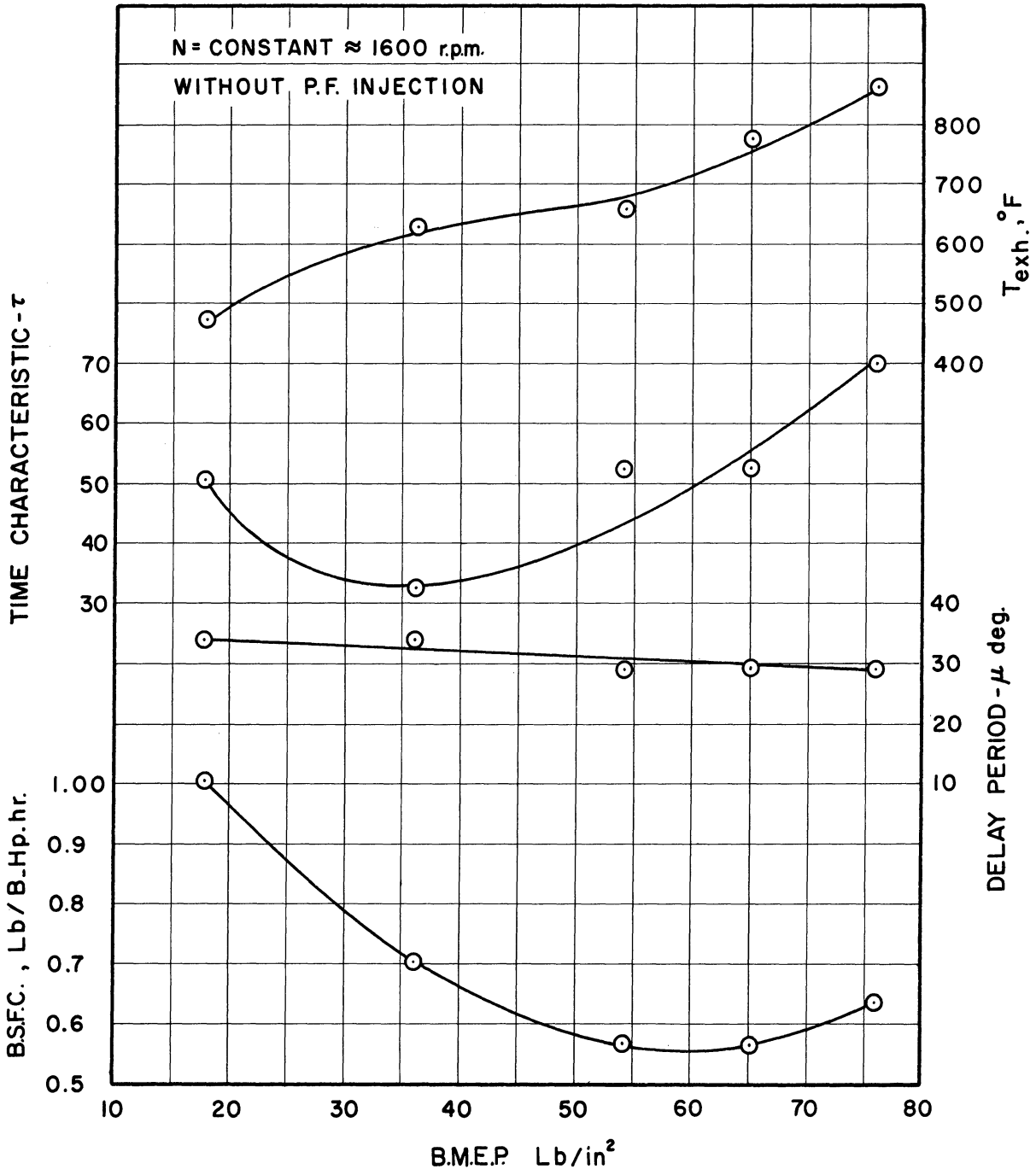

Figure 12. Engine Performance After Modification. (Series I).

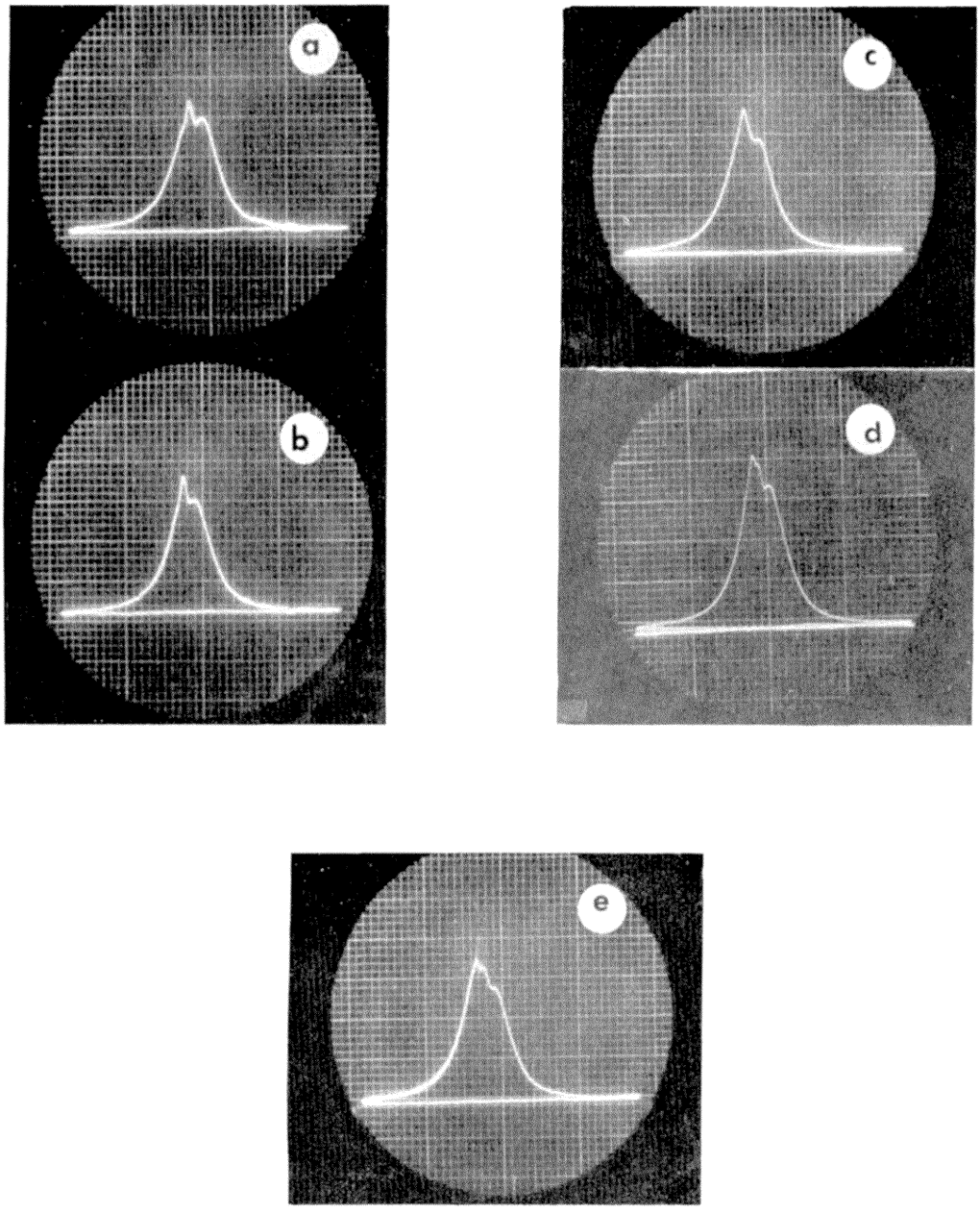

Figure 13. Pictorial Traces of Pressure-Time Diagrams (Series I).

P.F./T.F.% = 0

	Run No.	B.M.E.P.		Run No.	B.M.E.P.
a	1	18.1	d	4	65.1
b	2	36.2	e	5	76
c	3	54.3			

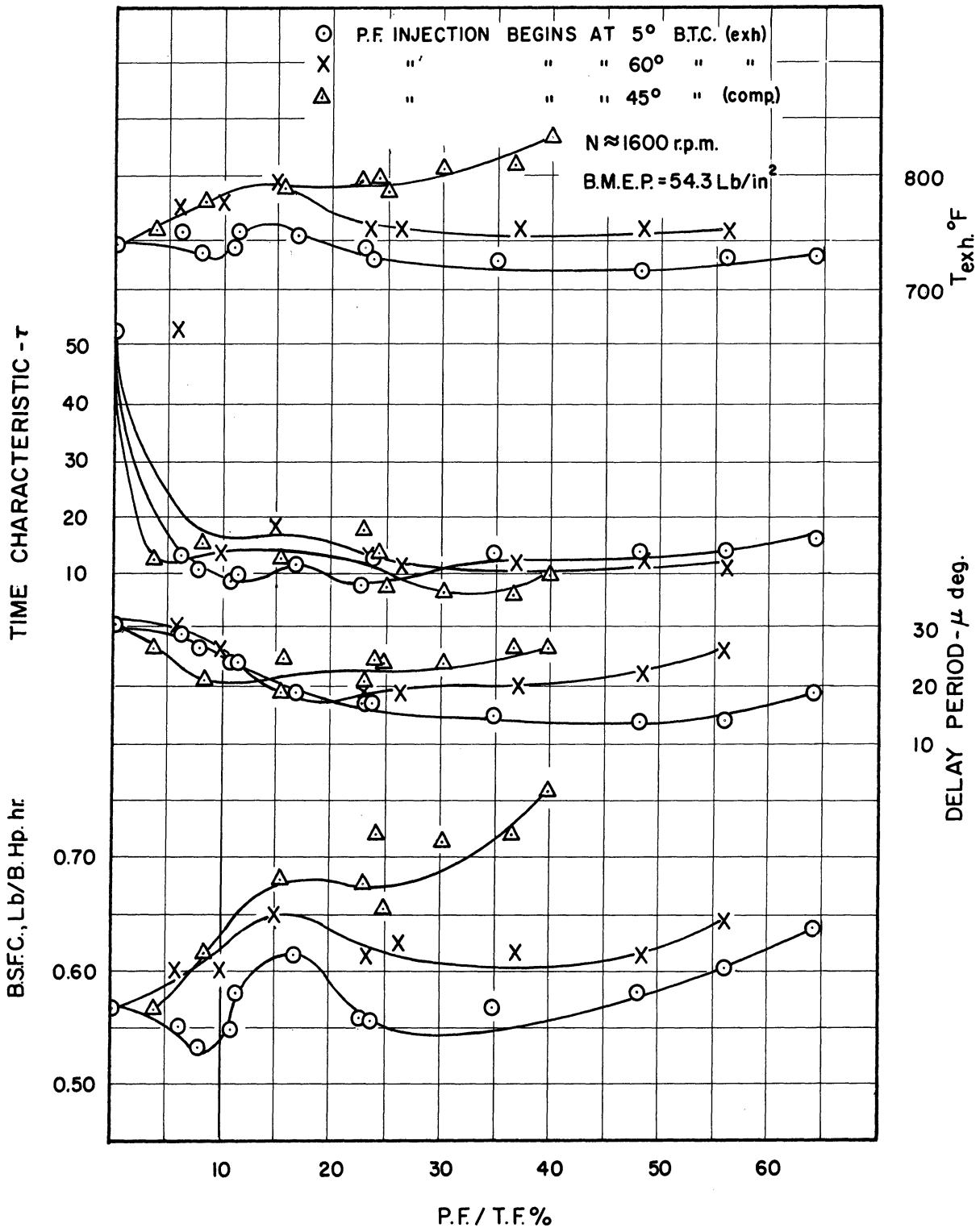

Figure 14. Effect of P.F. Injection Timing Upon Engine Performance. (Series II)

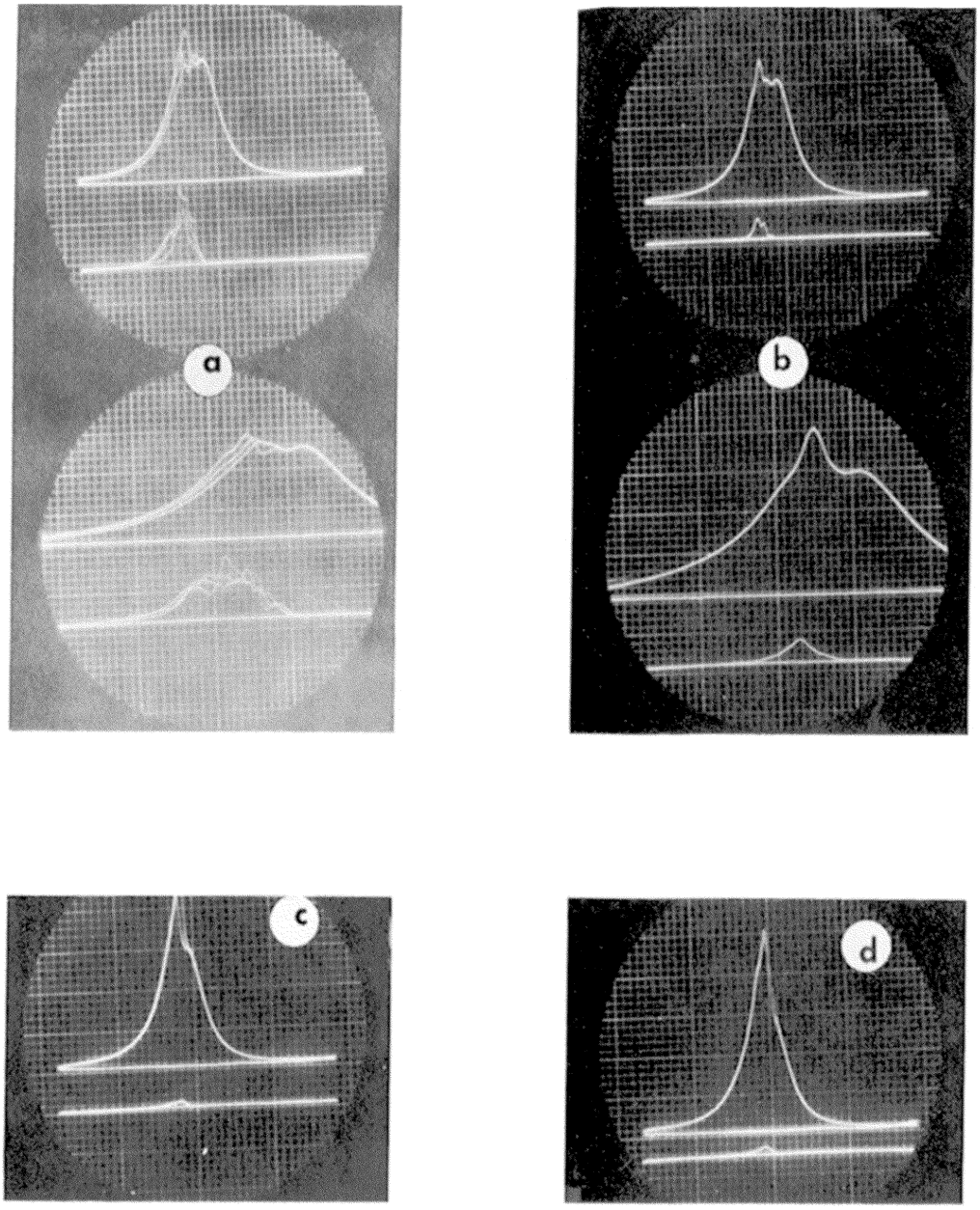

Figure 15. Pictorial Traces of Pressure-Time Diagrams at Various P.F./T.F.% (Series II)

P.F. Injection Begins 60° B.T.C. [exhaust]

	Run No.	P.F./T.F.%		Run No.	P.F./T.F.%
a	1	0	f	184	26.2
b	180	6.22	g	185	36.8
c	181	9.62	h	186	48.5
d	182	14.92	i	187	56
e	183	23.2	j	188	

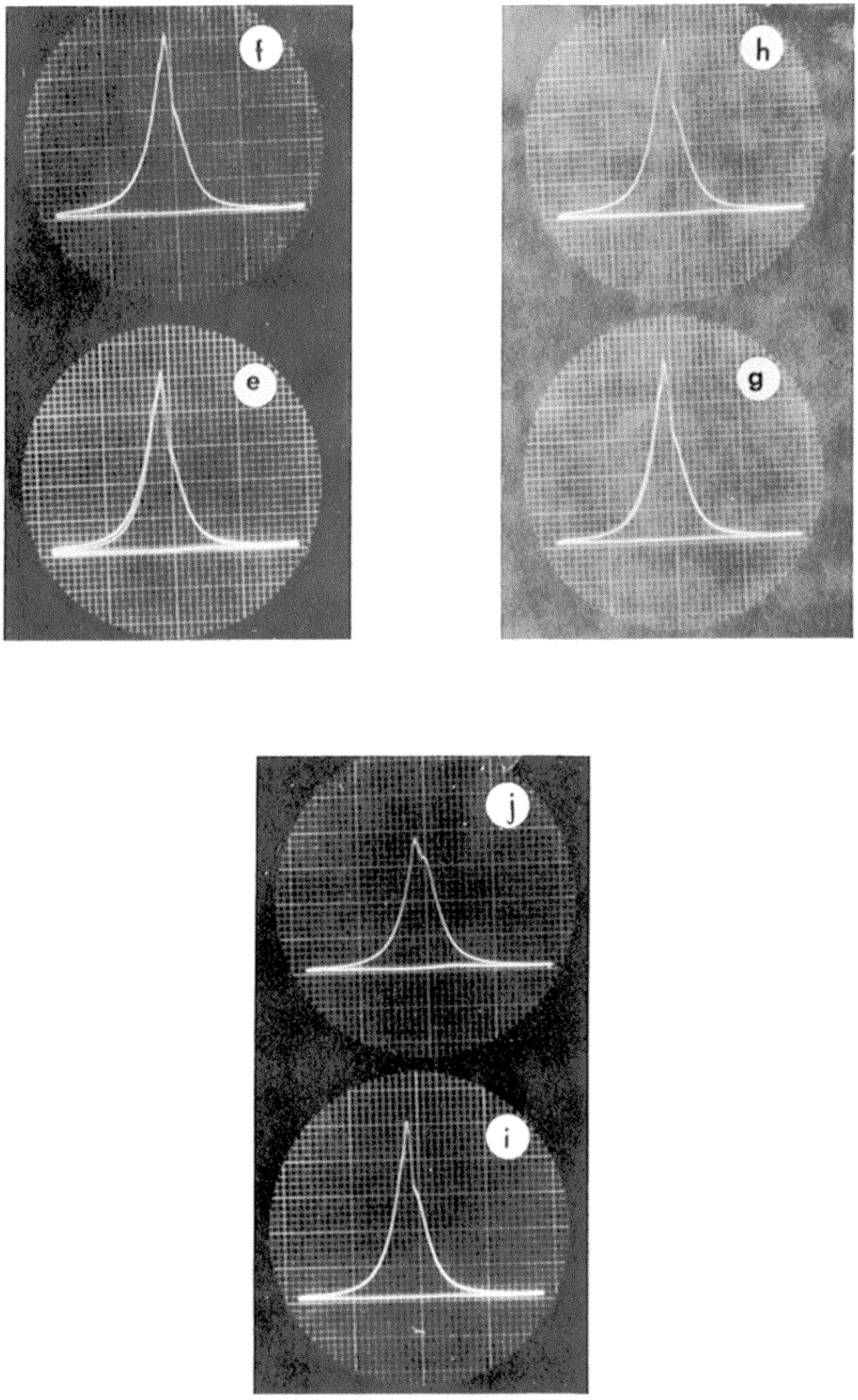

Figure 15. Pictorial Traces of Pressure-Time Diagrams at Various P.F./T.F.% (Series II), Lower Traces Show Flame Intensity.

fuel injection, and then decreases again. From this point on b.s.f.c. appeared to continually increase.

The delay period decreases to a minimum as the P.F./T.F.% increases, and then increases slightly. The delay period decreases first with an increasing rate, then the rate gradually decreases to zero at the inflection point (minimum delay), from this point on the delay period begins to increase.

Since the rate of decrease of delay period is very small at the very low P.F./T.F.%, while there is a similtaneous remarkable change in the pressure-time curve, a time characteristic value τ defined as follows is introduced.

$$\tau = \frac{\text{deg. crank angle elapsed during sudden pressure rise}}{\frac{\text{max pressure-comp.press.}}{\text{comp. press.}}}$$

$$= \theta_{max} - \theta_i \Big/ \frac{P_{max}-P_{comp}}{P_{comp}}$$

The time characteristic τ is inversely proportional to the reaction rate. It shows the effect of accelerating the reaction rate. The τ curves have the general form of the delay period but the rate of decrease of τ is magnified at the first part of the curve.

The exhaust gas temperature curve follows approximately the shape of the b.s.f.c. curve.

By injecting part of the fuel into the energy cell early in the cycle, it is exposed to high temperature and suffers preflame reactions in the τ_1 regime (cool flames) where suitable concentration of hydroperoxides are ready prepared, at the time of the main injection, to trigger the main fuel combustion with reduced delay.

Since the rate of formation of intermediates is a function of fuel concentration (Equation 4-11), this explains the first portion of the curves in Figure 14, i.e., as P.F./T.F.% increases (the concentration of P.F./A increases), the possibility of higher concentrations of intermediate products is evident. This shortens the delay* and most of the energy released from the main fuel is attained earlier in the cycle, i.e., at the highest possible temperature or in other words the highest possible availability. The accompanying effect is higher efficiency and lower exhaust gas temperature due to larger expansion ratio because of earlier maximum pressure rise, faster reaction and shorter afterburning as shown in Figure 15a and 15b. (Bottom traces)

As the P.F./T.F.% increases higher than the economical ratio three possibilities may exist:

1. The combustion rate increases to a point where maximum pressure occurs very early resulting in increased negative work on the piston during the compression stroke.

2. Some of the primary fuel burns in the energy cell early in the cycle at low level of availability.

3. The temperature of the energy cell increases and two other possibilities may arise:

   a. Part of the primary fuel evaporates which changes the reaction mechanism. The diffusion of radicals and their termination at the wall surface will increase (p. 26).

* Semenov has estimated the induction period of branched paraffins as 1/4 the reaction period of stoichiometric mixtures with oxygen at temperature of 400°K and atmospheric pressures.

b. The cell temperature achieves the negative coefficient range ($\approx$ 410°C, p. 24), that is the reaction rate decreases as shown in the humped portion of τ curves (Figure 14).

The coincidence of the point of minimum brake specific fuel consumption with the point of minimum τ supports this reasoning.

Further increase in P.F./T.F.% can cause decrease in the temperature of the energy cell due to the latent heat absorbed by the larger quantity of P.F. which can overcome part of the effect of the hot cell. The second minimum of b.s.f.c. is limited by the efficiency of fuel distributing and mixing in the combustion chamber due to its design and geometry.

The optimum timing of the P.F. injection was found to be at 5° B.T.C. during the exhaust stroke. The brake specific fuel consumption increases for P.F. injection on either sides of this point. When the primary fuel is injected too early during the exhaust stroke, it is probable that part of the P.F. escapes with the exhaust gas. On the other hand with P.F. injection during the compression stroke, the short period between the P.F. and the M.F. injections will not be sufficient for the production of the minimum required quantity of radicals in the preflame reaction for accelerating the main combustion.

Injection of P.F. in the exhaust stroke favors the engine performance since part of the P.F. may diffuse to the main chamber and some active intermediate products from the previous cycle may act as reacting centers to accelerate the reaction.

Series III. Variable Primary Fuel Injection Pressures

At low injection pressure, the fuel droplets are large and the surface to volume ratio is small. Since the reaction rate is a function of surface, then the τ is expected to be larger at the low injection pressure as shown in Figure 16. Moreover the penetration of the P.F. will be less i.e., less exposed to oxygen, as will also be the active radicals, which increases the tendency to higher b.s.f.c.

At higher P.F. injection pressure the atomization is better and the penetration is deeper.

Higher atomization increases the droplets surface to volume ratio resulting in higher rate of evaporation was well as a higher rate of reaction. If the rate of vaporization is high, the oxidation mechanism will differ and the rate of termination of the active radicals at the E.C. wall surface will increase.

Deeper penetration will increase the percentage of fuel injected through the E.C. throat and to the wall surface. The part of the fuel which will pass through the throat will be exposed to relatively low temperature resulting in retardation of pre-flame reaction and radical concentration. The part which will diffuse to the walls will suffer the termination of its active radicals.

Both actions, greater atomization and penetration, will probably act to retard the combustion. Figure 16 shows this trend, higher τ and $T_{exh.}$ are indications of slow combustion and longer afterburning.

Between the two extremes of the P.F. injection pressures, there is an optimum value. As far as brake specific fuel consumption is concerned, the optimum injection pressure was found to be about

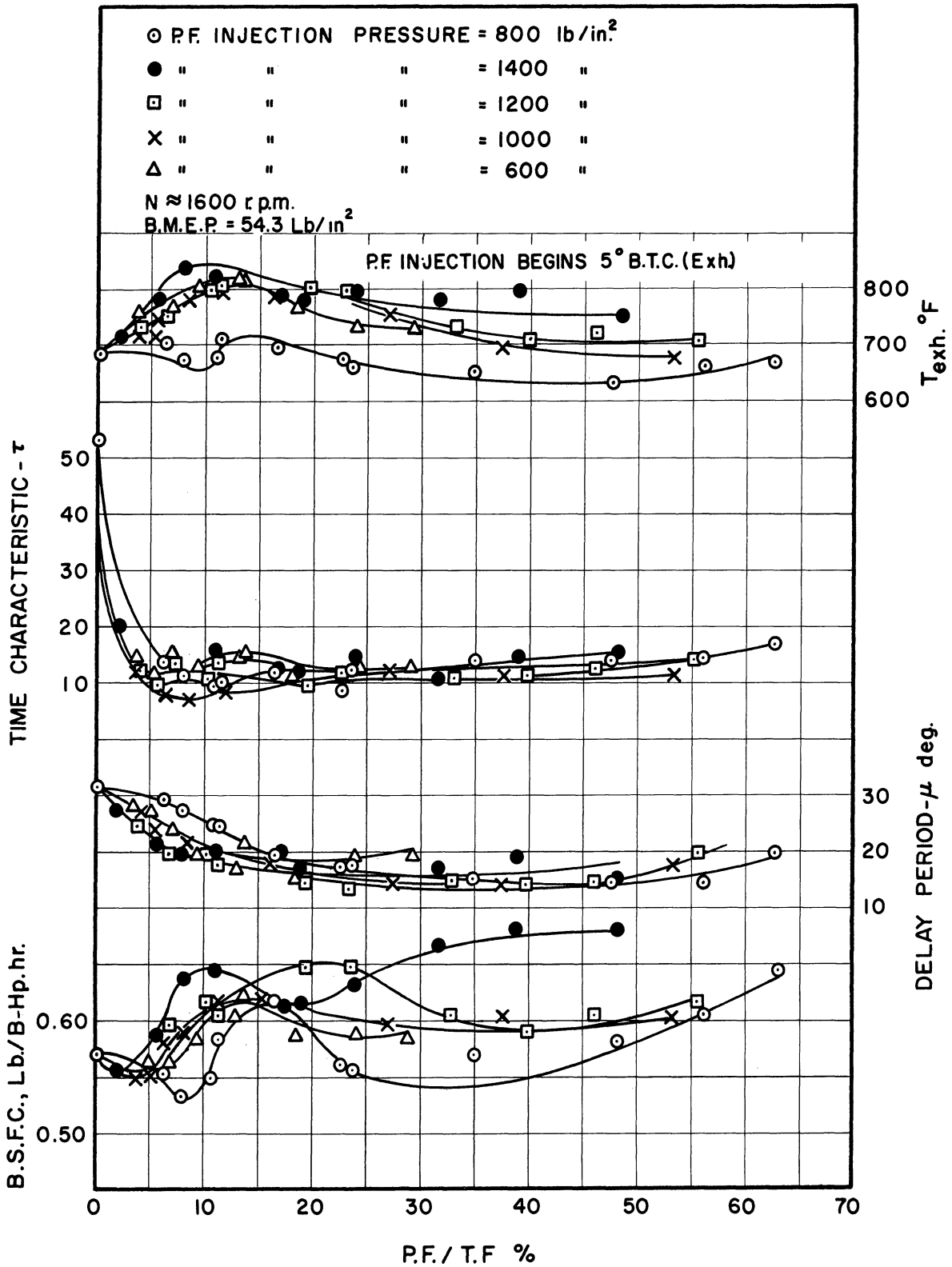

Figure 16. Effect of P.F. Injection Pressure Upon Engine Performance. (Series III).

800 lb/in^2. For minimum τ, injection pressure was found to be 1000 lb/in^2.

Series IV. Runs at Variable Cooling Water Temperature

At constant engine conditions, one run was carried out at each cooling water temperature. Figure 17 shows the b.s.f.c., μ, τ, and T_{exh} versus cooling water temperature for 54.3 b.m.e.p; 5° B.T.C. (exh.), 800 lb/in^2 for primary fuel injection timing and pressure respectively. As the cooling water temperature increases the b.s.f.c. decreases to a minimum at 142°F where it begins to increase. τ decreases with a decreasing rate as the temperature increases.

As the cooling water temperature increases, the engine runs hotter on the average and shorter delay is to be expected, due to faster reaction rate and shorter physical delay. The increase of b.s.f.c. after 142°F is due to the following reasons:

a. The earlier the ignition, the higher is the negative work on the piston during the compression stroke.

b. The higher the temperature, the greater the possibility for the energy cell to achieve the negative coefficient temperature range, which decreases the rate of reaction. In support of this, is that τ decreases with a decreased rate.

c. The higher the temperature, the faster is the vaporization of the P.F., which may affect the kinetics of reaction since the mechanism in the liquid phase is different from that in the vapor or gaseous phase.[15] Figure 18 shows the P-t diagrmas of this series.

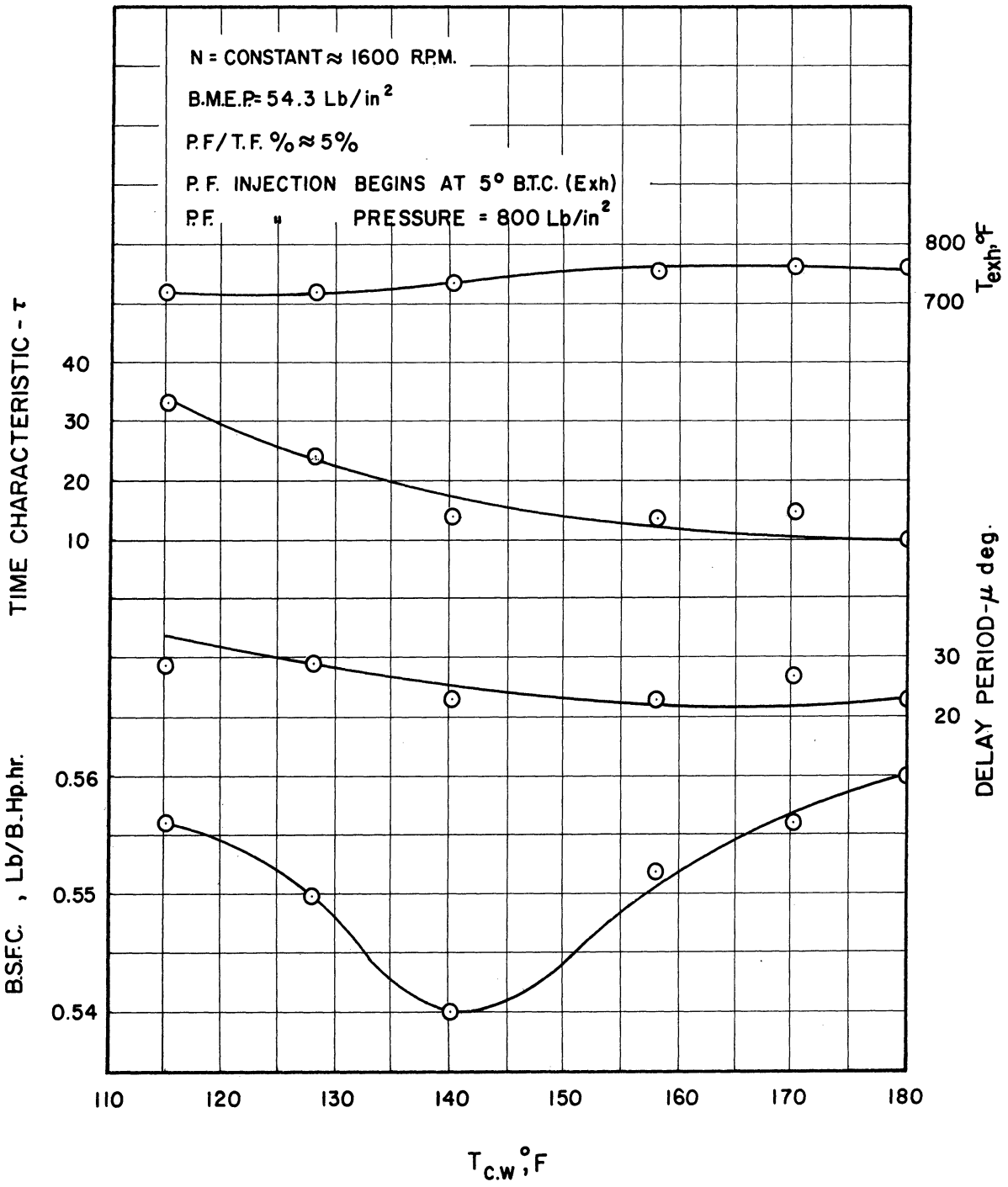

Figure 17. Effect of Cooling Water Temperature Upon Engine Performance. (Series IV).

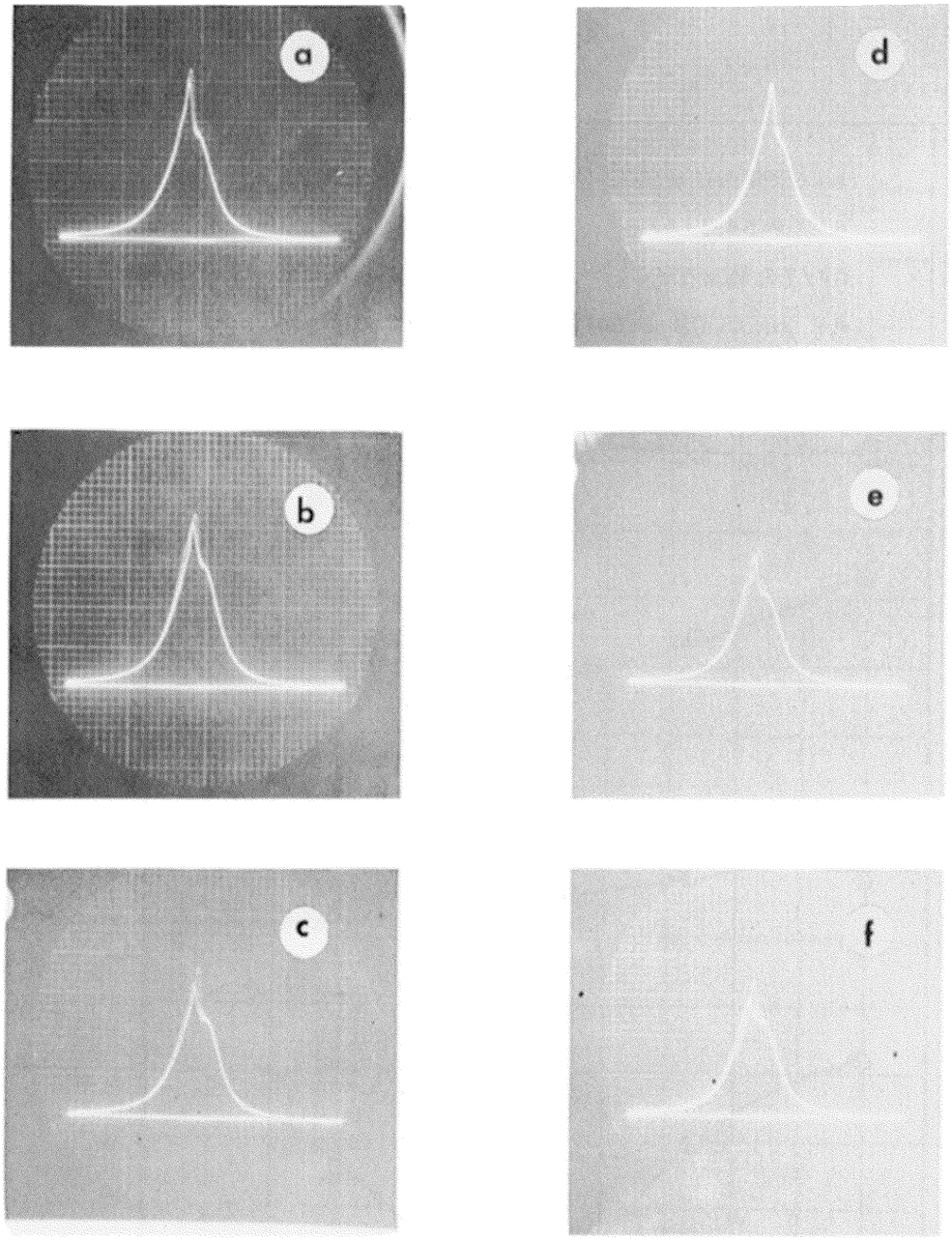

Figure 18. Pictorial Traces of Pressure-Time Diagrams at Various Cooling Water Temperature. (Series IV)

P.F. Injection Begins 5° B.T.C. [exhaust]
P.F./T.F.% = 5%

	Run No.	$T_{C.W.}$ °F		Run No.	$T_{C.W.}$ °F
a	364	180	d	367	140
b	365	170	e	368	128
c	366	158	f	369	115

Series V. Runs at Variable Speed

At constant engine conditions and the optimum performance as determined by the previous series of tests the engine was run at different speeds to determine the delay period. The injection pumps racks were locked to maintain approximately constant quantity of fuel injection per cycle. This assumption neglects the variation of volumetric efficiency of the pumps with the engine speed variation. The P.F./T.F.% was determined as the minimum quantity that the primary injection pump could supply and still produce ignition at the idling speed which amounted to 15.8.

The delay period decreases linearly as the speed increases and the rate of the decrease was the same in both cases, with and without P.F. injection. The decrease in the delay period due to the rise in speed from 950 to 2000 r.p.m. was, in either case, about 1.5 milliseconds which is probably due to higher air swirl and higher engine temperature. Figure 19 and Tables XXX and XXXI show the result of this test. Figure 20 shows the P-t diagrams at various speeds, with P.F./T.F.% = 15.8 (20a to 20h) and without primary fuel injection (20i to 20p). At 2000 r.p.m. without P.F., the combustion was almost at constant pressure (Figure 20m) and the end of the combustion was at 30° A.T.C., while with P.F. injection at the same speed and load, the combustion was almost at constant volume (Figure 20c) and the maximum pressure occurred at 15° A.T.C.

The test results show that (a) for a delay period of 2.8 milliseconds the engine speed was 1050 r.p.m. with P.F. and 1800 r.p.m. without P.F., and (b) for the same speed of 1800 r.p.m. the delay period with P.F. was 57.1% of that without P.F.

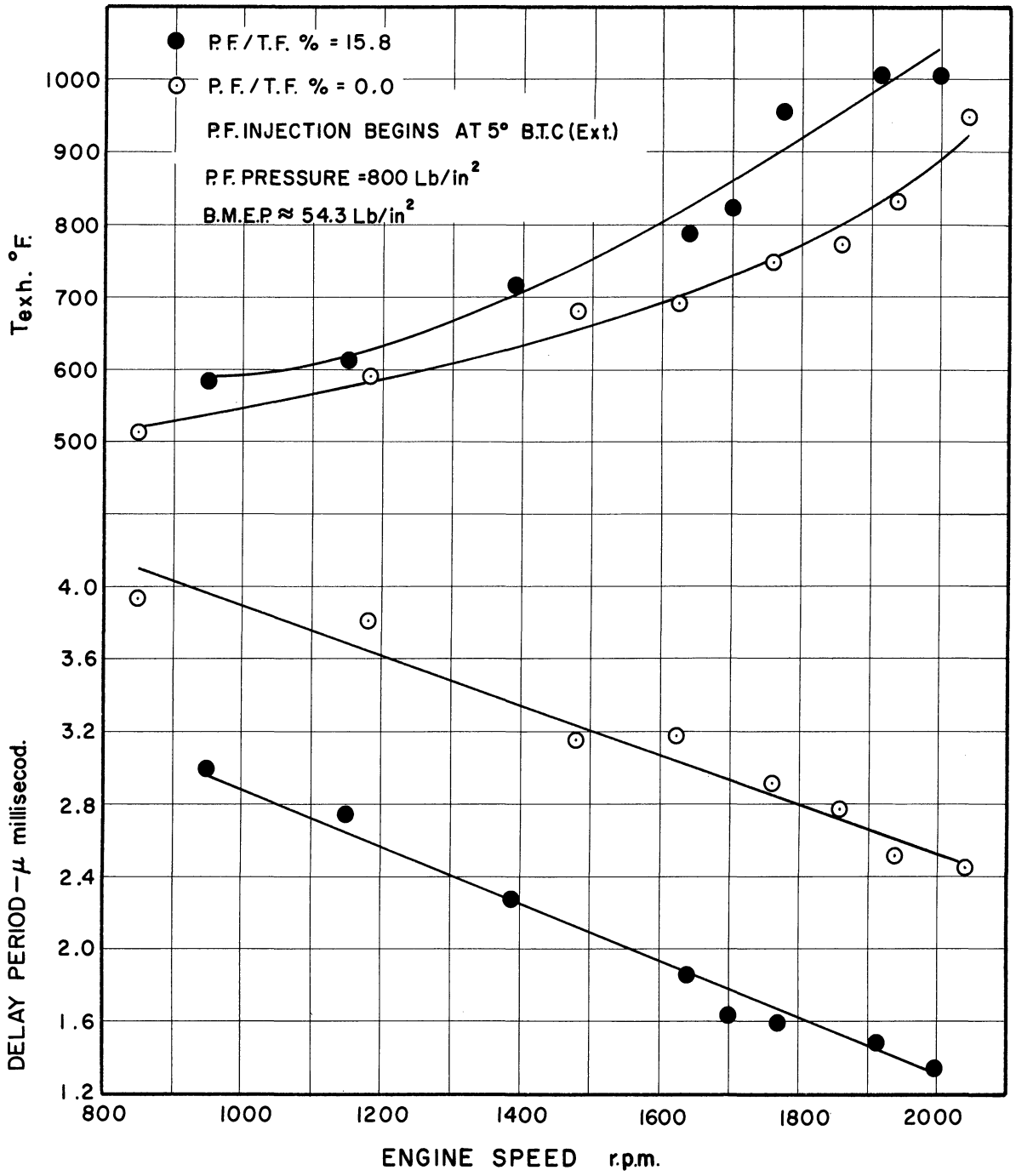

Figure 19. Effect of Engine Speed Upon Delay Period and Exhaust Gas Temperature. (Series V).

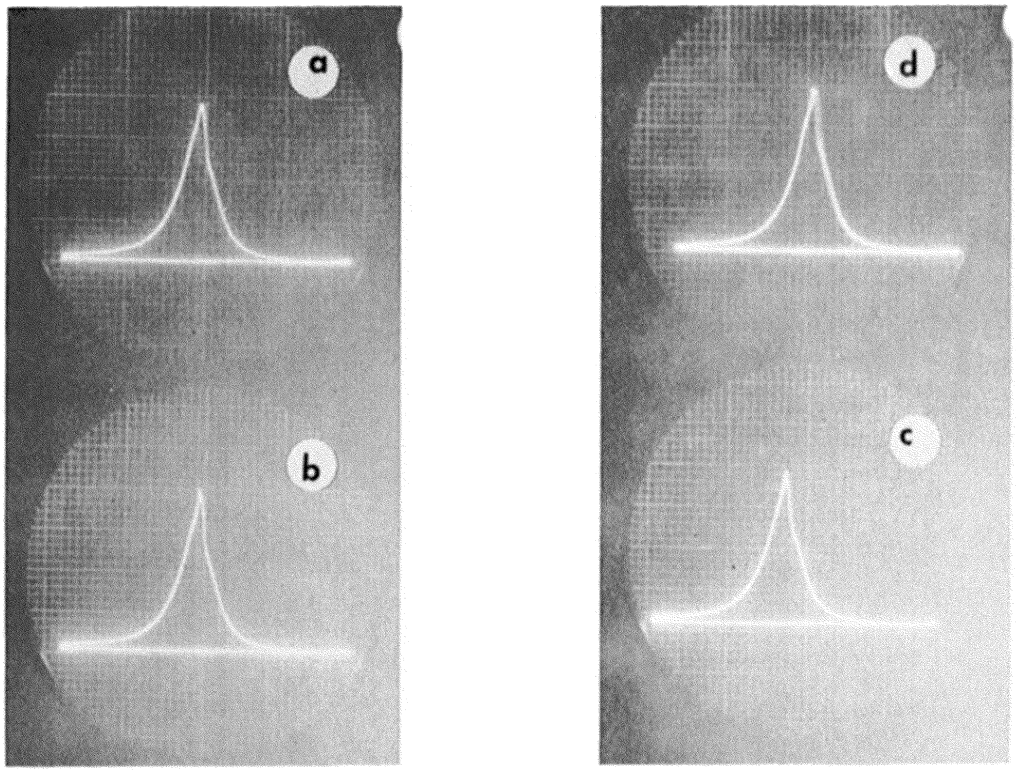

Figure 20. Pictorial Traces of Pressure-Time Diagrams at Variable Engine Speed. (Series V)

P.F. Injection Begins 5° B.T.C. [exhaust]
Constant Fuel Injection Per Cycle

	Run No.	N	P.F./T.F.		Run No.	N	P.F./T.F.
a	370	1775	15.8%	i	378	1625	0.0%
b	371	1915	15.8	j	379	1760	0.0
c	372	2000	15.8	k	380	1860	0.0
d	373	1700	15.8	l	381	1940	0.0
e	374	1390	15.8	m	382	2040	0.0
f	375	1150	15.8	n	383	1480	0.0
g	376	950	15.8	o	384	1180	0.0
h	377	1640	15.8	p	385	850	0.0

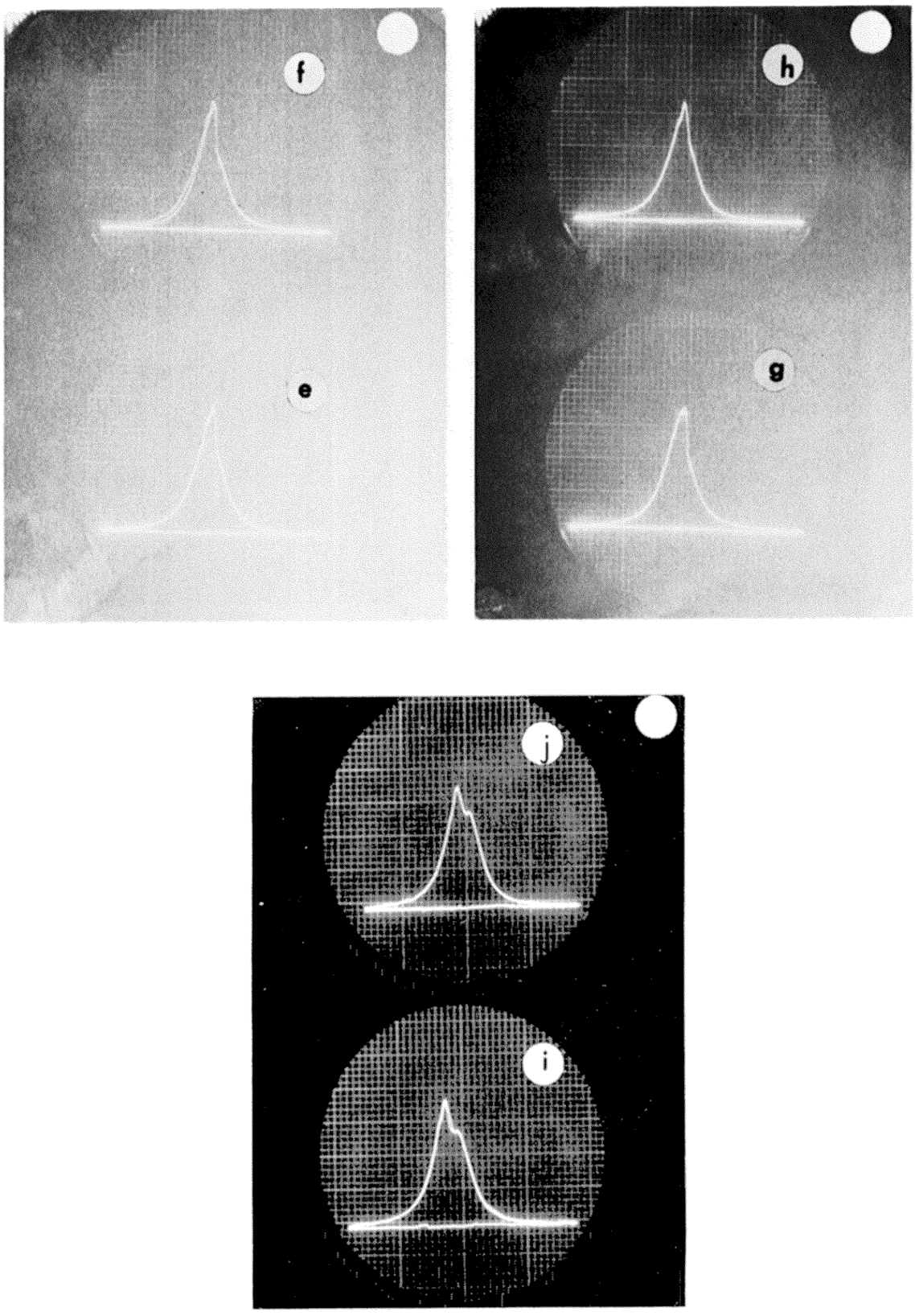

Figure 20. Continued.

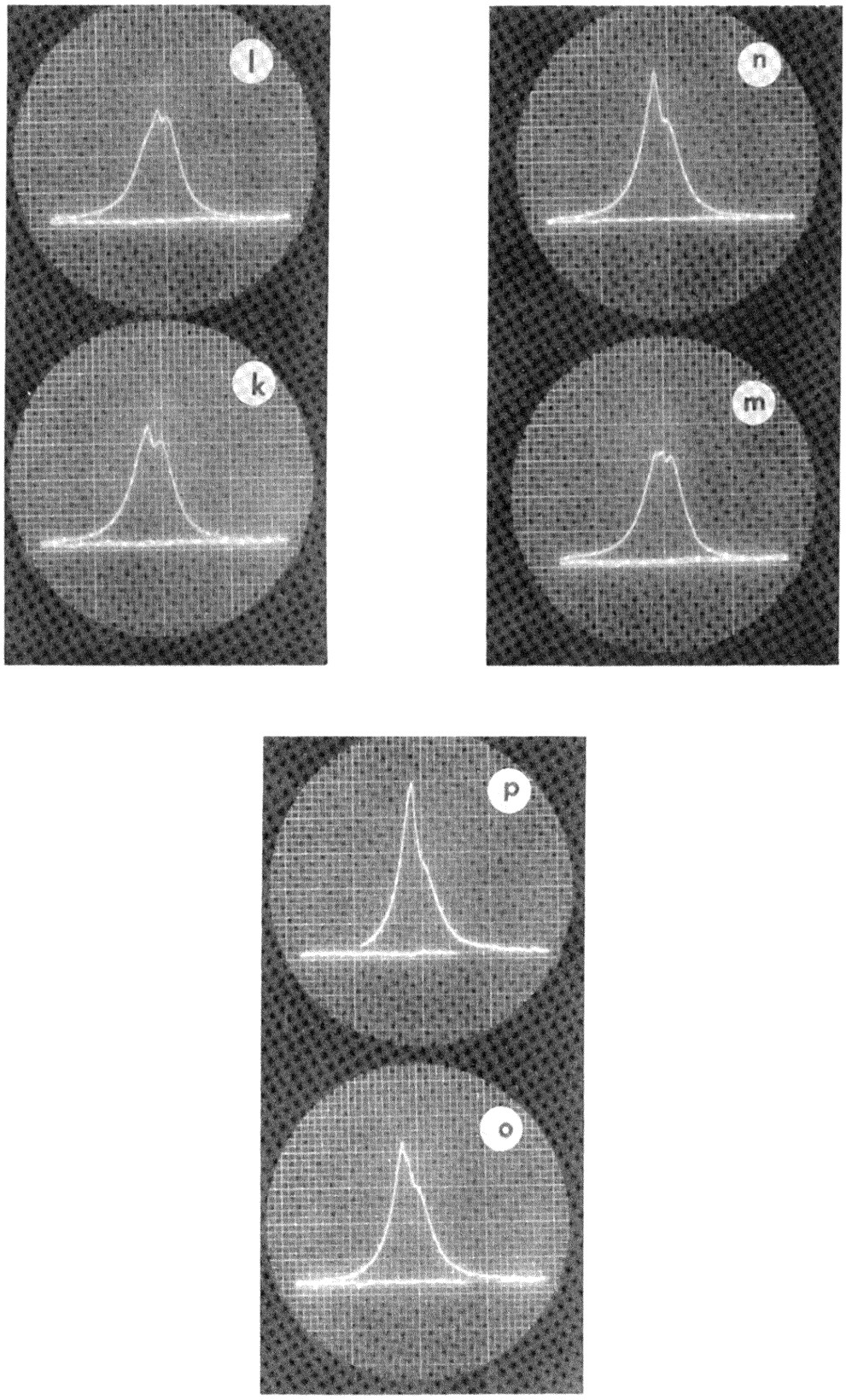

Figure 20. Contunued.

The decrease of the delay period and the increase of the reaction rate (combustion) that occurred in the test could permit a larger increase in speed of rotation of the engine than that actually used in this case (limited to engine safety condition) and it has been demonstrated that P.F. injection early in the cycle is one means of achieving the pre-flame reactions necessary for this.

Series VI. Runs at Different Main Fuel Injection Timing

At constant optimum engine conditions, series of runs at each main fuel injection time were carried out. The injection timing was altered by changing the clearance between the cam and the plunger follower. Although the acceleration behavior of the plunger is changed by the alteration of the clearance, because of the small range of clearance change (0.030"), this effect can be neglected.

Figure 21, to 24 and Tables X, XXXII to XL show the results of this series. For M.F. injection retarded to 9° B.T.C. the engine was not able to generate the 54.3 b.m.e.p. without P.F. injection, but as soon as a very small percentage of P.F. was injected it was easy for the engine to generate the load. This is due to earlier combustion and maximum pressure rise accompanied by an earlier end of the afterburning as indicated by the decrease of exhaust gas temperature. With P.F. injection the engine runs very smooth and the delay period was almost zero. Figure 25 shows the P-t diagrams for M.F. injection at 9° B.T.C.

At 14° B.T.C., the engine ran smooth and the delay period was very short. The engine was able to generate at this timing, with P.F. injection, 17.85% overload with 12% decrease in the b.s.f.c. and

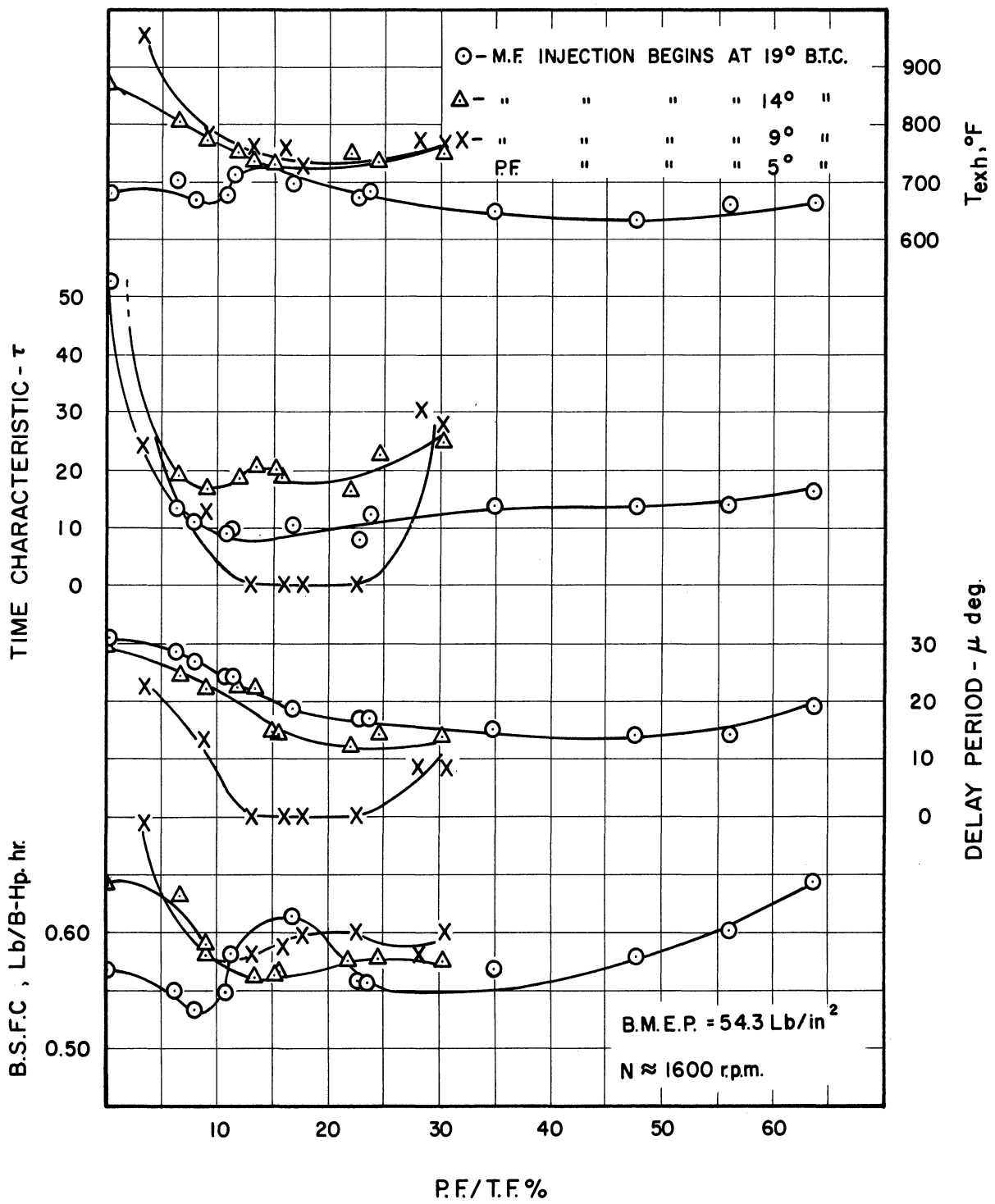

Figure 21. Effect of Main Fuel Injection Timing Upon Engine Performance. (Series VI).

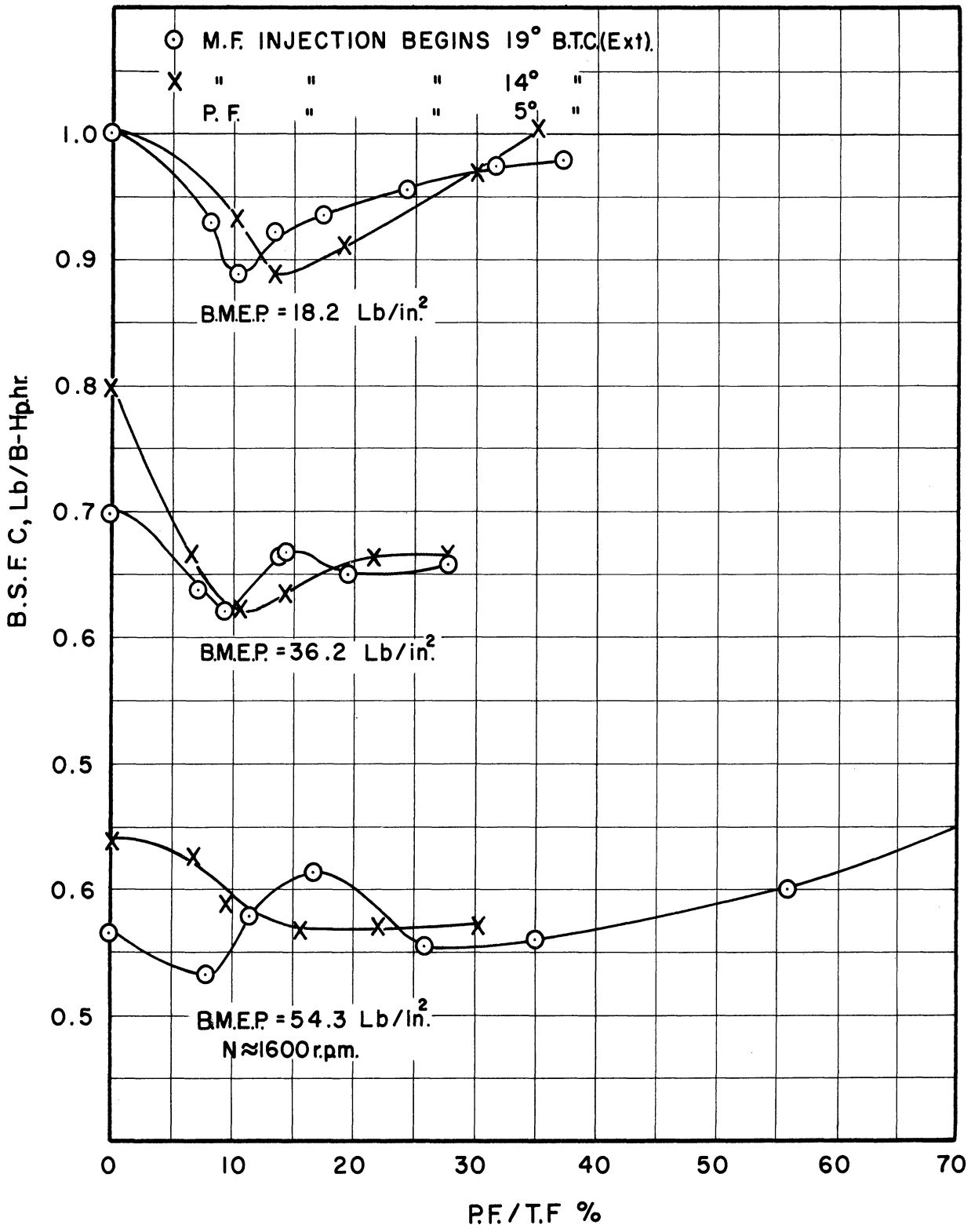

Figure 22. Effect of M.F. Injection Timing Upon B.S.F.C. (Series VI).

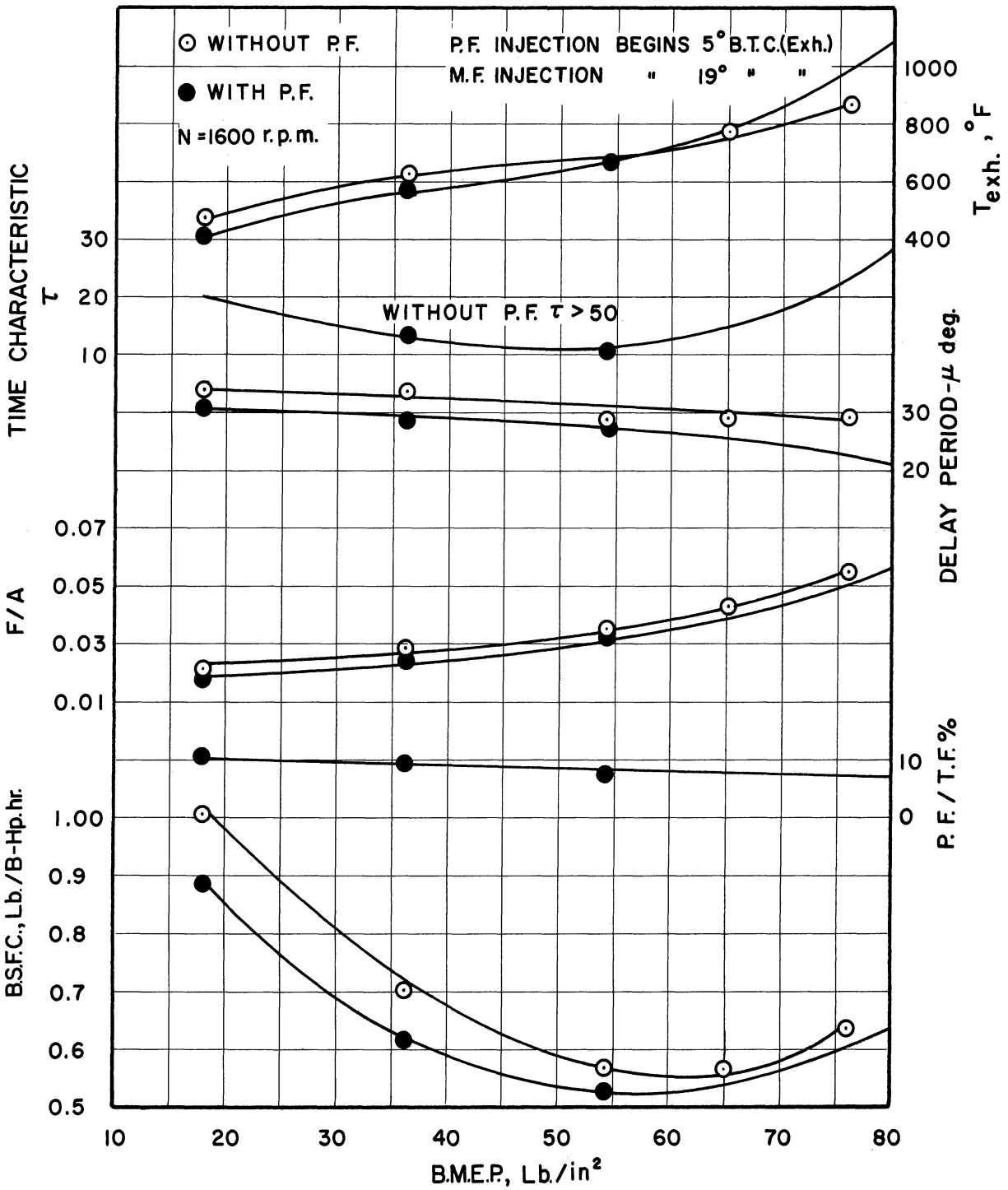

Figure 23. Effect of Primary Fuel Injection Upon Optimum Engine Performance. (Series VI).

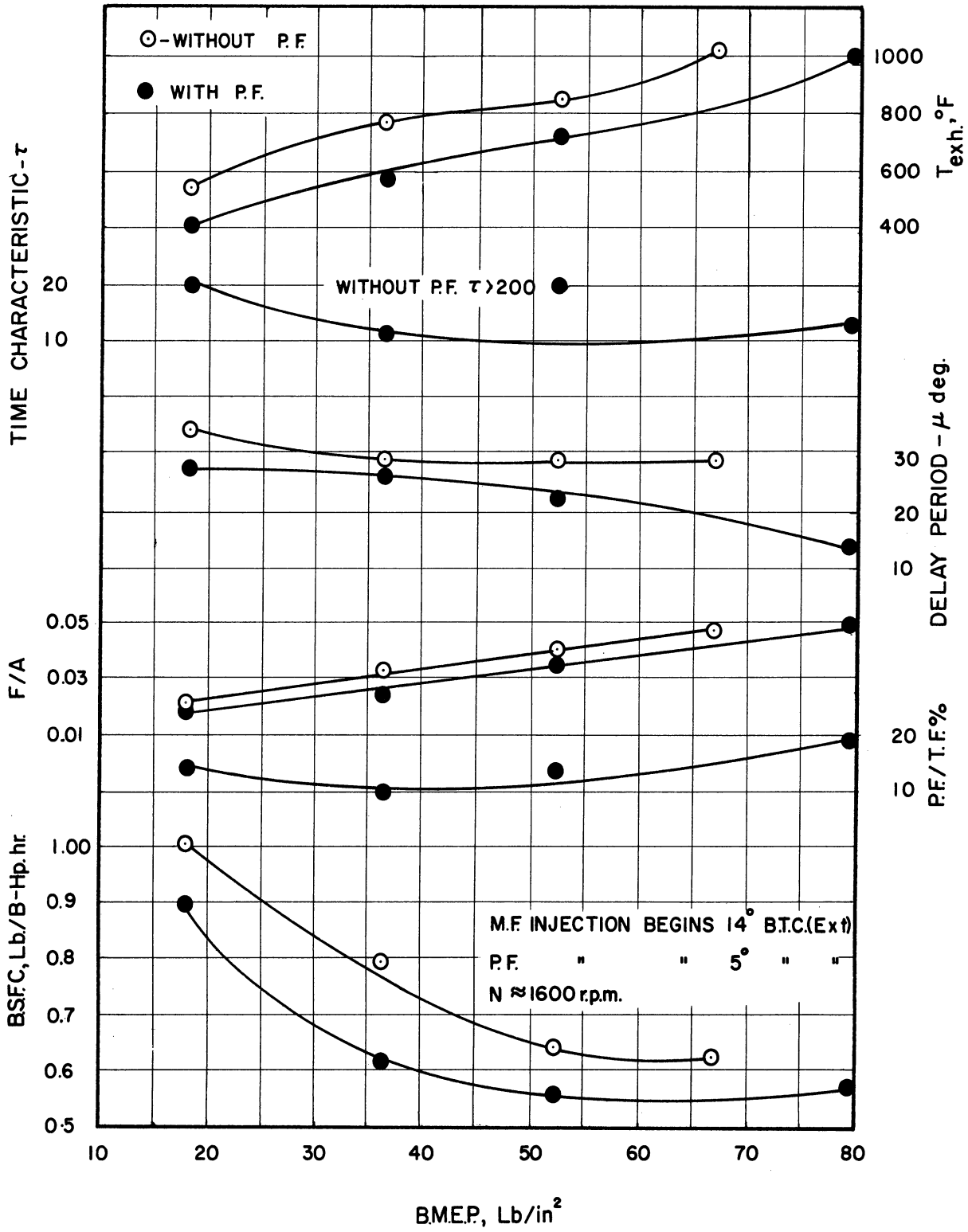

Figure 24. Effect of Primary Fuel Injection Upon Optimum Engine Performance. (Series VI).

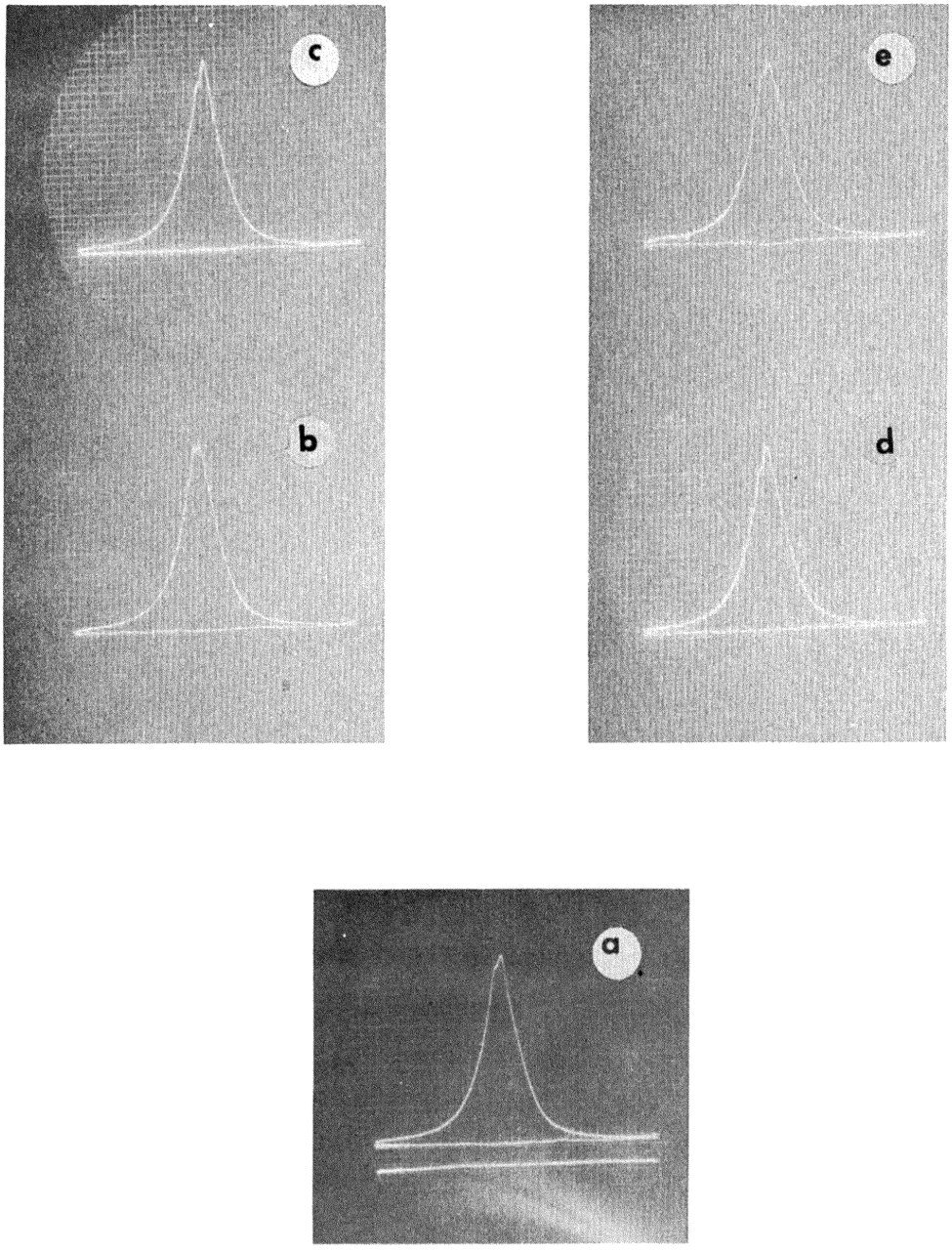

Figure 25. Pictorial Traces of Pressure-Time Diagrams (Series VI)

M.F. Injection Begins 9° B.T.C.
P.F. Injection Begins 5° B.T.C. [exhaust]
B.M.E.P. = 54.3 lb/in^2

	Run No.	P.F./T.F.%		Run No.	P.F./T.F.%
a	386	22.4	f	391	8.75
b	387	17.15	g	392	3.34
c	388	15.29	h	393	28.1
d	389	13	i	394	30.4
e	390	12.65	j	395	0 (B.M.E.P. = 45.6 lb/in^2)

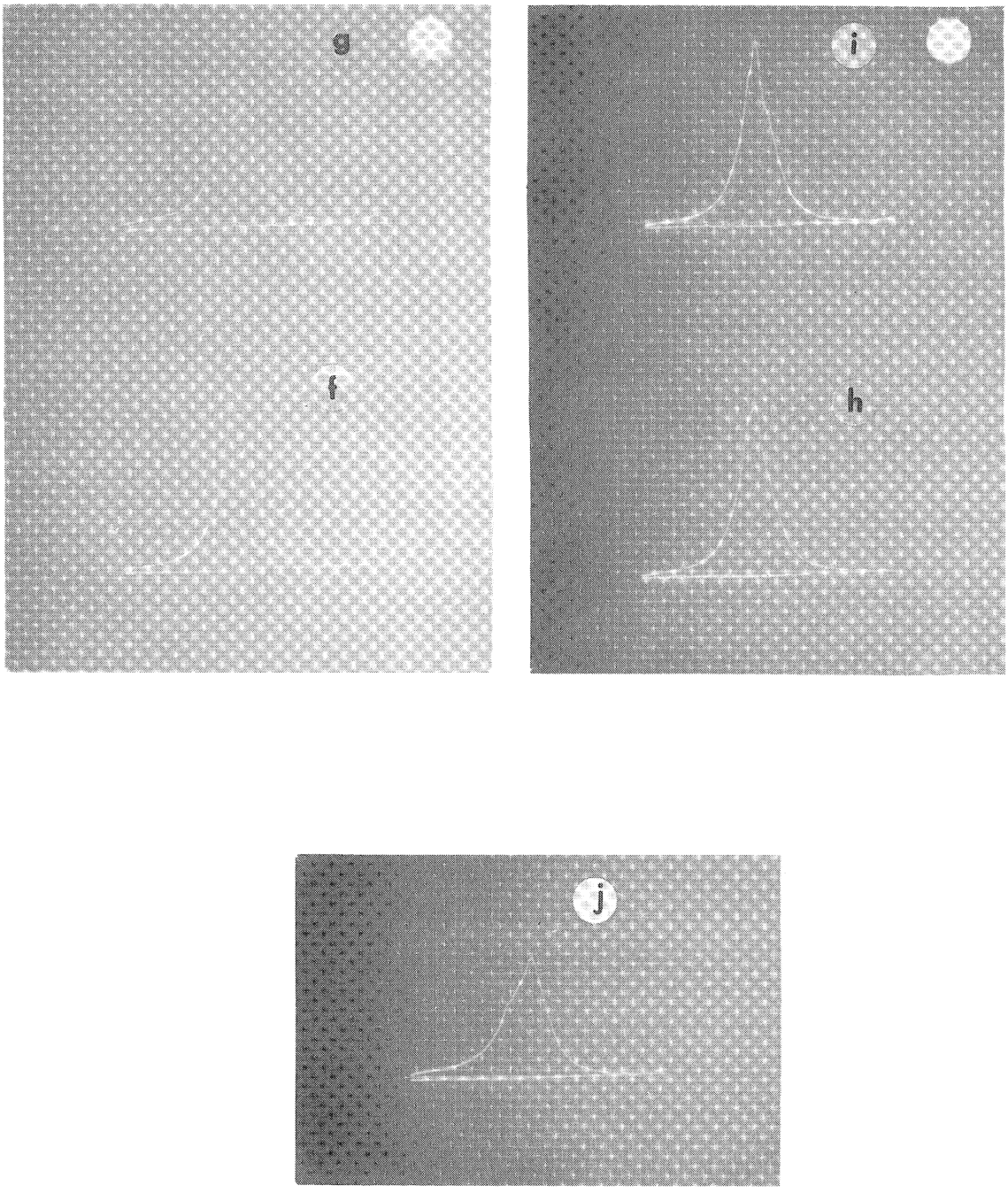

Figure 25. Continued.

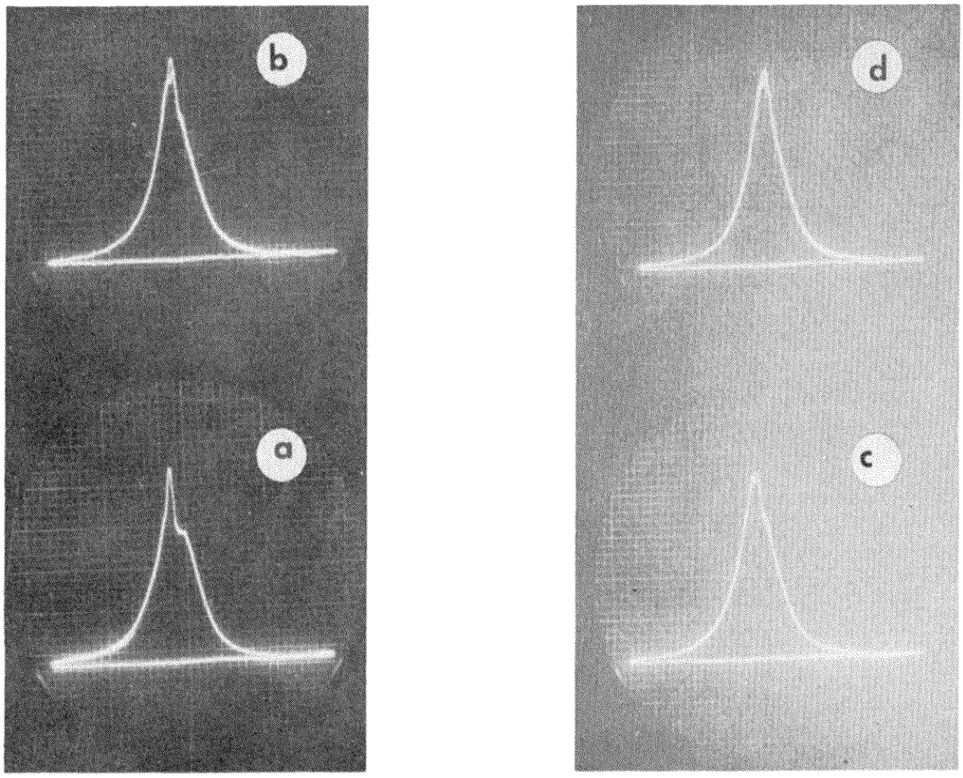

Figure 26. Pictorial Traces of Pressure-Time Diagrams (Series VI).

M.F. Injection Begins 14° B.T.C.
P.F. Injection Begins 5° B.T.C. [exhaust]
B.M.E.P. = 54.3 lb/in^2

	Run No.	P.F./T.F.%		Run No.	P.F./T.F.%
a	412	6.45	e	416	21.8
b	413	8.92	f	417	15.23
c	414	13.45	g	418	24.58
d	415	15.65	h	419	30.1

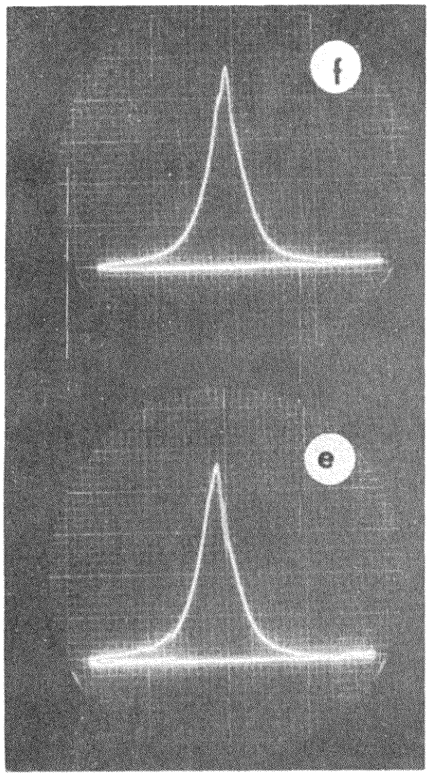

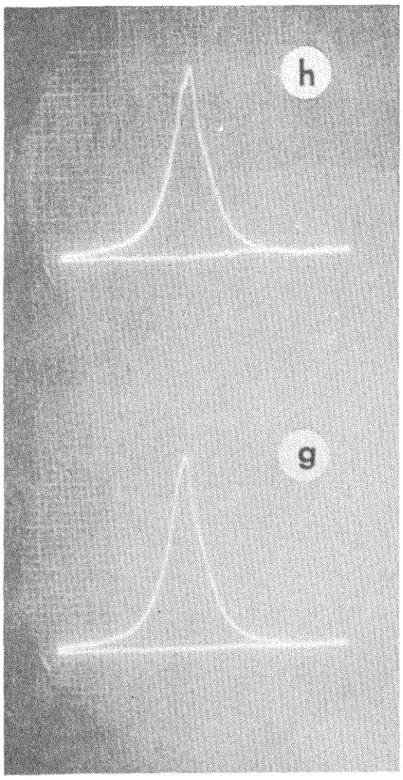

Figure 26. Continued.

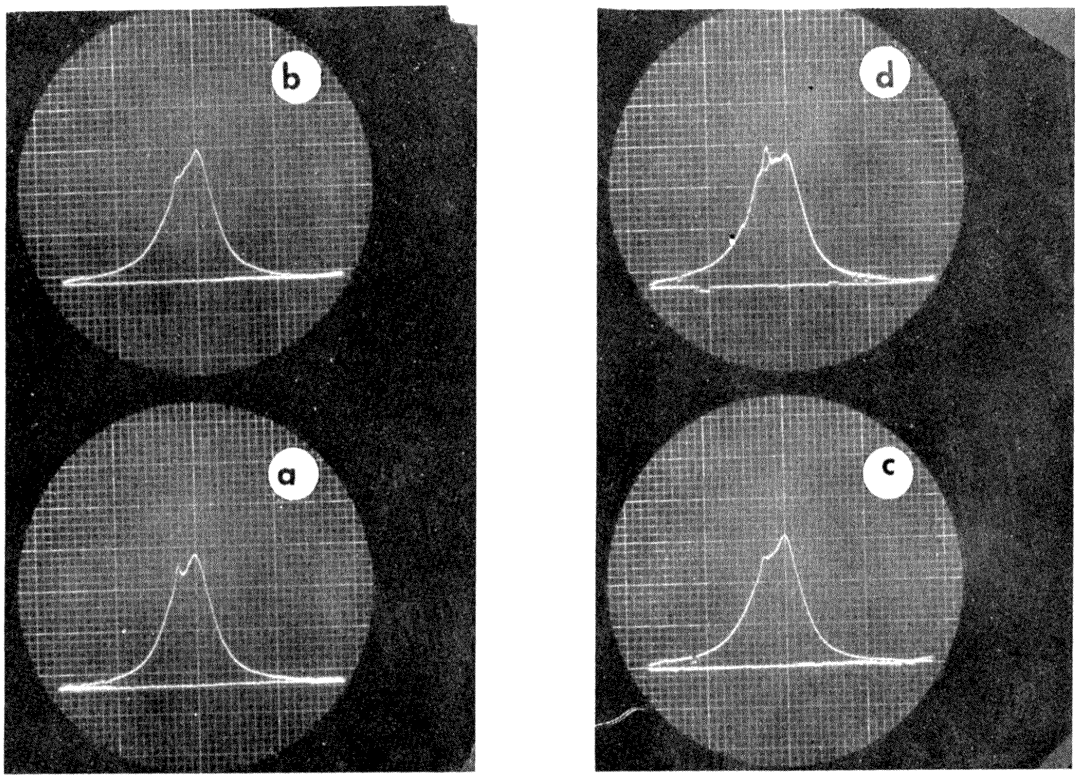

Figure 27. Pictorial Traces of Pressure-Time Diagrams (Series VI).

M.F. Injection Begins 14° B.T.C.
P.F./T.F.% = 0

	Run No.	B.M.E.P.
a	396	18.1
b	397	36.2
c	398	54.3
d	399	66.9

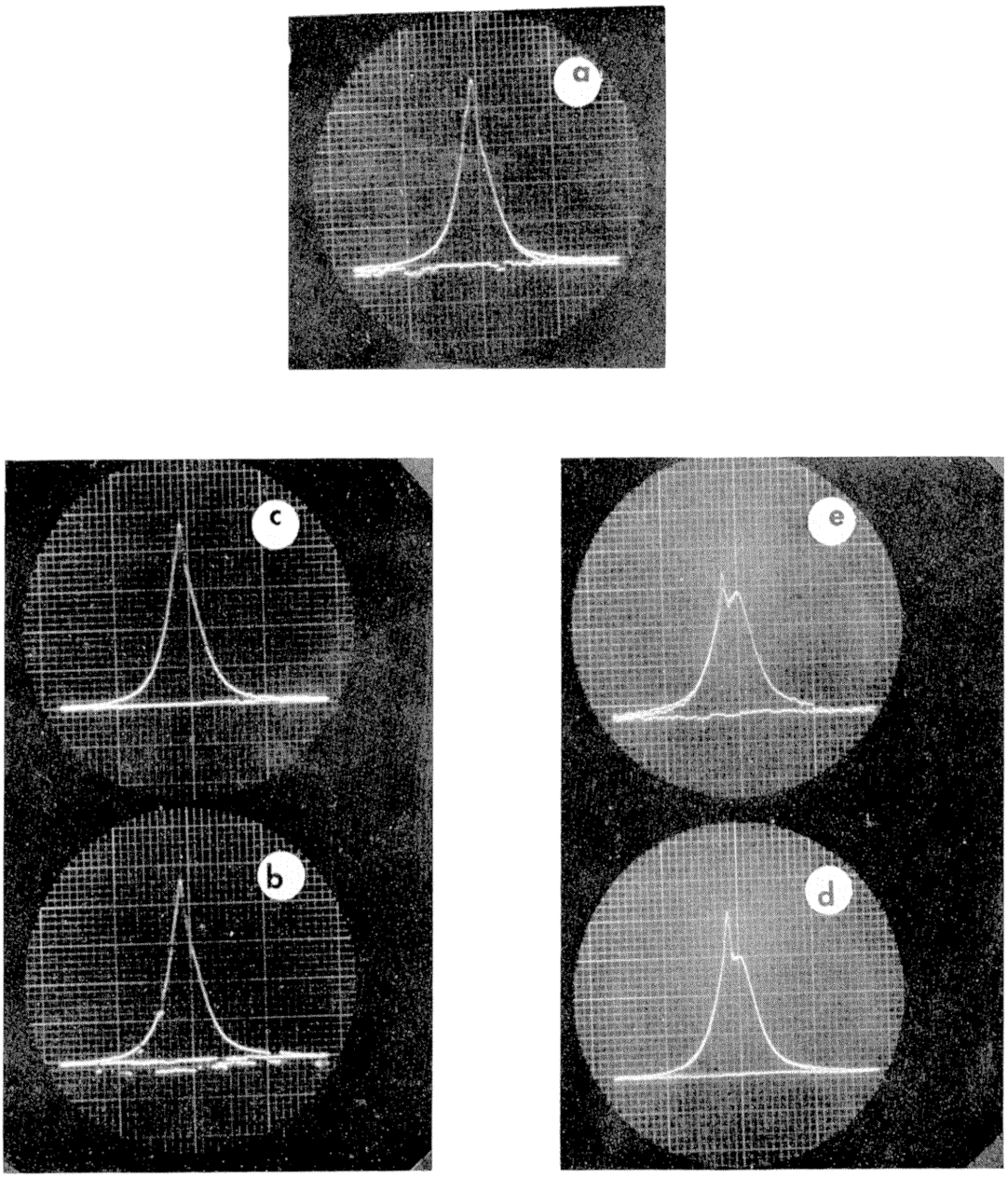

Figure 28. Pictorial Trace of Pressure-Time Diagrams (Series VI).

M.F. Injection Begins 14° B.T.C.
P.F. Injection Begins 5° B.T.C.
B.M.E.P. = 18.1

	Run No.	P.F./T.F.%		Run No.	P.F./T.F.%
a	400	35.3	d	403	13.85
b	401	35	e	404	10.1
c	402	19.35			

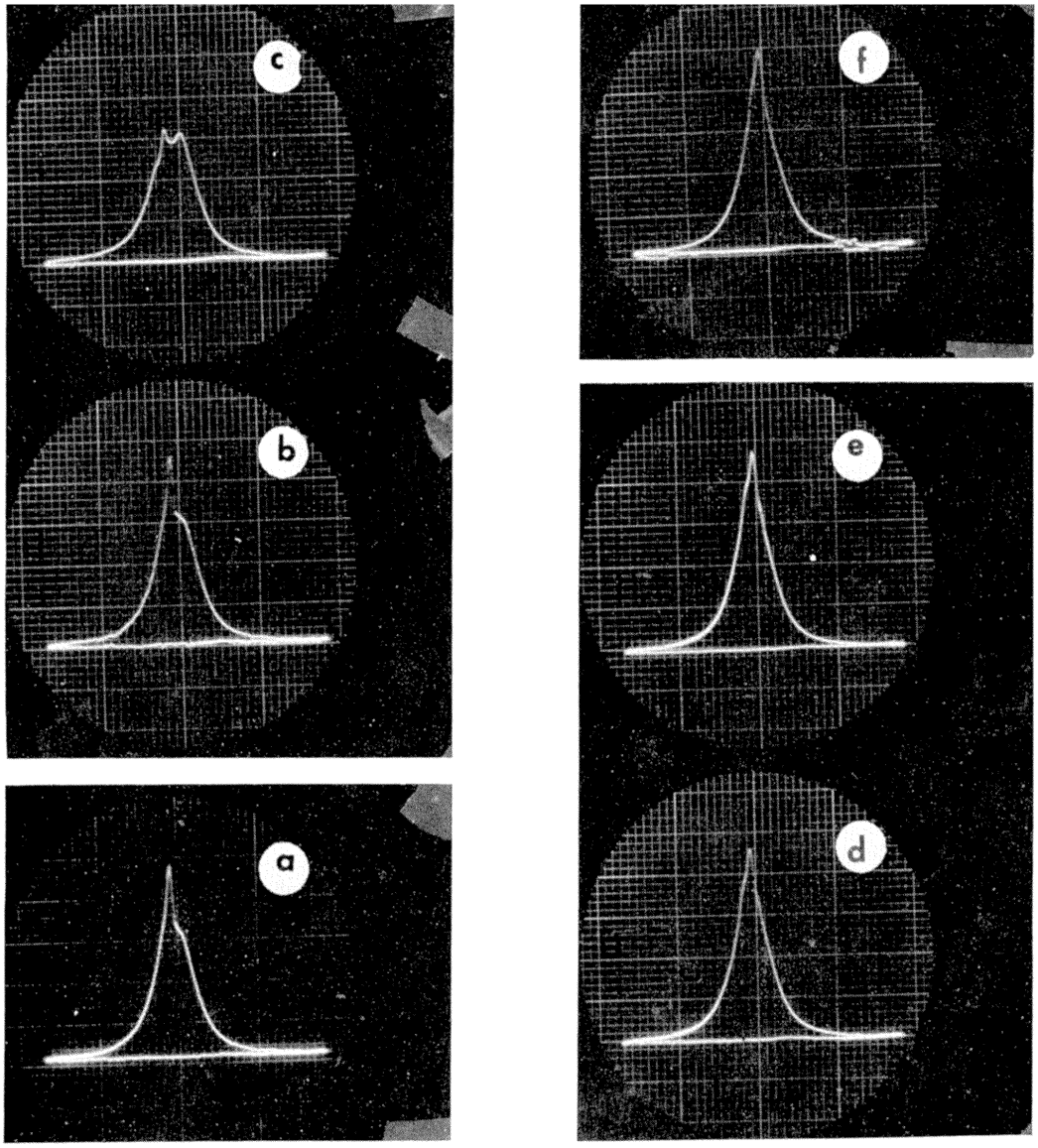

Figure 29. Pictorial Trace of Pressure-Time Diagrams (Series VI).

M.F. Injection Begins 14° B.T.C.
P.F. Injection Begins 5° B.T.C. [exhaust]
B.M.E.P. = 36.2

	Run No.	P.F./T.F.%		Run No.	P.F./T.F.%
a	405	14.25	d	408	16
b	406	9.99	e	409	21.5
c	407	6.45	f	410	27.9

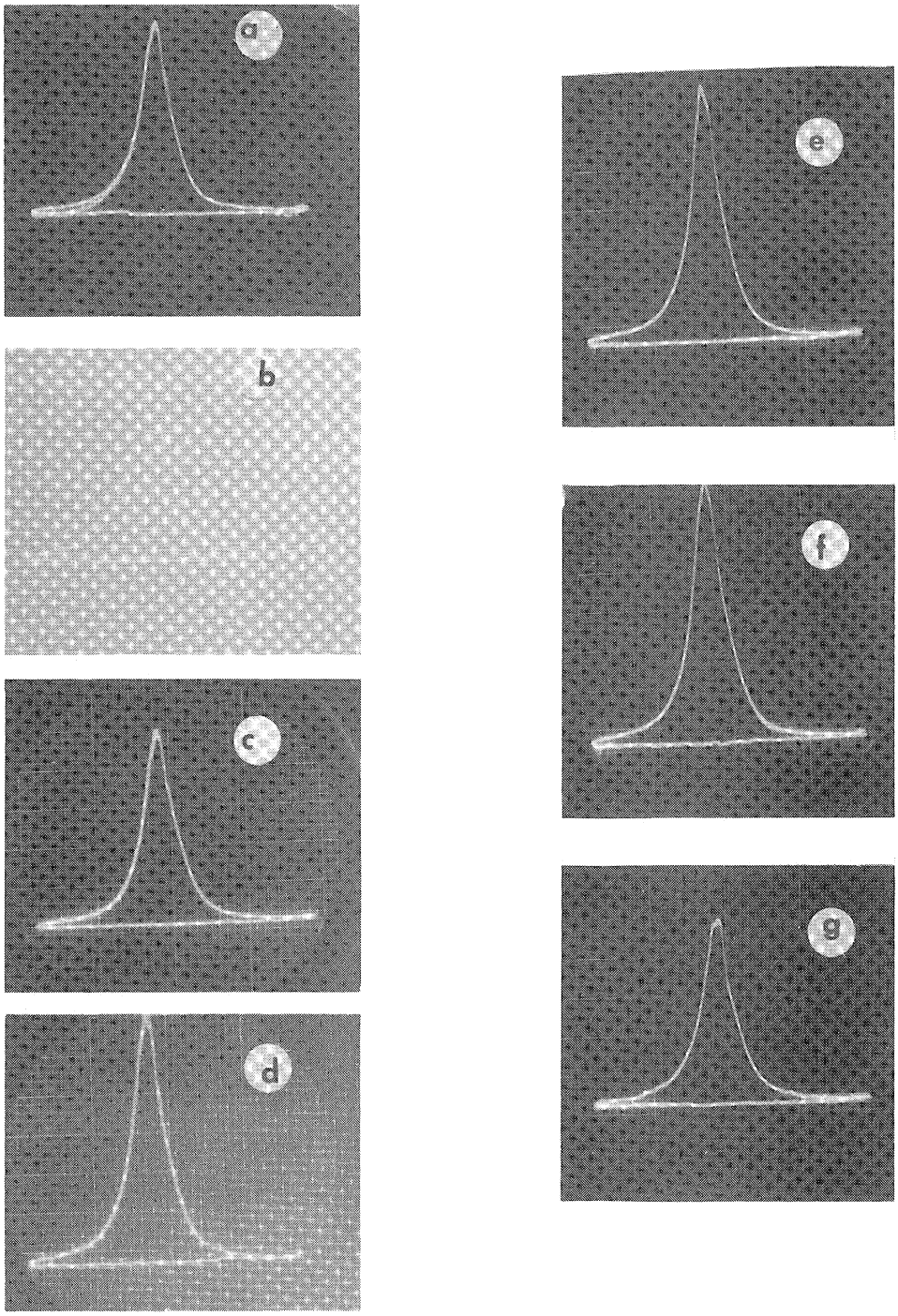

Figure 30. Pictorial Trace of Pressure-Time Diagrams, Maximum Loading (Series VI).

M.F. Injection Begins 14° B.T.C.
P.F. Injection Begins 5° B.T.C. [exhaust]

	Run No.	P.F./T.F.%	B.M.E.P.		Run No.	P.F./T.F.%	B.M.E.P.
a	420	7.89	74.2	e	424	16.25	77.7
b	421	3.87	69.6	f	425	18.6	79.6
c	422	8.13	72.4	g	426	19.8	79.6
d	423	11.85	76				

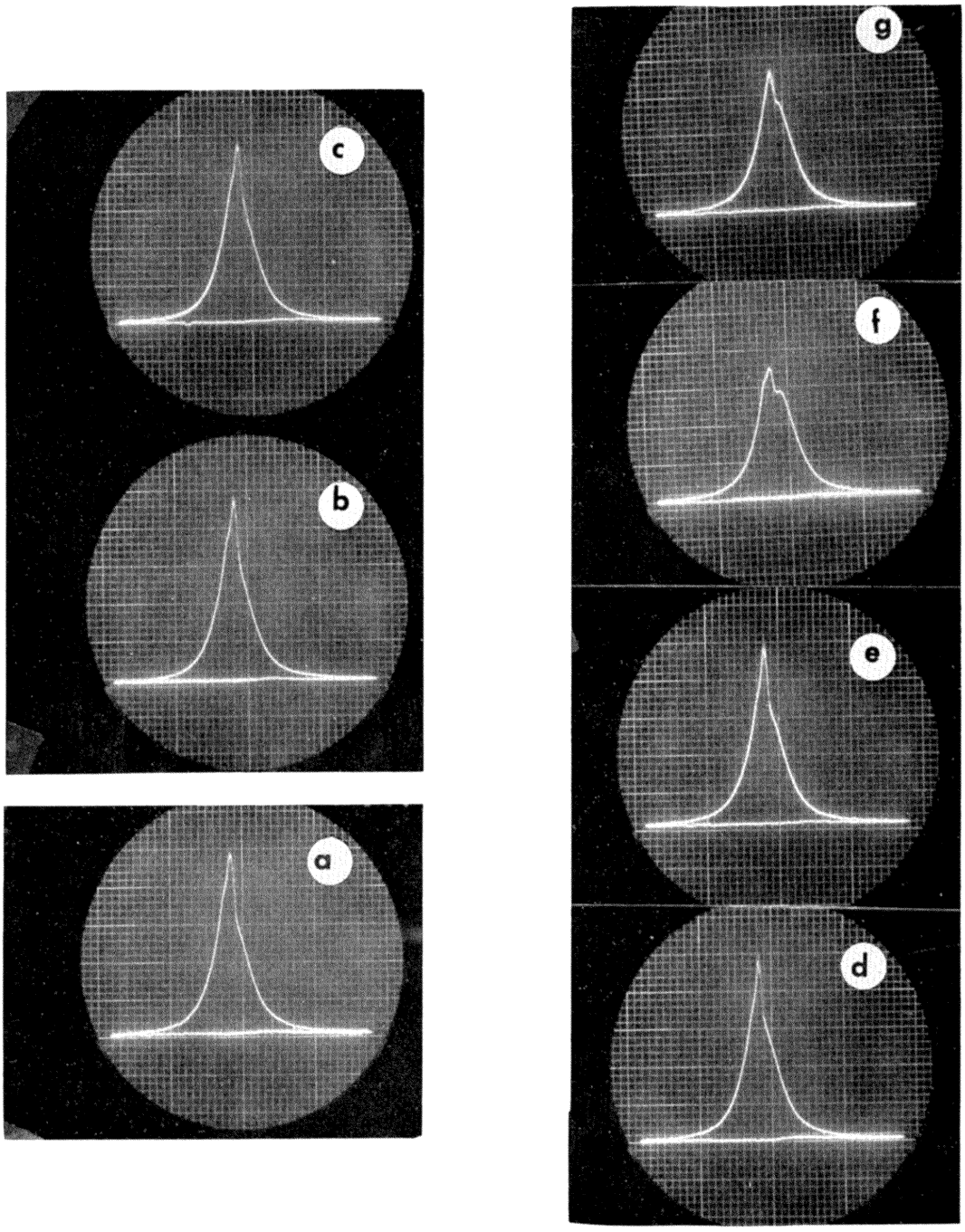

Figure 31. Pictorial Traces of Pressure-Time Diagrams (Series VI).

M.F. Injection Begins 19° B.T.C.
P.F. Injection Begins 5° B.T.C.
B.M.E.P. = 18.1 lb/in^2

	Run No.	P.F./T.F.%		Run No.	P.F./T.F.
a	427	37.3	e	430	17.6
b	428	31.9	f	431	13.5
c	429	24.41	g	432	10.55

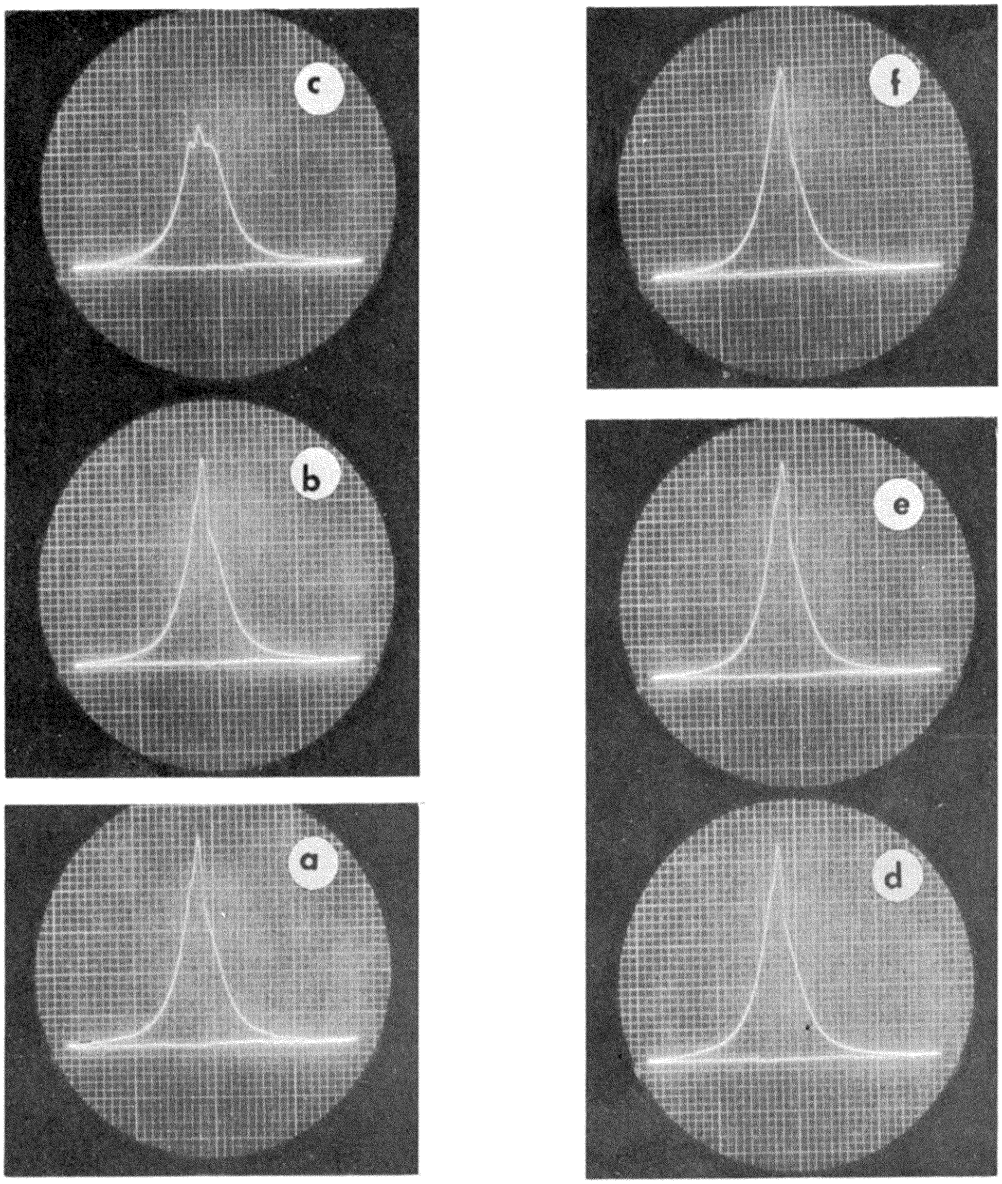

Figure 32. Pictorial Traces of Pressure-Time Diagrams (Series VI).

M.F. Injection Begins 19° B.T.C.
P.F. Injection Begins 5° B.T.C.
B.M.E.P. = 36.2 lb/in^2

	Run No.	P.F./T.F.%		Run No.	P.F./T.F.%
a	434	14.31	d	437	13.9
b	435	9.25	e	438	19.6
c	436	7.74	f	439	27.8

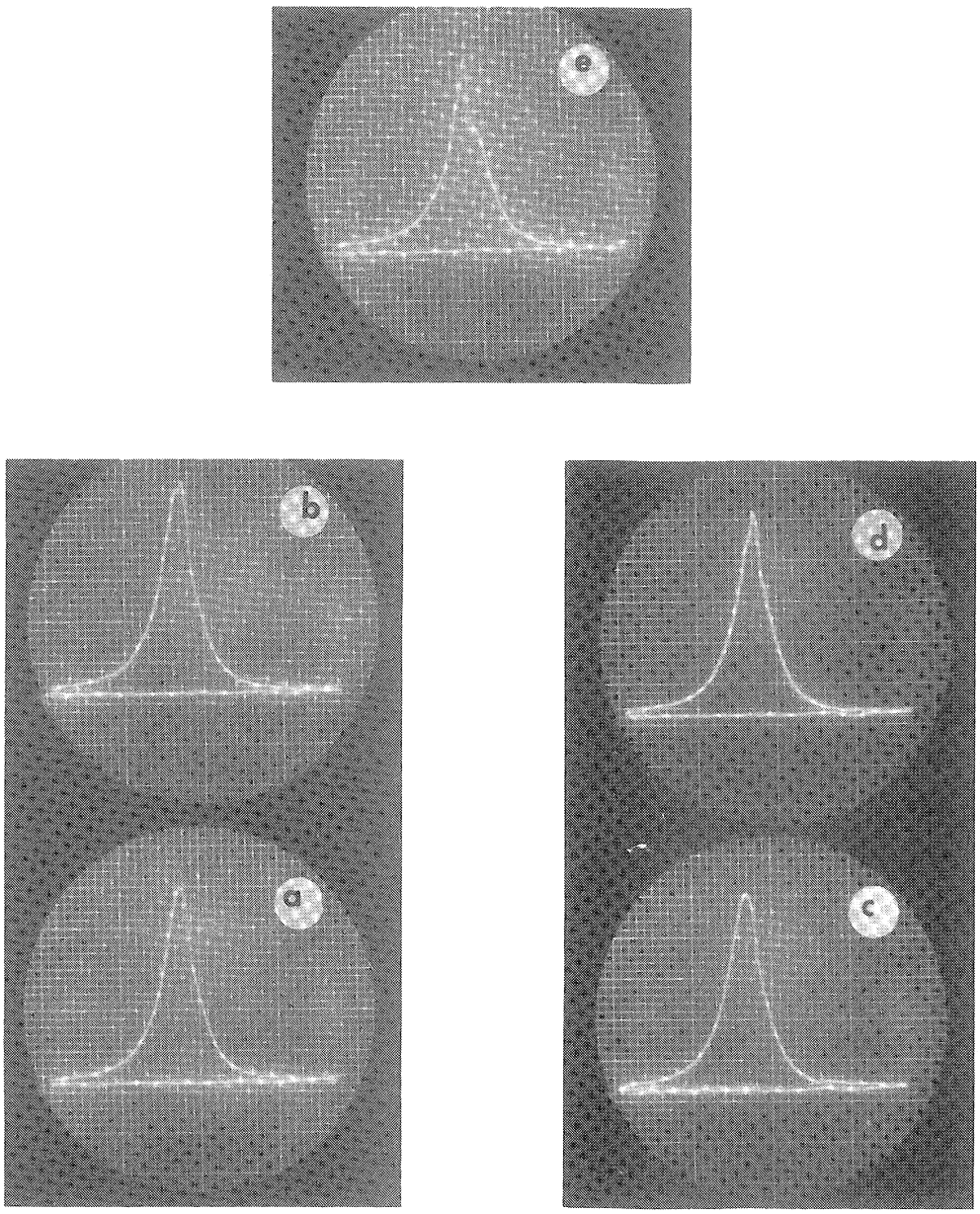

Figure 33. Pictorial Traces of Pressure-Time Diagrams, Maximum Loading (Series VI).

M.F. Injection Begins 19° B.T.C.
P.F. Injection Begins 5° B.T.C.

	Run No.	P.F./T.F.%	B.M.E.P.
a	440	15	76
b	441	17.85	78.6
c	442	7.55	82.2
d	443	5.15	76.9
e	444	3.5	72.4

6.97% decrease in the exhaust gases temperature (73°F). A decrease in the b.s.f.c. was noticed, over the whole range, when injecting the P.F., although the usual wavy curve still existed. The b.s.f.c. was lower within the range of 11 to 24% of P.F./T.F.% compared with the case of main injection at 19° B.T.C. Figure 24 shows the performance curves and Figures 26 to 30 show the P-t diagrams of the load range. The results are given in Tables XXXIII to XXXVII.

Series VII. Runs With Additive

Cumene hydroperoxide is known as a fast chain initiator, then its effect in shortening the delay period is a solid proof that the ignition of diesel fuel is of chain character.

A mixture of 1% by volume of cumene hydroperoxide in diesel fuel was used to investigate its effect and support the theoretical analysis.

Without P.F. injection and with diesel fuel-cumene hydroperoxide mixture as M.F., the delay period was shortened (μ was 24° as compared to 32° in case of no additive). This result substantiates the theory given before.

Table XLI shows the results and Figure 34 shows the P-t diagrams of this series.

Series VIII. Runs With Variation of Energy-Cell Throat Diameter*

The energy cell throat area was increased by 72%. The general b.s.f.c. was increased, but its minimum value was found to have shifted to about 25% of P.F./T.F. The engine runs smoother and the delay period

* $d_1 = 0.1495$ in., $A_1 = 0.01755$ in.^{2}
$d_2 = 0.196$ in., $A_2 = 0.030171$ in.

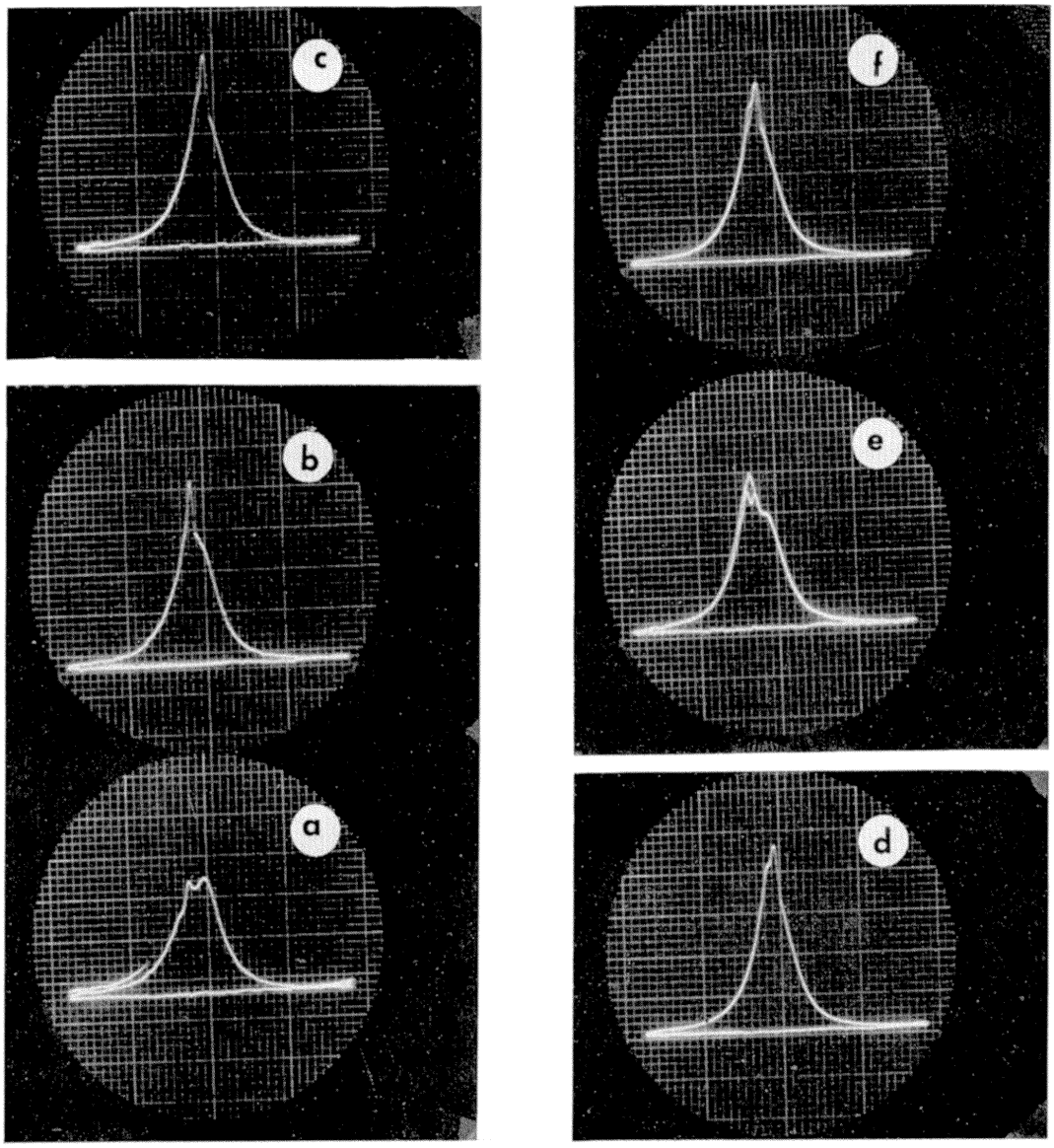

Figure 34. Pictorial Traces of Pressure-Time Diagrams, Additive Effect (Series VII)

M.F. Injection Begins 19° B.T.C.
P.F. Injection Begins 5° B.T.C.
B.M.E.P. = 54.3 lb/in^2

	Run No.	P.F./T.F.%	Additive P.F.	Additive M.F.
a	445	0	-	No
b	446	13.1	No	No
c	447	12.7	Yes	No
d	448	13.2	Yes	Yes
e	449	0	-	Yes
f	450	12.1	No	Yes

and $T_{exh.}$ are lower than that of the smaller throat area, but τ was larger. The relatively higher τ explains the smooth running conditions of the larger throat area.

There is a possibility of optimum throat area corresponding to primary injection timing and pressure which needs further investigation. By increasing the throat area, the energy cell surface area increased also. It is the surface which is responsible for chain termination, that is, the larger the surface the slower the chain propagation, which results in lower rate of reaction as seen from the higher τ.

Figure 35 shows the performance curves, Figure 36 shows the P-t diagrams, and Table XLII shows the test results of this series of runs.

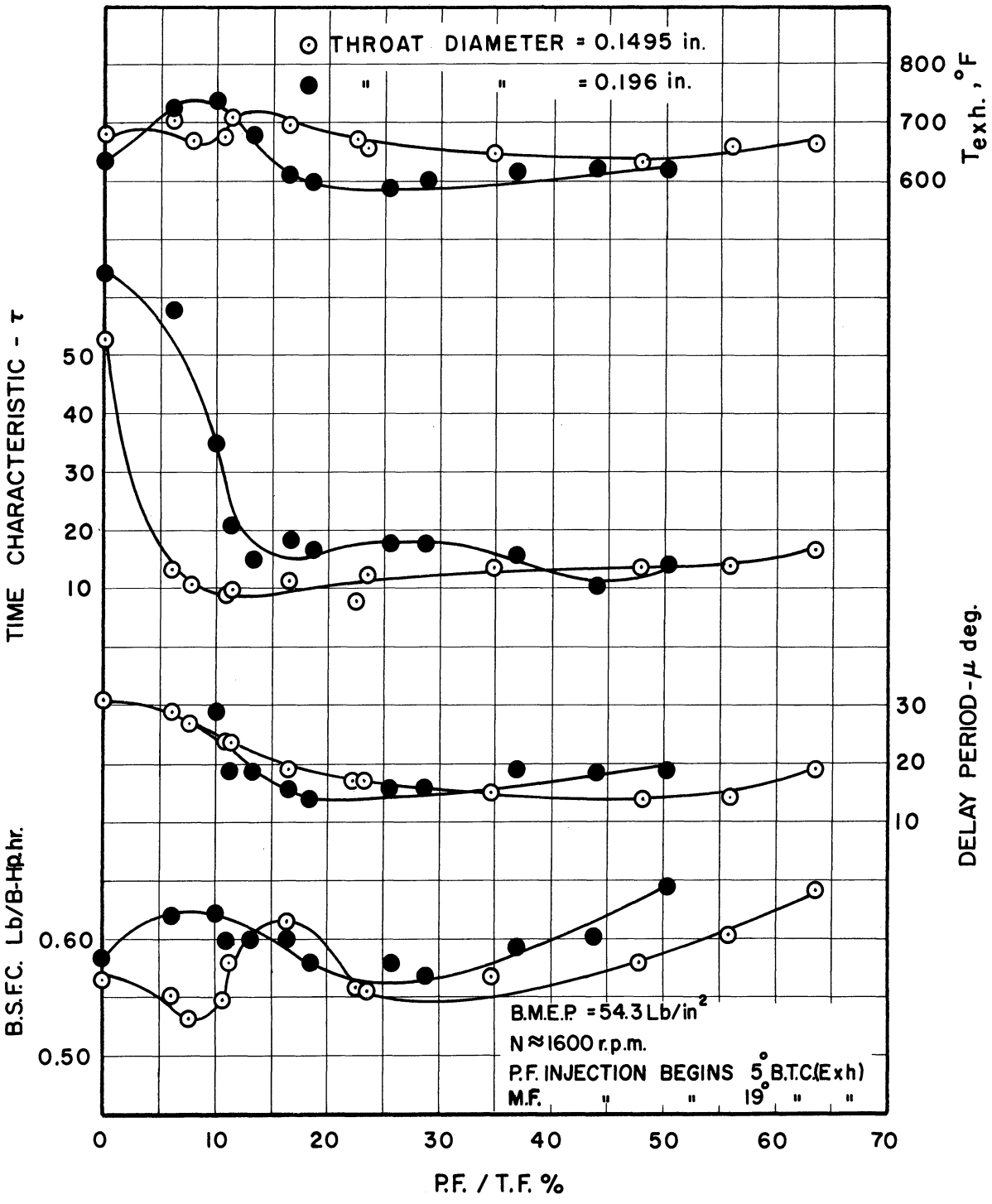

Figure 35. Effect of Energy-Cell Throat Diameter Upon Engine Performance. (Series VIII)

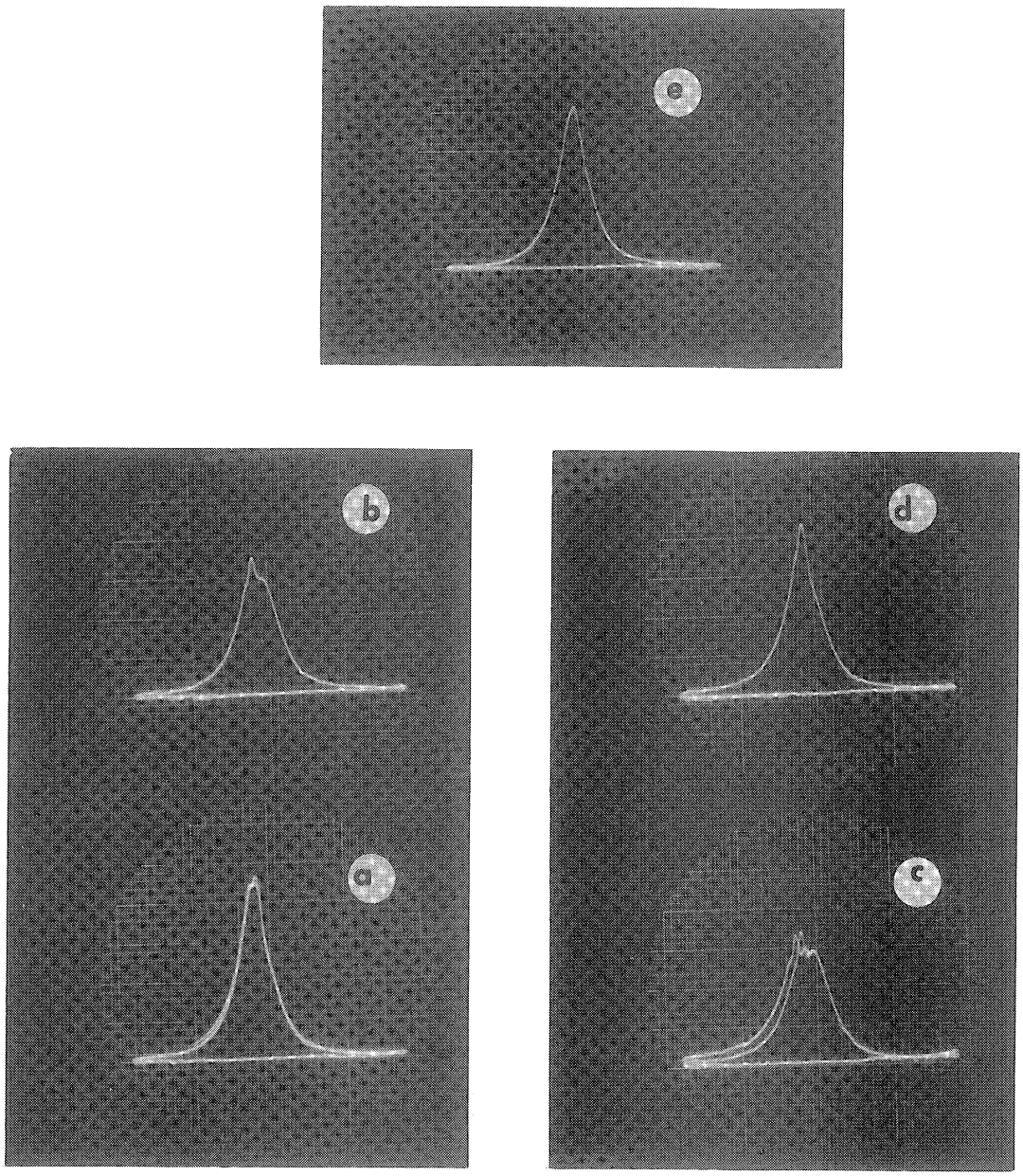

Figure 36. Pictorial Traces of Pressure-Time Diagrams (Series VIII)

Throat Diameter = 0.196
M.F. Injection Begins 19° B.T.C.
P.F. Injection Begins 5° B.T.C.
B.M.E.P. = 54.3 lbs/in^2

	Run No.	P.F./T.F.		Run No.	P.F./T.F.
a	451	13.45	g	457	25.6
b	452	10.1	h	458	28.9
c	453	6.05	i	459	37
d	454	11.3	j	460	44
e	455	16.6	k	461	50.4
f	465	18.65	l	462	0

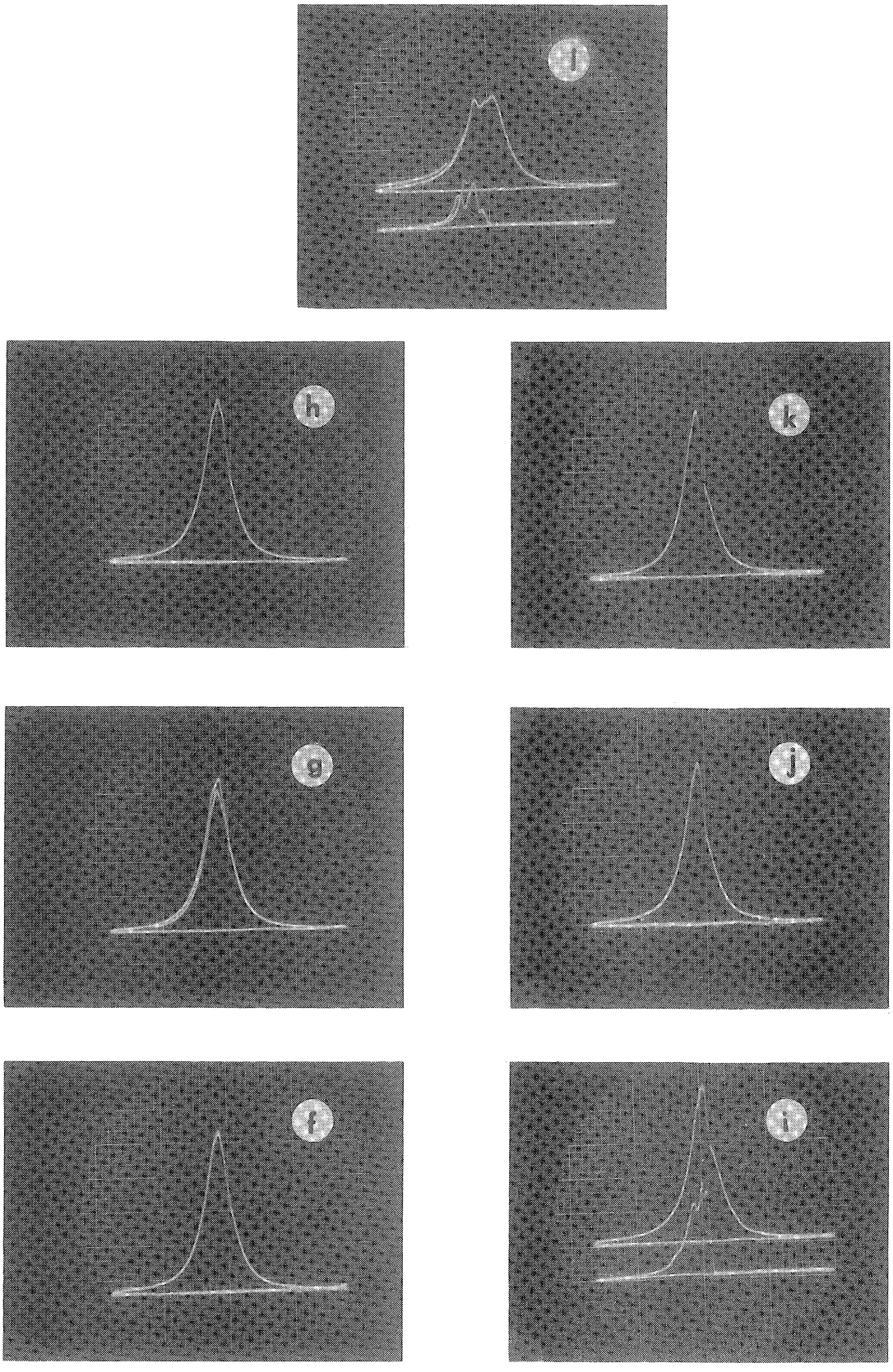

Figure 36. Continued.

VIII. GENERAL DISCUSSION

Figures 37, 38, and 39 show the P-t, P-v and log P-log v diagrams respectively. The superimposed diagrams represent the fuel air standard cycle considering the cooling losses, the actual cycle without P.F. (run 3), actual cycle for minimum fuel consumption (run 190), and actual cycle for minimum delay period (run 192). The corresponding oscilloscope pictoral traces are shown in Figure 37. The standard air fuel cycle was chosen to have the same initial condition and the same maximum pressure rise and F/A equal to that of run 3.

The negative work on the piston during the compression stroke of the standard cycle is smaller than the actual cycles due to the irreversibility of the compression process of the actual cycles. Due to the longer afterburning in run 3, the engine runs on the average at higher temperature, which causes the negative work to be higher in this case (afterburn for run 3 is up to 110° A.T.C. as compared to 80° A.T.C. in run 192). Figure 37a and 37c, the lower traces, show the flame intensity inside the cylinder.

With P.F. injected in any ratio, the ignition was almost at constant volume which increases the efficiency and improves the thermodynamic cycle at any P.F./T.F.%. But also with higher P.F./T.F.% the maximum pressure rise is higher and sudden which increases the cooling losses during the combustion process. With the maximum pressure rise occurring at 22° A.T.C. (run 190) the efficiency was maximum, but the maximum pressure and temperature were less than run 192, which favors the efficiency due to less cooling losses and dissociation. The solution of the air fuel standard cycle is shown in Appendix VI.

The photoelectric-cell was not able to detect the light of the cool flames. The beginning of the ignition (hot flames) coincided with the beginning of the sudden pressure rise. The log log diagrams (Figure 40) show that considerable reaction took place earlier than the point of sudden pressure rise and this can be explained that the cool flame reactions are taking place.

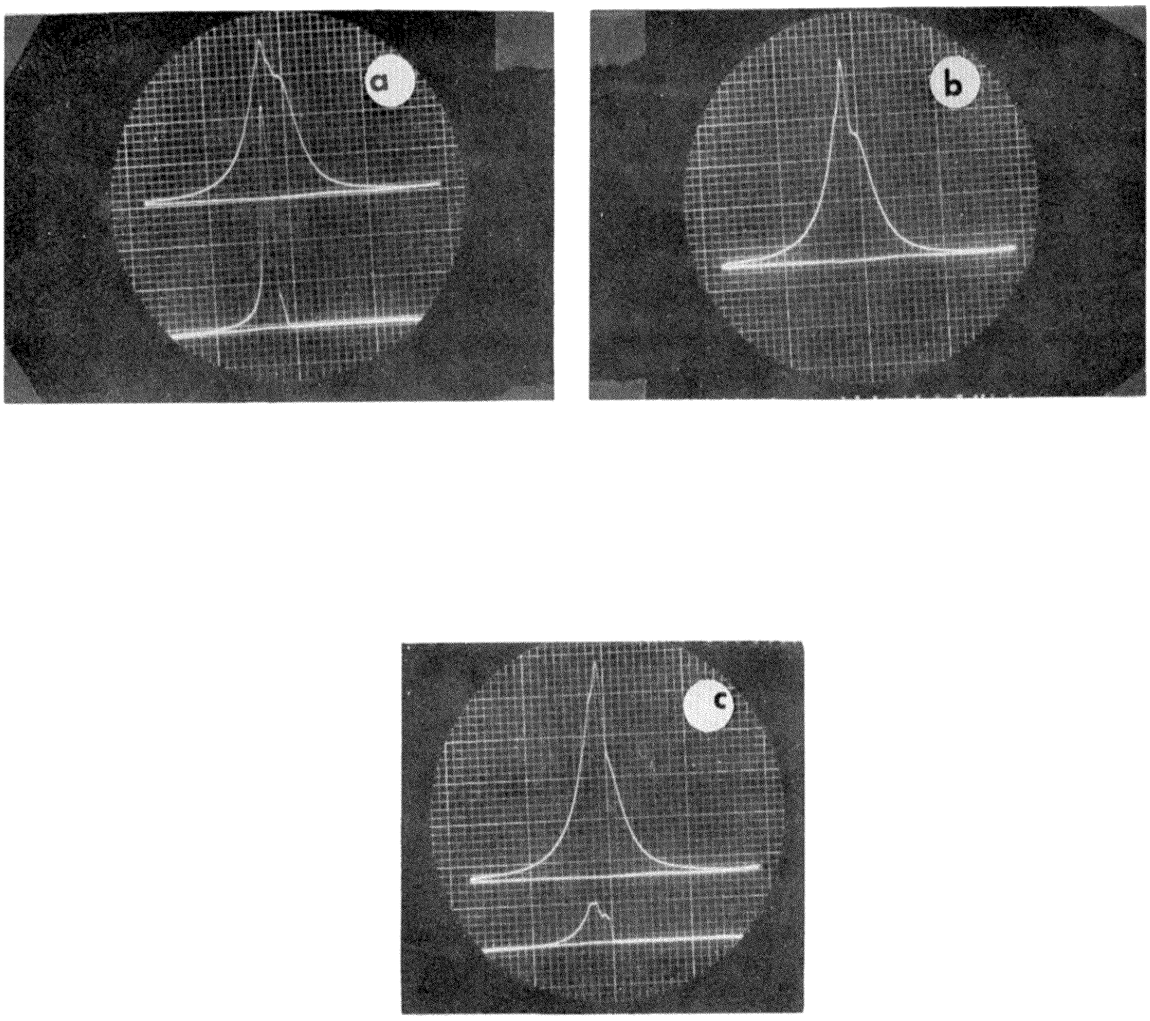

Figure 37. Pictorial Traces of Pressure-Time Diagrams (Lower Traces Show Flame Intensity).

B.M.E.P. = 54.3

	Run No.	P.F./T.F.	μ	B.S.F.C.
a	3	0	29	0.567
b	190	6.64	27	0.582
c	192	20.1	17	0.595

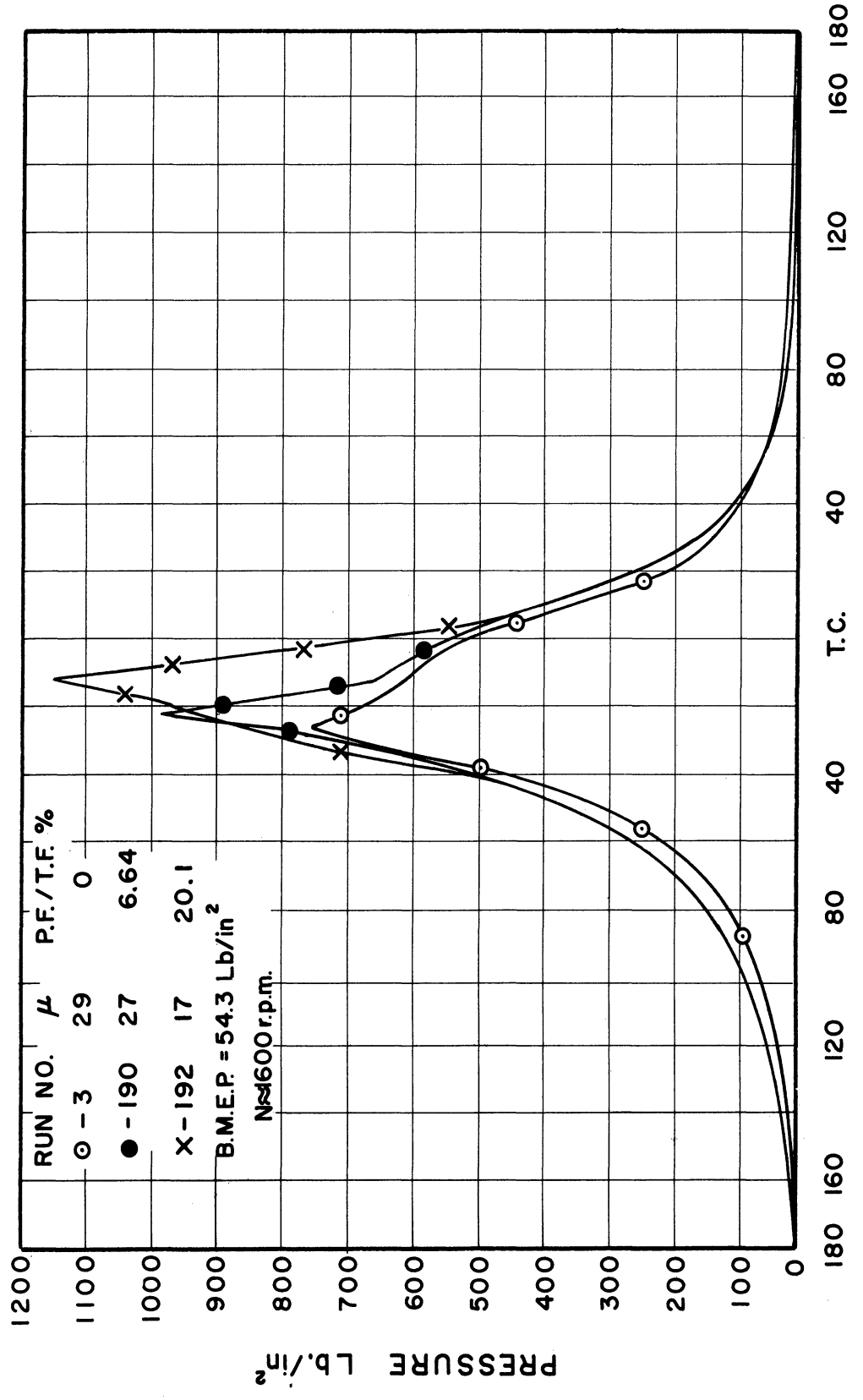

Figure 38. Pressure-Time Diagrams.

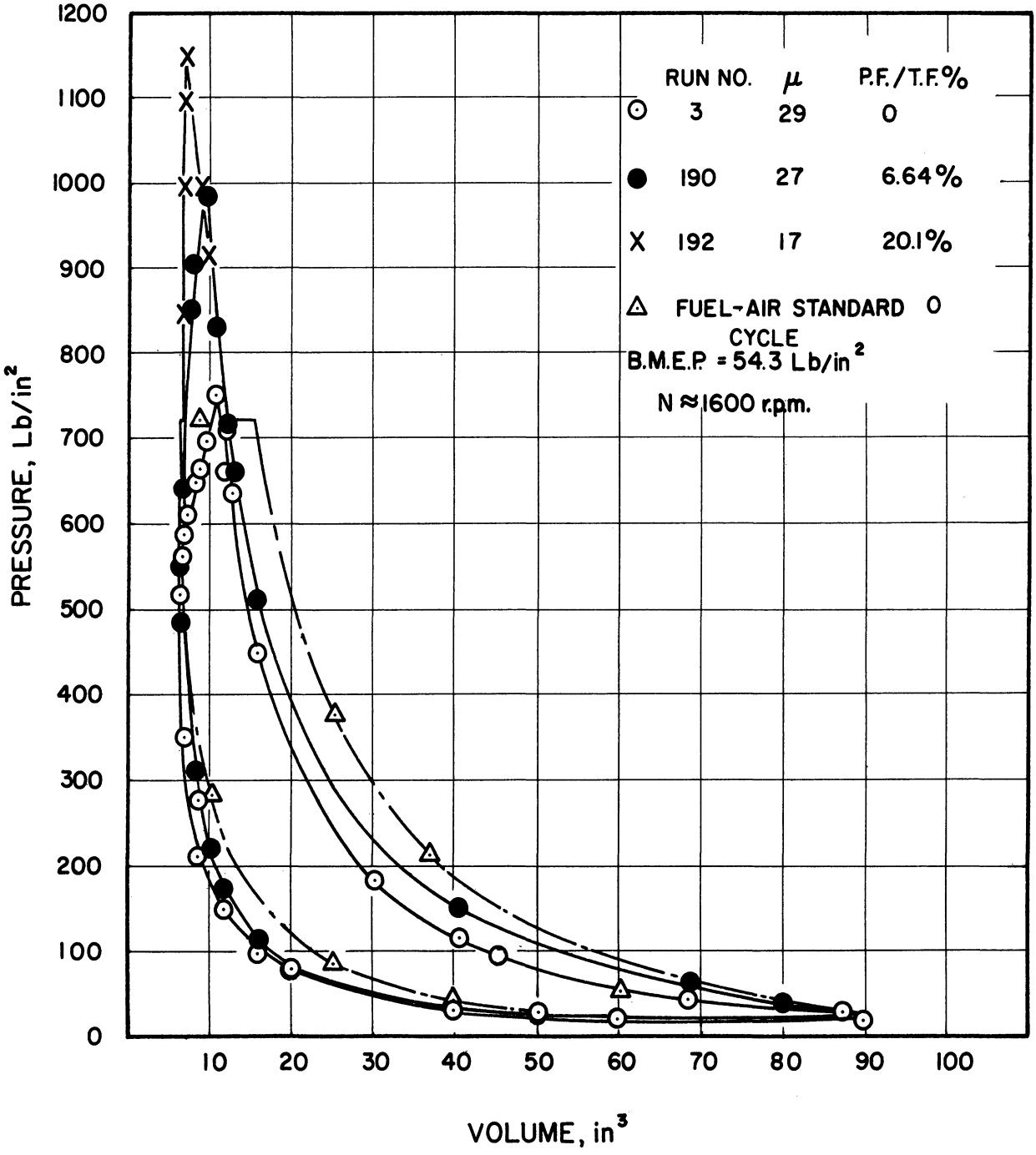

Figure 39. Pressure-Volume Diagrams.

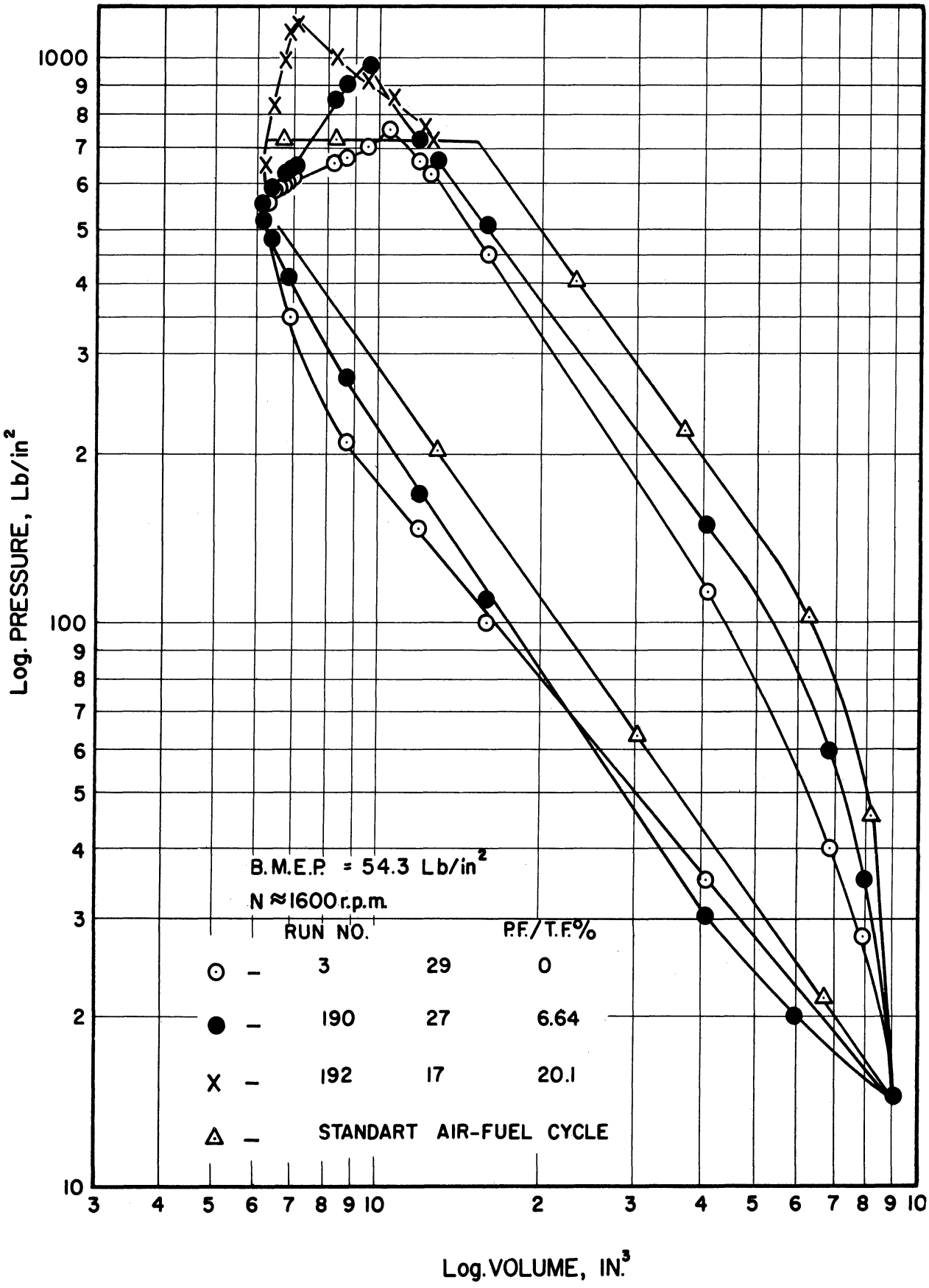

Figure 40. Log. Pressure-Log. Volume Diagrams for

X. SUMMARY OF RESULTS

From the foregoing results it is concluded that:

1. The b.s.f.c. could be decreased by 6.25% in the entire load range; the maximum load was increased by 10.7% limited by exhaust gas temperature of 1165°F; the delay period was decreased by 47%, and the engine speed could be raised to at least twice the designed engine speed despite the fuel injection system being designed for 1800 r.p.m. Moreover, the maximum output could be increased more than the above mentioned value by allowing the exhaust gas temperature to exceed 1165°F. The conditions under which these results were achieved were:

   a. M.F. injection begins at 19° B.T.C.
   b. P.F. injection begins at 5° B.T.C. during the exh. stroke.
   c. P.F. injection pressures is 800 lb/in^2.
   d. Cooling water and lubricating oil temperatures are 140, 160°F respectively.
   e. P.F./T.F.% equals about 6%.

2. By retarding the M.F. injection the engine runs smoother, with shorter delay, and higher economy in the over load (26% decrease in b.s.f.c. at 6.45% overload at M.F. injection begins 14° B.T.C.). When the M.F. injection begins at 9° B.T.C., the delay was practically eliminated at P.F./T.F.% of 12.5%.

3. Means for assisting the production of high and variable speed compression ignition engines are established by shortening the delay period and accelerating the reaction rate. At 2000 r.p.m. and

P.F./T.F.% of 15.8, the maximum pressure rise occurred at about 15° A.T.C., while it was at 30° A.T.C. in case of no P.F. injection at the same speed, and the heat addition was almost at constant pressure with the expected low efficiency. The delay period at 2000 r.p.m. with P.F. injection was 1.339 millisecond as compared to 2.45 milliseconds in case of no P.F. injection.

4. Increasing the energy cell throat area by 72%, increased the b.s.f.c. by about 6.77% but the engine ran smoother and the delay period was longer.

The utilization of two injection pumps and two injection valves is an additional complication or handicaps, but it is believed that this could be overcome by such a scheme as shown in Figure 41. A gear pump to compress fuel into a pressure vessel or header to supply two electrically operated injection valves, could be used. By using electrically operated injection valves, an optimum injection timing for each load and speed could be controlled and easily achieved. The possibility exists that such a scheme involves reduction in cost considerably.

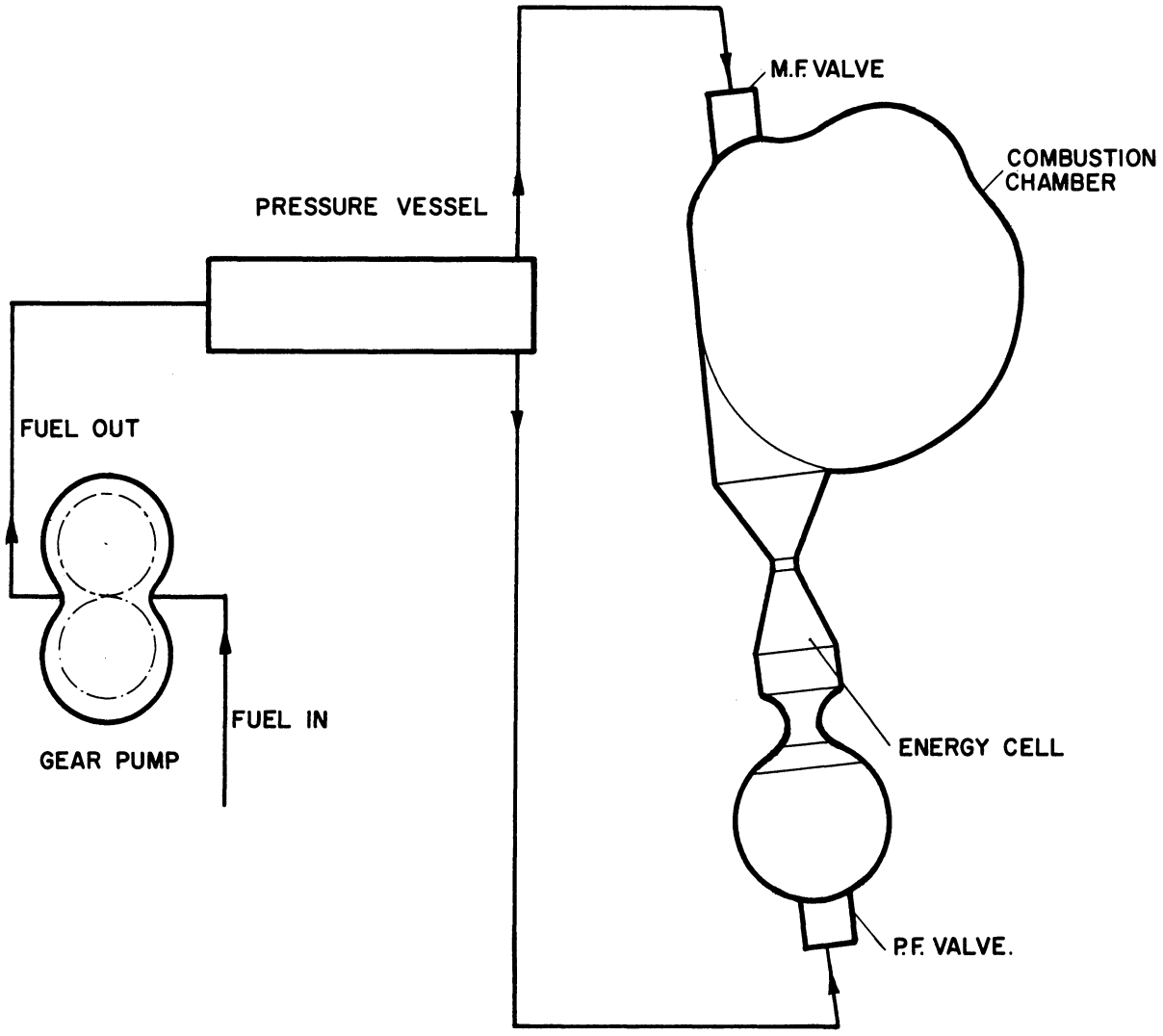

Figure 41. Suggested Injection System.

XI. CONCLUSIONS AND RECOMMENDATIONS

Conclusions

The results presented above show that it is possible to control the combustion in compression ignition engines by inducing sufficiently high concentration of radicals in the reaction zone inside the engine cylinder before the main injection. This was accomplished by injecting part of the fuel early in the cycle into the energy-cell.

It is believed that one means for increasing the engine speed of rotation and the specific power output was established by this technique.

Primary fuel injection timing and pressure, cooling water temperature, engine speed, main fuel injection timing, addition of cumene hydroperoxide to the fuel and energy-cell throat diameter influenced the combustion process and the engine performance. Maximum economy occurred when the primary fuel injection was at 5° B.T.C. during the exhaust stroke and of 800 lb/in^2 pressure. The combustion reaction rate was directly proportionate to the cooling water temperature. The delay period decreased linearly with engine speed. The engine ran smoother when the main injection was retarded and with larger throat diameter. Cumene hydroperoxide addition to the fuel had less affect on both the ignition delay and the reaction rate.

The correlations which are derived from this combustion chamber, and the combustion behavior may be applied to other combustion chambers particularly the pre- and ante- combustion chambers.

Recommendations

It is recommended that further investigations be made along the following lines:

1. Determination of optimum energy-cell throat diameter and volume, with the corresponding M.F. and P.F. injections timing.

2. The possibility of injecting the two quantities through one injection valve located in some favorable position should be examined.

3. Investigate the possibility of applying this technique in other types of combustion chambers.

4. Examine the effect of the energy cell temperature on the preflame reactions.

5. Spectroscopic analysis of the gases inside the engine cylinder at different positions could be made to detect the concentrations of the different species of intermediate and final products.

6. Examine the effect of air vitiation at high pressures and temperature on the delay period.

APPENDIX I

SAMPLE CALCULATIONS

Run Number 148

Readings

Torque F = 30 lbs.ft

Time for consumption of 1/8 lb of main fuel = t_m = 1.64 minute

Revolution counter reading for the time t_m = N_m = 2674 revs.

Time for consumption of 1/16 lb of primary fuel = t_p = 9.59 minute

Compression pressure = P_{comp} = 17.5 divisions

Maximum pressure = P_{max} = 29 divisions

Location of maximum pressure = θ_{max} = 15 degrees A.T.C.

Location of start of sudden pressure rise = θ_i = 8 degrees A.T.C.

Exhaust temperature = $T_{exh.}$ = 670°F

Results

Average engine speed = $\frac{N_m}{t_m} = \frac{2674}{1.64}$ = 1630 r.p.m.

Brakepower = $\frac{FN}{5250} = \frac{30 \times 1630}{5250}$ = 9.32 B.H.P.

B.M.E.P. = $150.8 \frac{F}{V_s} = \frac{150.8 \times 30}{83.48}$ = 54.3 lb/in^2

$S.F.C._m = \frac{1 \times 60}{8 \times B.H.P. \times t_m} = \frac{60}{8 \times 9.32 \times 1.64}$ = 0.491 lb/B.H.P. hr.

$S.F.C._p = \frac{1 \times 60}{16 \times B.H.P. \times t_p} = \frac{60}{16 \times 9.32 \times 9.8}$ = 0.041 lb/B.H.P. hr.

$\therefore$ B.S.F.C. = ΣS.F.C. = 0.491 + 0.041 = 0.532 lb/B.H.P. hr.

$\frac{\text{Primary fuel}}{\text{Total fuel}}\ \% = \frac{P.F.}{T.F.}\ \% = \frac{0.041}{0.532} \times 100$ = 7.87%

Ignition delay = $19 + \theta_i$ = 19 + 8 = 27 degrees (crank angles)

$$\tau = \frac{\theta_{max} - \theta_i}{\frac{P_{max} - P_{comp}}{P_{comp}}} = \frac{15 - 8}{\frac{29 - 17.5}{17.5}} = \frac{17.5 \times 7}{11.5} = 10.65$$

Run Number 372

Location of start of sudden pressure rise = θ_i = 2.92 degrees B.T.C.

Engine speed = N = 2000 rpm

T_{exh} = 1005

Ignition delay = $\frac{(19 + \theta_i) \times 60 \times 1000}{N \times 360} = \frac{(19 - 2.92)\ 1000}{60 \times 2000}$

= 1.339 milliseconds.

APPENDIX II

ENGINE SPECIFICATIONS

Bore (inches)	= 4 1/2
Stroke (inches)	= 5 1/4
Compression ratio	= 14 1/2
Piston displacement	= 83.48 in^3
Maximum rated speed	= 1800 rpm
Number of revolutions per cycle	= 2
Cooling system	water
Main injection begins	19° before top center
Intake valve opens	16° before top center
Intake valve closes	38° after bottom center
Exhaust valve opens	45° before bottom center
Exhaust valve closes	20° after top center
Main injection pump	AFFIA-80N-2400A } American Bosch
Primary injection pump	APEIB-50P-300/30 S632 } American Bosch

APPENDIX III

FUELS SPECIFICATIONS

Standard Diesel Fuel

H/C% by weight	=	14.5
Gravity, °A.P.I.	=	43.0
Cetane Number	=	51.1
Kinematic Viscosity	=	1.63
Flash (Tag closed)	=	130°F
Sulfur %	=	0.113
Pour	=	- 30°F
Heating Value	=	126,000 Btu/gallon
Initial Boiling Point	=	335°F
10% Recovery	=	376°F
50% Recovery	=	437°F
90% Recovery	=	486°F
End Point	=	540°F

Temperature °F	Pressure m.m.Hg.
60	0.8
80	1.6
100	2.8
120	5.0
140	8.3
160	13.3
180	21.0
200	33.0

APPENDIX IV

SOLUTIONS OF THE DIFFERENTIAL EQUATIONS 4-9, 4-10, 4-11

$$\frac{d[RCHCH_3]}{dt} = W_o - k_2[RCHCH_3][O_2] + k_3[R(CH_3)CHOO][RCH_2CH_3] + k_1[R(CH_3)CHOOH] \qquad (4\text{-}9)$$

$$\frac{d[R(CH_3)CHOO]}{dt} = k_2[RCHCH_3][O_2] - k_3[R(CH_3)CHOO][RCH_2CH_3] - k_{3'}[R(CH_3)CHOO]^2 \qquad (4\text{-}10)$$

$$\frac{d[R(CH_3)CHOOH]}{dt} = k_3[R(CH_3)CHOO][RCH_2CH_3] \qquad (4\text{-}11)$$

At the oxygen pressure normally employed (few hundreds of millimeters Hg), the radical $RCHCH_3$ reacts much faster than the radical $R(CH_3)CHOO$ and the concentration of $RCHCH_3$ may be treated as quasi-steady. This reduces the number of equations to two.

$$\therefore \frac{d[RCHCH_3]}{dt} = o = W_o - k_2[RCHCH_3][O_2] + k_3[R(CH_3)CHOO][RCH_2CH_3] + k_1[R(CH_3)CHOOH]$$

$$k_2[RCHCH_3][O_2] - k_3[R(CH_3)CHOO][RCH_2CH_3] = W_o + k_1[R(CH_3)CHOOH]$$

Equations (4-10) and (4-11) become:

$$\frac{d[R(CH_3)CHOO]}{dt} = W_o + k_1[R(CH_3)CHOOH] - k_{3'}[R(CH_3)CHOO]^2 \qquad (4\text{-}10)$$

$$\frac{d[R(CH_3)CHOOH]}{dt} = k_3[R(CH_3)CHOO][RCH_2CH_3] \qquad (4\text{-}11)$$

Using the following substitutions:

$$\xi = \frac{k_{3'}[R(CH_3)CHOO]}{\sqrt{k_3 k_1 [RCH_2CH_3]}}, \qquad (1)$$

$$\eta = \frac{k_{3'}[R(CH_3)CHOOH]}{k_3 [RCH_2CH_3]}, \qquad (2)$$

$$W_o' = \frac{W_o k_3'}{k_3 k_1 [RCH_2CH_3]} , \qquad (3)$$

$$\tau = \sqrt{k_3 k_1 [RCH_2CH_3] t} . \qquad (4)$$

Then the system of Equations (4-10) and (4-11) can be written in the form:

$$\frac{d\xi}{d\tau} = W_o' + \eta - \xi^2 \qquad (4\text{-}10)$$

$$\frac{d\eta}{d\tau} = \xi \qquad (4\text{-}11)$$

But

$$\frac{d\xi}{d\eta} = \frac{d\xi}{d\tau} \cdot \frac{d\tau}{d\eta} = \frac{W_o' + \eta - \xi^2}{\xi}$$

$$\therefore 2\xi \frac{d\xi}{d\eta} = 2(W_o' + \eta - \xi^2)$$

Substitute $\xi^2 = y$, $2\xi \frac{d\xi}{d\eta} = \frac{dy}{d\eta}$

$$\therefore \frac{dy}{d\eta} = 2(W_o' + \eta - y)$$

$$\frac{dy}{d\eta} + 2y = 2 W_o' + 2\eta$$

$$y_{C.F.} = C e^{-2\eta}$$

$$y_{P.I.} = \left(\frac{1}{D + 2}\right)[2W_o' + 2\eta] = W_o' + \left(\frac{2}{D + 2}\right)[\eta]$$

$$= W_o' + \frac{1}{(D/2 + 1)} [\eta] = W_o' + [1 - \frac{D}{2} + \text{--}] \eta$$

$$= W_o' + \eta - 1/2$$

$\therefore$ y general solution $= W_o' + \eta - 1/2 + C e^{-2\eta}$

at $y = o \qquad \eta = o$

$\therefore \quad C = 1/2 - W_o'$

$\therefore \quad y = W_o' + \eta - 1/2 + (1/2 - W_o') e^{-2\eta}$

$= \eta + (W_o' - 1/2)(1 - e^{-2\eta})$

and

$$\frac{d\eta}{d\tau} = \xi = \sqrt{y} = \sqrt{\eta + (W_o' - 1/2)(1 - e^{-2\eta})}$$

$$\tau = \int_{\eta_o}^{\eta_1} \frac{d\eta}{\sqrt{\eta + (W_o' - 1/2)(1 - e^{-2\eta})}}$$

By expansion $(1 - e^{-2\eta})$ and neglecting powers 3 and up*, then

$$\tau_1 = \int_{o}^{\eta_1} \frac{d\eta}{\sqrt{\eta^2(1 - 2W_o') + 2W_o'\eta}} = \left[\cosh^{-1} \frac{\eta_1}{W_o'}\right]_o^{\eta_1}$$

and

$$t = \frac{\tau^2}{k_3 k_1 [RCH_2CH_3]} = \text{time of reaction in seconds.}$$

* $(1 - e^{-2\eta}) = 1 - (1 - 2\eta + \frac{4\eta^2}{21.}) = 2\eta - 2\eta^2$.

APPENDIX V

THERMAL THEORY OF EXPLOSION[15]

According to this theory the sharp transition between slow reaction and violent explosion is explained as follows:

Under certain conditions of temperature and pressure, the reaction rate reaches a critical value for which equality between the heat release due to reaction and heat loss to the surroundings become impossible. Since reaction rate coefficients are exponential functions of temperature, the overall reaction is auto-accelerated and the temperature rises.

This shows the fallacy of the concept of the ignition temperature as a specific property of a subsistance; it is rather a result of the heat released by a reaction feeding back on the reaction that generates the heat and is a function of the whole system.

Ignition Temperature

The quantity of heat of reaction released per second

$q_1 = VQ/N_a\ W.$

The rate of reaction per unit volume $= W = ka^n \exp(-E/RT)$ molecules/second

$$\therefore q_1 = \frac{VQka^n \exp(-E/RT)}{N_a} \qquad (A\text{-}1)$$

where n = 1 or 2 for unimolecular or bimolecular process respectively. q_1 is an exponential function with respect to T.

The quantity of heat transferred through the reactor walls

$$q_2 = \lambda(T - T_o)s \qquad (A\text{-}2)$$

For constant λ, s, q_2 is a straight line function with respect to T.

On Figure 42, q_1 and q_2 are represented as a function of temperature. If the reactor wall temperature is maintained at T_o', the heat supply q_1 at the start is larger than the heat removal q_2. Therefore the reactants will become warmer than the reactor walls until it reaches some value T_i' where the temperature will not increase more than that since q_2 (heat removal) would become larger than q_1. Thus in this case the reaction does not lead to auto-ignition.

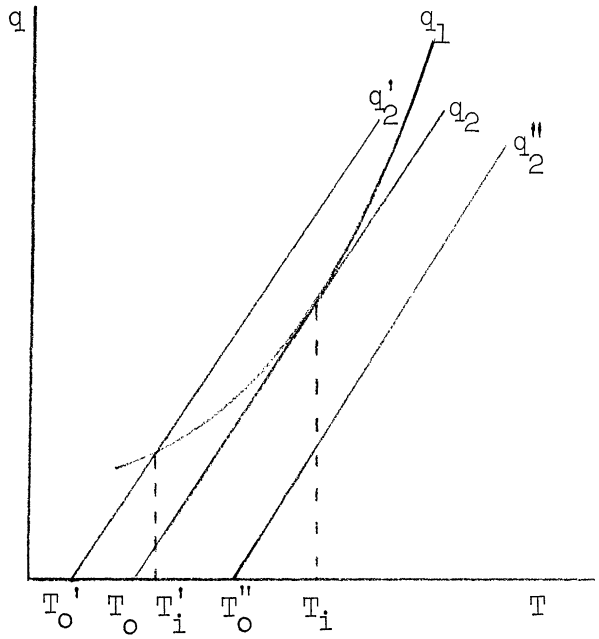

Figure 42
q-T Diagram

If the wall temperature is at T_o'', q_1 curve does not intersect the straight line q_2. In this case, the heat supply q_1 is larger, at all temperatures, than the heat removal q_2 and thus the reactants will become continuously warmer and auto-ignition takes place.

If the wall temperature is at T_o, the curve q_1 is tangent at one point to the straight line q_2 and the corresponding temperature is T_i. T_i is the lowest temperature at which auto-ignition takes place and T_i is defined as the auto-ignition temperature.

At T_i the boundary conditions are:

$$q_1 = q_2 \qquad (a)$$

and

$$-\frac{dq_1}{dT} = \frac{dq_2}{dT} \qquad (b)$$

$$\therefore \frac{VQka^n \exp(-E/RT)}{N_a} = \lambda s(T - T_o) \qquad (a.1)$$

$$\frac{E}{RT^2} \frac{VQka^n \exp}{N_a} (-E/RT)\, dT = \lambda s\, dT \qquad (b.1)$$

substitute λs from a.1 into b.1, then

$$\frac{E}{RT^2} \frac{VQ}{N_a} ka^n \exp(-E/RT) = \frac{VQka^n}{N_a(T-T_o)} \exp(-E/RT) \qquad (b.2)$$

$$\therefore \frac{E}{RT^2} = \frac{1}{T-T_o}$$

$$\frac{RT^2}{E} = T-T_o \qquad (A\text{-}3)$$

$$\therefore T = \frac{1 \pm \sqrt{1 - (4RT_o/E)}}{2\,R/E} \quad \frac{1 \pm \{1 - (4RT_o/E)\}^{1/2}}{2\,R/E}$$

By binomial expansion

$$T = \frac{1 \pm \{1 - 2RT_o/E + 2(\frac{RT_o}{E})^2 + --\}}{2R/E}$$

since RT_o/E is a small quantity, ($E \approx 20000$ cal. $T_o \approx 400$), then terms of second order and up can be neglected and since the plus sign gives T_i above 10000°K then its solution must be rejected

$$\therefore T_i = T_o + \frac{RT_o^2}{E} \qquad (A\text{-}4)$$

Define ΔT as $T_i - T_o = \frac{RT_o^2}{E}$

$$T_i = T_o + \Delta T$$

$$\frac{1}{T_i} = \frac{1}{T\left(1 + \frac{\Delta T}{T_o}\right)} \approx \frac{1}{T_o}\left(1 - \frac{\Delta T}{T_o}\right) \qquad \text{binomial approx.}$$

and $$\frac{1}{T_i^2} = \frac{1}{T_o^2}\left(1 - \frac{2\Delta T}{T_o}\right)$$

Substitute in b.1

$$\therefore \frac{EQVka^n}{N_a RT_o^2}\left(1 - \frac{2\Delta T}{T_o}\right) \exp\left\{-E/RT_o\left(1 - \frac{\Delta T}{T_o}\right\}\right. = \lambda s \qquad \text{(A-5)}$$

Since $2\Delta T/T_o = 2RT_o/E$ is of order 0.1, it may be neglected in the first term and Equation (A-5) becomes

$$\frac{EQVka^n}{\lambda s N_a RT_o^2} \exp\{-E/RT_o + 1\} = \frac{QVka^n Ee}{\lambda s N_a RT_o^2} \exp(-E/RT_o) = 1 \qquad \text{(A-6)}$$

Equation (A-6) determines T_o which consequently determines T_i according to the relation given by Equation (A-4). From Equations (A-4) and (A-6) one can see that the ignition temperature is a characteristic of the system as represented by the reaction rate (k,E), heat quantities and vessel geometry and material (Q, λ, s, V and T_o).

Delay Period[25]

Assume that the reaction rate is constant* and has its initial value and the medium is homogeneous and isotropic. The equation of energy is:

net rate of evolution of heat = heat generated by chemical reaction - heat loss by conduction

$$\frac{CaV}{N_a}\frac{dT}{dt} = \frac{QV}{N_a} ka^n \exp(-E/RT) - \lambda s (T - T_o) \qquad \text{(A-7)}$$

* This assumption is not correct since the concentration of reactants decrease with time but it does not introduce substantial error.

Assume that the heat loss during the development of an explosion is negligible compared with the heat generated by chemical reaction[25] then Equation (A-7) becomes

$$\frac{dT}{dt} = \frac{1}{C} ka^{n-1} Q \exp(-E/RT)$$

or

$$\frac{dT}{e^{-E/RT}} = \frac{1}{C} ka^{n-1} Qdt \qquad (A-8)$$

Using the exponential approximation[28] by replacing E/RT by a Taylor expansion

$$\frac{E}{RT} \simeq \frac{E}{RT_o} - (T-T_o)\frac{E}{RT_o^2} + (T-T_o)^2 \frac{ER}{T_o^3} + \cdots$$

omitting all but the first terms of the expansion since $(T-T_o) \gg T_o$, then Equation (A-8) becomes

$$\frac{dT}{e^{-E/RT_o} \cdot e^{(T-T_o)E/RT_o^2}} = \frac{1}{C} ka^{n-1} Qdt$$

which can be easily integrated

$$\int_{T_o}^{T_o+\Delta T} \exp(E/RT_o) \exp - (T-T_o) E/RT_o^2 \, dT = 1/C \, ka^{n-1} Qt$$

$$\left[\exp(E/RT_o) \cdot \left(\frac{-RT_o^2}{E}\right) \exp - (T-T_o) E/RT_o^2\right]_{T_o}^{T_o+\frac{RT_o^2}{E}} = \frac{1}{C} ka^{n-1} Qt$$

$$-\frac{RT_o^2}{E} \exp(E/RT_o)(e^{-1} - 1) = \frac{1}{C} ka^{n-1} Qt$$

and the induction period t, the time elapsed from the beginning of reaction to the preheat before explosion or the chemical delay, is

$$t = \frac{RT_o^2 C}{Eka^{n-1}Q} e^{E/RT_o} (1 - e^{-1}) \; *$$

* Todes[29] approximation gives $t = \frac{RT_o^2 C}{EQka^{n-1}} \exp(E/RT)$

At the moment of the sudden increase in temperature not more than 1% of the original reactants has reacted* in a way which justifies the assumption made concerning the constancy of the reaction rate during the induction period.

* Semenov [ref. 15, vol. II] p. 102.

APPENDIX VI

AIR-FUEL CYCLE

Compression ratio r	= 14.5
Piston displacement V_s	= 83.48 in^3
Clearance volume V_c	= 6.18 in^3
Maximum pressure P_{max}	= 720 lb/in^2
F/A	= 0.0378*
Volumetric efficiency	= 0.866**
Cooling losses (26)	
Compression stroke	0.75% of heat input
Cobmustion	2.5% of heat input
Incomplete combustion	2% of heat input
Expansion stroke	6.5% of heat input
Exhaust stroke	7.25% of heat input

Assumptions

1. Cooling losses are distributed lineary during each individual stroke.
2. Molecular weight of combustion products*** = 28.925, k = 1.296
3. Residuals from the previous cycle = 0.033
4. Calculation for one pound of air

---

*As measured in an actual cycle run 3.
**Assumption based on previous work on the same engine.
***Products of combustion - 200% theoretical air.

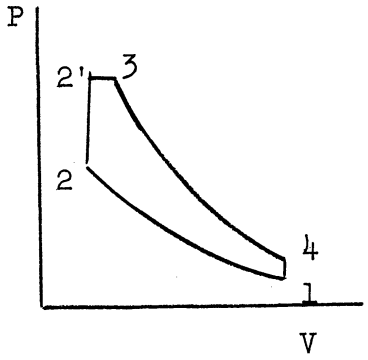

Point 1.

$T_1 = 560°R$

$h_1^{(30)} = 133.86$ Btu/lb.

$P_{r_1} = 1.5742$; $P_1 = 14.5$ lb/in^2

$V_{r_1} = 131.78$

$u_1 = 95.47$

Heat addition u_C = (1-f)F/A x H.V. = (1-0.033) 0.0378 x 19000 = 695 Btu.

Point 2.

$$V_{r_2} = \frac{V_{r_1}}{r} = \frac{131.78}{14.5} = 9.075$$

$u_{r_{21}} = 275.95$

Cooling losses in compression stroke = 695 x 0.0075 = 5.21 Btu.

Actual $u_{r_2} = 275.95 - 5.21 = 270.74$ Btu.

$T_2 = 1522.5°R$

$P_{r_{21}} = 59.15$

$V_{r_{21}} = 9.533$

$$\therefore P_{r_2} = \frac{P_{r_{21}} V_{r_{21}}}{V_{r_2}} = \frac{59.15 \times 9.533}{9.075} = 62.1$$

$$P_2 = \frac{62.1}{1.5742} \times 14.5 = 572 \text{ lb/in}^2$$

Point 3.

Cooling losses in combustion and incomplete combustion =

= 695 x 0.045 = 31.25 Btu.

$$\bar{h}_3 = (u_2 + u_C - \text{cooling losses} + P_3V_2)M$$

$$= \left(270.74 + 695 - 31.25 + \frac{720 \times 0.977 \times 144}{778}\right) 28.925$$

$$= (1096.24 - 31.25)\ 28.925 = 30800 \text{ Btu/mol}$$

$\bar{u}_3 = 3747$

$V_{r_3} = 11.330$

$P_{r_3} = 3553$

$T_3 = 3658°R$

$$V_3 = \frac{P_{r_3} V_{r_3}}{M} \frac{V_2}{P_r V_{r_2}} = \frac{3553 \times 11.33}{28.925} \times \frac{6.18}{62.1 \times 9.075} = 15.52 \text{ in}^3$$

Point 4.

$$V_{r_{41}} = V_{r_3} \times \frac{11.33 \times 89.66}{15.25} = 66.8$$

$\bar{u}_{41} = 12980$

$P_{r_{41}} = 363.8$

$T_{41} = 2267°R$

Cooling losses = $695 \times 0.065 \times 28.95 = 130.9$ Btu/mol.

$\bar{u}_4 = 12980 - 130.9 = 12849.1$ Btu/mol.

$V_{r_{41}} = 68.89$

$P_{r_{42}} = 350$

$T_4 = 2247°R$

$$P_{r_4} = \frac{P_{r_{42}} V_{r_{42}}}{V_r} = \frac{350 \times 68.89}{66.8} = 361$$

$$\therefore P_4 = \frac{P_{r_4}}{P_{r_3}} \times P_3 = \frac{361}{3553} \times 720 = 73.2$$

Point	P	V	T
1	14.5	89.66	560
2	572	6.18	1522.5
3	720	15.25	3658
4	73.2	89.66	2247

APPENDIX VII

ENGINE TEST RUNS - SERIES I THROUGH VIII

TABLE I

ENGINE TEST RESULTS - SERIES I

Run No.	N R.P.M.	B.H.P.	B.M.E.P. lb/in^2	B.S.F.C. $\frac{lb.}{B.H.P.hr.}$	$\frac{P.F.}{T.F.}$%	μ deg. crank angle	τ	$T_{exh.}$ °F	F/A
1	1625	3.09	18.1	1.037	0	34	50.7	475	0.0204
2	1610	6.14	36.2	0.701	0	34	32.7	628	0.02855
3	1600	9.15	54.3	0.567	0	29	52.5	660	0.035
4	1590	10.9	65.1	0.567	0	29	52.5	775	0.0421
5	1575	12.6	76.0	0.633	0	29	70	860	0.0547

TABLE II

ENGINE TEST RESULTS - SERIES II

Runs at: P.F. Injection Begins at 38° A.T.C. (suc.)

Run No.	N R.P.M.	B.H.P.	B.M.E.P. lb/in^2	B.S.F.C. $\frac{lb}{B.H.P.\ hr.}$	$\frac{P.F.}{T.F.}\%$	μ deg. crank angle	τ	$T_{exh.}$ °F
6	1625	3.09	18.1	1.037	0	29	17.5	475
7	1635	3.12	18.1	0.96	16.42	27	12.5	425
8	1635	3.12	18.1	0.984	8.4	28	16.8	450
9	1635	3.12	18.1	0.971	5.13	29	22.2	460
10	1635	3.12	18.1	0.965	13.39	27	12.5	430
11	1635	3.12	18.1	0.954	13.78	26	10.5	437
12	1635	3.12	18.1	0.953	14	24	10.5	435
13	1635	3.12	18.1	0.965	15.23	24	14	435
14	1635	3.12	18.1	1.015	25.7	17	19.4	415
15	1635	3.12	18.1	1.03	29.6	19	17.5	415
16	1630	3.11	18.1	1.078	38.1	19	17.5	410
17	1625	3.09	18.1	1.16	43.6	18	14	405
18	1622	3.095	18.1	1.152	44.1	15	14	405
19	1630	3.11	18.1	1.248	50.8	19	13.2	405
20	1628	3.1	18.1	1.24	50.4	19	13.2	405
21	1628	3.1	18.1	1.338	55.4	15	14	405
22	1625	3.09	18.1	1.455	60	15	18	405
23	1625	3.09	18.1	1.532	62.8	15	15.72	405
24	1625	3.09	18.1	1.58	65.5	17	12.25	405
25	1635	3.12	18.1	1.645	70.2	19	17.5	402
26	1638	3.122	18.1	1.67	72.4	19	20	402

TABLE III

ENGINE TEST RESULTS - SERIES II

Runs at: P.F. Injection Begins at 38° A.T.C. (suc.)

Run No.	N R.P.M.	B.H.P.	B.M.E.P. lb/in^2	B.S.F.C. $\frac{\text{lb}}{\text{B.H.P. hr.}}$	P.F. / T.F. %	μ deg. crank angle	τ	$T_{exh.}$ °F
27	1620	6.16	36.2	0.66	13.40	27	13.15	535
28	1625	6.19	36.2	0.654	11.85	29	18	543
29	1620	6.16	36.2	0.654	4.43	29	30	543
30	1615	6.15	36.2	0.675	5.76	29	37.5	535
31	1620	6.16	36.2	0.647	8.00	27	25	535
32	1620	6.16	36.2	0.63	2.99	27	21	535
33	1630	6.21	36.2	0.644	4.72	27	17.5	530
34	1630	6.21	36.2	0.653	14.2	24	13.15	530
35	1630	6.21	36.2	0.651	13.65	24	13.15	538
36	1635	6.22	36.2	0.67	19.15	17	10.5	528
37	1638	6.24	36.2	0.688	23.8	17	10.5	528
38	1645	6.26	36.2	0.582	30.1	17	11.05	518
39	1645	6.26	36.2	0.745	35.2	17	13.1	520
40	1642	6.25	36.2	0.791	41.5	17	13.1	510
41	1642	6.25	36.2	0.787	41.1	19	16.7	518
42	1640	6.248	36.2	0.902	49.98	19	16.7	510
43	1638	6.24	36.2	0.946	52.5	19	17.65	510
44	1645	6.26	36.2	0.954	55.7	19	17.65	510
45	1648	6.27	36.2	0.988	57.15	19	17.65	510
46	1642	6.25	36.2	1.025	58.5	19	16.7	505
47	1642	6.25	36.2	1.052	60.0	19	21.4	505
48	1630	6.21	36.2	0.64	13.48	24	17.5	533
49	1632	6.22	36.2	0.614	12.65	24	17.5	540
50	1615	6.15	36.2	0.701	0	34	32.7	628

TABLE IV

ENGINE TEST RESULTS - SERIES II

Runs at: P.F. Injection Begins at 38° A.T.C. (suc.)

Run No.	N R.P.M.	B.H.P.	B.M.E.P. lb/in^2	B.S.F.C. $\frac{lb.}{B.H.P.\ hr}$	P.F./T.F. %	μ deg. crank angle	τ	$T_{exh.}$ °F
51	1615	9.24	54.3	0.585	10.95	19	9.52	712
52	1605	9.16	54.3	0.55	7.8	23	11.1	670
53	1605	9.16	54.3	0.575	7.4	27	15	698
54	1605	9.16	54.3	0.562	6.55	27	19.25	698
55	1605	9.16	54.3	0.56	5.08	29	19.25	698
56	1598	9.12	54.3	0.564	4.63	29	19.25	708
57	1605	9.16	54.3	0.62	17.15	21	10.5	745
58	1615	9.23	54.3	0.615	15.55	19	13.15	748
59	1612	9.21	54.3	0.622	18.3	19	13.15	748
60	1615	9.23	54.3	0.621	18.9	19	13.15	748
61	1615	9.23	54.3	0.645	25.5	17	13.15	740
62	1615	9.23	54.3	0.666	28.3	17	13.15	740
63	1630	9.32	54.3	0.668	32.1	19	13.15	720
64	1620	9.25	54.3	0.686	34.6	17	16.05	704
65	1625	9.29	54.3	0.716	48.6	16	10.5	700
66	1625	9.29	54.3	0.752	41.75	16	11.11	700
67	1630	9.32	54.3	0.778	44.6	16	11.11	695
68	1622	9.27	54.3	0.805	48.9	19	13.9	670
69	1625	9.29	54.3	0.822	48.9	17	9.72	680
70	1600	9.15	54.3	0.568	51.4	27	9.06	660

TABLE V

ENGINE TEST RESULT - SERIES II

Runs at: P.F. Injection Begins at 38° A.T.C. (suc.)

Run No.	N R.P.M.	B.H.P.	B.M.E.P. lb/in^2	B.S.F.C. $\frac{lb.}{B.H.P.\ hr}$	P.F./T.F. %	μ deg. crank angle	τ	$T_{exh.}$ °F
71	1572	10.78	65.1	0.676	7.18	19	11.55	1000
72	1575	10.8	65.1	0.624	7.07	21	11.55	890
73	1575	10.8	65.1	0.645	7.3	21	13	960
74	1585	10.86	65.1	0.576	5.68	27	10.1	870
75	1585	10.86	65.1	0.577	3.11	27	10.1	750
76	1595	10.93	65.1	0.645	4.06	24	10.1	820
77	1585	10.86	65.1	0.619	12.7	17	10.1	900
78	1585	10.86	65.1	0.599	13.3	15	9.6	875
79	1588	10.88	65.1	0.644	19.55	14	10.1	875
80	1598	10.95	65.1	0.634	22.1	15	14.65	860
81	1595	10.93	65.1	0.645	24.4	17	11.35	810
82	1610	11.03	65.1	0.622	34.3	19	10.95	760
83	1620	11.11	65.1	0.579	39.2	24	8.45	755
84	1625	11.14	65.1	0.576	44.8	27	8.45	770
85	1625	11.14	65.1	0.625	50	27	8.46	775
86	1615	11.09	65.1	0.667	51.4	27	9.06	785

TABLE VI

ENGINE TEST RESULTS - SERIES II

Runs at: P.F. Injection Begins at 15° A.T.C. (suc.)

Run No.	N R.P.M.	B.H.P.	B.M.E.P. lb./in^2	B.S.F.C. $\frac{lb}{B.H.P.\ hr}$	$\frac{P.F.}{T.F.}$ %	μ deg. crank angle	τ	$T_{exh.}$ °F
87	1640	3.125	18.1	0.973	15	27	12	412
88	1635	3.12	18.1	0.97	9.08	27	14	415
89	1650	3.15	18.1	0.982	12.5	29	24	415
90	1645	3.14	18.1	0.946	23.7	31	25.1	415
91	1650	3.15	18.1	0.898	19.85	27	12	395
92	1650	3.15	18.1	0.926	22.1	23	14.5	395
93	1660	3.165	18.1	0.988	35.5	21	17.45	392
94	1660	3.165	18.1	1.032	41	19	16	402
95	1655	3.16	18.1	1.07	46.2	19	12	395
96	1655	3.16	18.1	1.086	48.2	19	12	395
97	1660	3.165	18.1	1.292	50.5	19	12	395
98	1615	3.08	18.1	1.178	59.6	17	11.2	385

TABLE VII

ENGINE TEST RESULTS - SERIES II

Runs at: P.F. Injection Begins at 15° A.T.C. (suc.)

Run No.	N R.P.M.	B.H.P.	B.M.E.P. lb/in^2	B.S.F.C. $\frac{lb.}{B.H.P.\ hr}$	$\frac{P.F.}{T.F.}$ %	μ deg. crank angle	τ	$T_{exh.}$ °F
99	1635	6.22	36.2	0.615	19.2	19	15	503
100	1635	6.22	36.2	0.627	21.3	23	9	508
101	1640	6.248	36.2	0.611	18.05	24	10.5	512
102	1635	6.22	36.2	0.614	17.75	21	12	512
103	1635	6.22	36.2	0.606	14.3	21	12	512
104	1635	6.22	36.2	0.60	7.83	27	12	535
105	1635	6.22	36.2	0.586	9	27	12	525
106	1628	6.2	36.2	0.63	7.32	34	60	545
107	1645	6.26	36.2	0.62	18.42	19	12	520
108	1635	6.22	36.2	0.646	24.9	21	12	510
109	1645	6.26	36.2	0.644	25.7	19	12	510
110	1645	6.26	36.2	0.678	33.4	19	12	510
111	1645	6.26	36.2	0.682	35.2	19	12	510
112	1645	6.26	36.2	0.71	40.2	17	13.5	510
113	1645	6.26	36.2	0.755	46.3	17	13.5	512
114	1645	6.26	36.2	0.825	53.9	19	9.6	517
115	1650	6.29	36.2	0.895	58.1	19	9.6	528
116	1650	6.29	36.2	0.922	62.5	19	9.6	528

TABLE VIII

ENGINE TEST RESULTS - SERIES II

Runs at: P.F. Injection Begins at 15° A.T.C. (suc.)

Run No.	N R.P.M.	B.H.P.	B.M.E.P. lb/in^2	B.S.F.C. $\frac{\text{lb}}{\text{B.H.P. hr}}$	$\frac{\text{P.F.}}{\text{T.F.}}$ %	μ deg. crank angle	τ	$T_{exh.}$ °F
117	1615	9.24	54.3	0.577	10.38	31	11.25	738
118	1600	9.14	54.3	0.607	12.32	23	11.25	735
119	1610	9.2	54.3	0.555	10.12	23	7.5	705
120	1595	9.12	54.3	0.575	9.65	27	11.65	735
121	1605	9.16	54.3	0.59	10.2	27	11.65	730
122	1605	9.16	54.3	0.574	8.13	27	7.5	730
123	1615	9.24	54.3	0.548	8.45	24	10.5	705
124	1612	9.21	54.3	0.562	4.87	24	8.32	705
125	1602	9.155	54.3	0.605	17.4	29	8.5	738
126	1605	9.16	54.3	0.625	28.2	27	17	708
127	1610	9.2	54.3	0.64	33.1	21	15.1	710
128	1614	9.24	54.3	0.656	38.2	21	17	700
129	1618	9.25	54.3	0.844	40	21	17	700
130	1618	9.25	54.3	0.727	52.5	21	17	705

TABLE IX

ENGINE TEST RESULTS - SERIES II

Runs at: P.F. Injection Begins at 15° A.T.C. (suc.)

Run No.	N R.P.M.	B.H.P.	B.M.E.P. lb/in^2	B.S.F.C. $\frac{\text{lb}}{\text{B.H.P. hr}}$	$\frac{\text{P.F.}}{\text{T.F.}}$ %	μ deg. crank angle	τ	$T_{exh.}$ °F
131	1615	11.09	65.1	0.615	10.85	21	26	922
132	1620	11.11	65.1	0.647	10.47	19	18.2	962
133	1615	11.09	65.1	0.623	9.48	24	11.66	938
134	1610	11.03	65.1	0.546	5.17	27	18.76	765
135	1600	10.98	65.1	0.56	6.8	27	15	790
136	1612	11.05	65.1	0.586	14.95	19	15.1	855
137	1625	11.14	65.1	0.587	24.48	17	17.78	835
138	1615	11.09	65.1	0.573	15.3	19	17.78	840
139	1615	11.09	65.1	0.574	13.2	24	15.4	860
140	1630	11.19	65.1	0.5738	31.9	19	26.4	770
141	1635	11.21	65.1	0.56	33.4	21	14	740
142	1640	11.25	65.1	0.591	42.3	21	12.45	740
143	1635	11.21	65.1	0.634	51.2	24	17.5	725
144	1615	11.09	65.1	0.518	7.67	27	14	775

TABLE X

ENGINE TEST RESULTS - SERIES II

Runs at: P.F. Injection Begins at 5° B.T.C. (exh.)

Run No.	N R.P.M.	B.H.P.	B.M.E.P. lb/in^2	B.S.F.C. $\frac{lb}{B.H.P.\ hr}$	$\frac{P.F.}{T.F.}$ %	μ deg. crank angle	τ	$T_{exh.}$ °F
145	1621	9.26	54.3	0.615	16.65	19	11.55	695
146	1628	9.3	54.3	0.581	11.42	24	9.8	710
147	1630	9.32	54.3	0.548	10.8	24	9	675
148	1630	9.32	54.3	0.532	7.88	27	10.65	670*
149	1635	9.34	54.3	0.551	6.2	29	13.32	702
150	1638	9.35	54.3	0.558	22.6	17	8	672
151	1638	9.35	54.3	0.555	23.6	17	12.3	658
152	1635	9.34	54.3	0.567	34.8	15	13.7	650
153	1648	9.42	54.3	0.58	48.15	14	13.85	631
154	1650	9.44	54.3	0.606	56	14	14	660
155	1652	9.45	54.3	0.643	63.6	19	16.35	662

* F/A = 0.0329

TABLE XI

ENGINE TEST RESULTS - SERIES II

Runs at: P.F. Injection Begins at 25° B.T.C. (exh.)

Run No.	N R.P.M.	B.H.P.	B.M.E.P. lb/in^2	B.S.F.C. $\frac{lb}{B.H.P.\ hr}$	$\frac{P.F.}{T.F.}$ %	μ deg. crank angle	τ	$T_{exh.}$ °F
156	1610	9.2	54.3	0.573	9.17	24	19.5	708
157	1615	9.24	54.3	0.561	8.26	27	15	708
158	1620	9.25	54.3	0.549	8.1	27	10.5	702
159	1625	9.28	54.3	0.55	8.22	27	9.55	702
160	1635	9.34	54.3	0.54	6.65	29	13.33	692
161	1625	9.28	54.3	0.546	5.09	31	18.75	700
162	1645	9.4	54.3	0.612	19.65	19	10	675
163	1640	9.37	54.3	0.558	17.95	19	10.72	668
164	1645	9.4	54.3	0.561	32.9	19	10	650
165	1645	9.4	54.3	0.551	35.2	23	9.22	635
166	1655	9.45	54.3	0.583	46.5	23	11.78	650
167	1654	9.45	54.3	0.592	54	23	8	655
168	1655	9.45	54.3	0.615	64.2	23	8	662

TABLE XII

ENGINE TEST RESULTS - SERIES II

Runs at: P.F. Injection Begins at 42° B.T.C. (exh.)

Run No.	N R.P.M.	B.H.P.	B.M.E.P. lb/in^2	B.S.F.C. $\frac{lb}{B.H.P.hr}$	$\frac{P.F.}{T.F.}$ %	μ deg. crank angle	τ	$T_{exh.}$ °F
169	1632	9.33	54.3	0.558	15.05	19	12.5	668
170	1635	9.34	54.3	0.556	9.55	23	10	668
171	1635	9.34	54.3	0.53	9.42	27	10.5	650
172	1635	9.34	54.3	0.552	7.25	27	18.75	680
173	1635	9.34	54.3	0.571	17.95	16	15	695
174	1640	9.37	54.3	0.566	25.9	18	19	670
175	1645	9.4	54.3	0.555	34.9	21	12.3	625
176	1642	9.38	54.3	0.557	41.8	24	13.35	650
177	1650	9.42	54.3	0.561	52.1	27	10.72	665
178	1653	9.44	54.3	0.592	60.02	24	10.45	672
179	1653	9.44	54.3	0.606	63.5	24	9.8	688

TABLE XIII

ENGINE TEST RESULTS - SERIES II

Runs at: P. F. Injection Begins at 60° B.T.C. (exh.)

Run No.	N R.P.M.	B.H.P.	B.M.E.P. lb/in^2	B.S.F.C. $\frac{lb}{B.H.P.\ hr}$	$\frac{P.F.}{T.F.}$ %	μ deg. crank angle	τ	$T_{exh.}$ °F
180	1588	9.06	54.3	0.60	6.22	31	53.4	755
181	1605	9.16	54.3	0.602	9.62	27	14	760
182	1615	9.24	54.3	0.651	14.92	19	18	795
183	1630	9.32	54.3	0.615	23.2	19	13.65	712
184	1605	9.16	54.3	0.626	26.2	19	12	712
185	1625	9.28	54.3	0.612	36.8	21	12	712
186	1635	9.34	54.3	0.626	48.5	23	12	710
187	1647	9.41	54.3	0.645	56	27	11.5	710

TABLE XIV

ENGINE TEST RESULTS - SERIES II

Runs at: P. F. Injection Begins at 50° A.T.C. (suc.)

Run No.	N R.P.M.	B.H.P.	B.M.E.P. lb/in^2	B.S.F.C. $\frac{lb}{B.H.P.\ hr}$	$\frac{P.F.}{T.F.}$ %	μ deg. crank angle	τ	$T_{exh.}$ °F
188	1612	9.21	54.3	0.64	18.6	17	16.25	765
189	1605	9.16	54.3	0.639	13.15	19	11	768
190	1595	9.12	54.3	0.582	6.64	27	15	745
191	1600	9.14	54.3	0.622	15.57	27	12.89	750
192	1625	9.28	54.3	0.595	20.1	17	12.5	755
193	1625	9.28	54.3	0.63	18.8	19	13.9	760
194	1635	9.34	54.3	0.615	22.2	19	12	745
195	1630	9.32	54.3	0.662	33.3	19	11.55	735
196	1625	9.28	54.3	0.734	40.6	24	11.85	705
197	1630	9.32	54.3	0.801	46.2	24	11.4	690
198	1635	9.34	54.3	0.602	9.35	27	10.5	785
199	1625	9.28	54.3	0.615	10.15	19	13.33	788
200	1625	9.28	54.3	0.589	7.4	21	11.03	745
201	1630	9.32	54.3	0.557	5.71	24	32.5	665

TABLE XV

ENGINE TEST RESULTS - SERIES II

Runs at: P.F. Injection Begins at 70° A.T.C. (suc.)

Run No.	N R.P.M.	B.H.P.	B.M.E.P. lb/in^2	B.S.F.C. $\frac{lb}{B.H.P.\ hr}$	$\frac{P.F.}{T.F.}$ %	μ deg. crank angle	τ	$T_{exh.}$ °F
202	1620	9.25	54.3	0.618	12.8	24	15.45	765
203	1615	9.24	54.3	0.626	9.45	27	8.34	800
204	1630	9.32	54.3	0.578	9.27	27	11.43	752
205	1635	9.34	54.3	0.58	9.13	29	8.16	745
206	1628	9.3	54.3	0.549	4.48	29	17.6	710
207	1630	9.32	54.3	0.592	18.15	23	12.15	740
208	1620	9.25	54.3	0.626	14.6	19	12.65	765
209	1630	9.32	54.3	0.654	22.8	22	9	765
210	1635	9.34	54.3	0.663	28.2	19	12.85	740
211	1635	9.34	54.3	0.694	35	16	11.35	710
212	1635	9.34	54.3	0.76	41.7	14	11.35	695
213	1635	9.34	54.3	0.842	45.5	16	12.86	718
214	1628	9.3	54.3	0.876	46	19	10.58	730

TABLE XVI

ENGINE TEST RESULTS - SERIES II

Runs at: P.F. Injection Begins at 95° A.T.C. (suc.)

Run No.	N R.P.M.	B.H.P.	B.M.E.P. lb/in^2	B.S.F.C. $\frac{lb}{B.H.P.\ hr}$	$\frac{P.F.}{T.F.}$ %	μ deg. crank angle	τ	$T_{exh.}$ °F
215	1630	9.32	54.3	0.646	14.8	19	7.1	805
216	1620	9.25	54.3	0.619	10.3	21	9.6	790
217	1630	9.32	54.3	0.599	10.55	21	9.6	728
218	1615	9.24	54.3	0.572	7.2	-	-	728
219	1625	9.28	54.3	0.541	2.48	-	-	670
220	1630	9.32	54.3	0.549	11.9	21	10.4	715
221	1620	9.25	54.3	0.644	19.2	24	15.1	730
222	1630	9.32	54.3	0.647	25.5	21	7.3	768
223	1650	9.42	54.3	0.669	32.8	17	15.5	725
224	1640	9.37	54.3	0.701	36.6	16	9.6	730
225	1645	9.4	54.3	0.706	38.2	17	14.55	735
226	1650	9.42	54.3	0.752	45.4	21	14.4	710
227	1635	9.34	54.3	0.765	49.3	27	10.3	680
228	1645	9.4	54.3	0.785	50.5	27	6.65	675

TABLE XVII

ENGINE TEST RESULTS - SERIES II

Runs at: P.F. Injection Begins at 120° A.T.C. (suc.)

Run No.	N R.P.M.	B.H.P.	B.M.E.P. lb/in^2	B.S.F.C. $\frac{lb}{B.H.P.\ hr}$	$\frac{P.F.}{T.F.}$ %	μ deg. crank angle	τ	$T_{exh.}$ °F
229	1625	9.28	54.3	0.566	8.91	24	12.45	738
230	1615	9.24	54.3	0.569	7.53	27	12.7	738
231	1625	9.28	54.3	0.564	5.1	27	21.4	725
232	1635	9.34	54.3	0.565	11.22	22	11.25	702
233	1630	9.32	54.3	0.566	12.6	19	11.48	725
234	1615	9.24	54.3	0.654	17.95	16	9.15	795
235	1612	9.21	54.3	0.672	20.4	17	12.8	775
236	1632	9.33	54.3	0.66	24.1	14	10	735
237	1630	9.32	54.3	0.672	29.6	14	15	720
238	1640	9.37	54.3	0.685	39.8	13	12.25	690
239	1640	9.37	54.3	0.73	44.1	19	12.85	670
240	1640	9.37	54.3	0.766	50.2	21	9	670
241	1640	9.37	54.3	0.74	54.2	24	10	670

TABLE XVIII

ENGINE TEST RESULTS - SERIES II

Runs at: P.F. Injection Begins at 152° A.T.C. (suc.)

Run No.	N R.P.M.	B.H.P.	B.M.E.P. lb/in^2	B.S.F.C. $\frac{lb}{B.H.P.\ hr}$	$\frac{P.F.}{T.F.}\%$	μ deg. crank angle	τ	$T_{exh.}$ °F
242	1615	9.24	54.3	0.66	17.9	19	13.35	773
243	1625	9.28	54.3	0.606	15.15	19	15.63	732
244	1625	9.28	54.3	0.574	14.1	21	11.65	725
245	1630	9.32	54.3	0.563	13.35	17	13.7	712
246	1630	9.32	54.3	0.556	8.3	27	6.95	695
247	1620	9.25	54.3	0.555	6.6	27	15.1	675
248	1625	9.28	54.3	0.546	6.97	27	7.15	710
249	1625	9.28	54.3	0.543	5.93	27	8.6	715
250	1620	9.25	54.3	0.553	5.65	27	10	705
251	1630	9.32	54.3	0.57	24.6	17	14.5	685
252	1628	9.3	54.3	0.601	26.1	16	8.55	695
253	1635	9.34	54.3	0.58	28.3	17	12.25	670
254	1632	9.33	54.3	0.637	28.7	14	11.1	700
255	1620	9.25	54.3	0.691	32.9	14	12.1	700
256	1625	9.28	54.3	0.736	36.2	17	8.65	695
257	1630	9.32	54.3	0.752	39.3	17	11.68	695
258	1630	9.32	54.3	0.8	42.8	17	9.46	695
259	1628	9.3	54.3	0.856	46.7	17	9.46	695

TABLE XIX

ENGINE TEST RESULTS - SERIES II

Runs at: P.F. Injection Begins at B. C. (comp.)

Run No.	N R.P.M.	B.H.P.	B.M.E.P. lb/in^2	B.S.F.C. $\frac{lb}{B.H.P.\ hr}$	$\frac{P.F.}{T.F.}$ %	μ deg. crank angle	τ	$T_{exh.}$ °F
260	1615	9.24	54.3	0.631	15.35	22	12	758
261	1615	9.24	54.3	0.606	13.7	21	10	745
262	1625	9.28	54.3	0.57	10.83	21	10.3	725
263	1620	9.25	54.3	0.552	8.37	27	10.3	708
264	1615	9.24	54.3	0.555	7.34	27	11	730
265	1615	9.24	54.3	0.55	4.83	27	18.35	742
266	1615	9.24	54.3	0.582	11.55	17	10.7	750
267	1605	9.16	54.3	0.624	16.4	15	10.7	745
268	1615	9.24	54.3	0.644	18.8	15	12.4	750
269	1602	9.14	54.3	0.716	25.4	14	11.1	752
270	1615	9.24	54.3	0.713	28.1	15	14.1	752
271	1610	9.2	54.3	0.76	31.4	15	14.1	762
272	1615	9.24	54.3	0.792	35.3	15	14.1	762
273	1630	9.32	54.3	0.805	40	17	11	715
274	1620	9.25	54.3	0.87	42.1	19	12.57	740

TABLE XX

ENGINE TEST RESULTS - SERIES II

Runs at: P.F. Injection Begins at 35° A.B.C. (comp.)

Run No.	N R.P.M.	B.H.P.	B.M.E.P. lb/in^2	B.S.F.C. $\frac{lb}{B.H.P.\ hr}$	$\frac{P.F.}{T.F.}$ %	μ deg. crank angle	τ	$T_{exh.}$ °F
275	1625	9.28	54.3	0.615	13.5	19	13.7	750
276	1620	9.25	54.3	0.568	10.58	24	6.8	720
277	1620	9.25	54.3	0.572	10.5	24	7.85	718
278	1625	9.28	54.3	0.561	8.52	27	8.45	710
279	1612	9.21	54.3	0.55	5.26	27	15.4	705
280	1610	9.2	54.3	0.641	15.65	19	14.16	758
281	1605	9.16	54.3	0.644	16.45	17	11	765
282	1612	9.21	54.3	0.697	22.7	17	11	760
283	1625	9.28	54.3	0.752	33.1	17	8.75	765
284	1615	9.24	54.3	0.825	37.5	17	8.75	765

TABLE XXI

ENGINE TEST RESULTS - SERIES II

Runs at: P.F. Injection Begins at 110° B.T.C.(comp.)

Run No.	N R.P.M.	B.H.P.	B.M.E.P. lb/in^2	B.S.F.C. $\frac{\text{lb.}}{\text{B.H.P.hr.}}$	$\frac{\text{P.F.}\%}{\text{T.F.}}$	μ deg. crank angle	τ	T_{exh} °F
285	1625	9.28	54.3	0.594	16.75	24	11.65	690
286	1625	9.28	54.3	0.561	11.73	24	8.3	690
287	1605	9.16	54.3	0.571	7.65	27	15	705
288	1610	9.2	54.3	0.606	14	17	11.65	710
289	1620	9.25	54.3	0.656	21.8	17	11.65	715
290	1615	9.24	54.3	0.68	24.5	19	15	728
291	1625	9.28	54.3	0.733	30.77	19	15	728
292	1615	9.24	54.3	0.788	34.8	19	7.8	740
293	1630	9.32	54.3	0.816	40.3	17	12.25	720
294	1630	9.32	54.3	0.841	41.9	19	16	710

TABLE XXII

ENGINE TEST RESULTS - SERIES II

Runs at: P.F. Injection begins at 75° B.T.C. (Comp.)

Run No.	N R.P.M.	B.H.P.	B.M.E.P. lb/in^2	B.S.F.C. $\frac{\text{lb.}}{\text{B.H.P.hr.}}$	$\frac{\text{P.F.}\%}{\text{T.F.}}$	μ deg. crank angle	τ	T_{exh} °F
295	1593	9.1	54.3	0.62	14.2	27	13	745
296	1592	9.1	54.3	0.615	9.85	27	21.7	770
297	1585	9.05	54.3	0.606	9.25	29	22.75	750
298	1595	9.12	54.3	0.624	15	27	6.67	760
299	1595	9.12	54.3	0.686	19.6	24	10.83	835
300	1600	9.14	54.3	0.715	24.6	21	11.55	852
301	1585	9.05	54.3	0.766	30.3	17	15.9	880
302	1615	9.24	54.3	0.822	37.8	19	7.1	890
303	1620	9.25	54.3	0.875	42.2	21	11.42	910

TABLE XXIII

ENGINE TESTS RESULTS - SERIES II

Runs at: P.F. Injection begins at 75° B.T.C.(Comp.)
P.F. Injection pressure = 1400 lb/in^2

Run No.	N R.P.M.	B.H.P.	B.M.E.P. lb/in^2	B.S.F.C. $\frac{\text{lb.}}{\text{B.H.P.hr.}}$	$\frac{\text{P.F.}}{\text{T.F.}}$ %	μ deg. crank angle	τ	T_{exh} °F	
304	1610	9.2	54.3	0.582	8.16	27	12.25	730	
305	1605	9.16	54.3	0.566	6.4	24	26	722	
306	1612	9.21	54.3	0.635	16.0	21	11.55	750	
307	1610	9.2	54.3	0.674	19.5	17	9.1	785	
308	1610	9.2	54.3	0.704	24.2	17	10.1	785	
309	1620	9.25	54.3	0.724	27.5	17	11.38	795	
310	1610	9.2	54.3	0.791	33.3	19	13	850	
311	1622	9.26	54.3	0.818	36.1	19	9.76	855	
312	1610	9.2	54.3	0.876	38.5	17	11	870	*

* Irregular firing

TABLE XXIV

ENGINE TEST RESULTS - SERIES II

Runs at: P.F. Injection begins at 45° B.T.C.(Comp.)
P.F. Injection Pressure = 1400 lb/in^2

Run No.	N R.P.M.	B.H.P.	B.M.E.P. lb/in^2	B.S.F.C. $\frac{\text{lb.}}{\text{B.H.P.hr.}}$	P.F. / T.F. %	μ deg. crank angle	τ	T_{exh} °F
313	1615	9.24	54.3	0.72	24	25	12.85	800
314	1610	9.2	54.3	0.68	15.4	25	12.85	775
315	1612	9.21	54.3	0.616	8.3	21	15.2	752
316	1632	9.33	54.3	0.565	3.6	27	12.1	705
317	1630	9.32	54.3	0.675	22.8	21	18	792
318	1625	9.28	54.3	0.656	24.9	24	7.5	775
319	1625	9.28	54.3	0.711	30.3	24	6.43	812
320	1622	9.26	54.3	0.72	36.3	27	6	825
321	1628	9.3	54.3	0.757	39.9	27	9.35	870

TABLE XXV

ENGINE TEST RESULTS - SERIES III

Runs at: P.F. Injection begins 5° B.T.C.(exh.)
P.F. Injection pressure = 1400 lb/in^2

Run No.	N R.P.M.	B.H.P.	B.M.E.P. lb/in^2	B.S.F.C. $\frac{\text{lb.}}{\text{B.H.P.hr.}}$	$\frac{\text{P.F.}\%}{\text{T.F.}}$	μ deg. crank angle	τ	T_{exh} °F
322	1595	9.12	54.3	0.644	10.8	19	15.45	825
323	1608	9.19	54.3	0.637	8.05	19	10.5	835
324	1600	9.14	54.3	0.586	5.6	21	9.23	780
325	1605	9.16	54.3	0.555	1.89	27	19.85	708
326	1625	9.28	54.3	0.615	18.8	17	12.6	780
327	1625	9.28	54.3	0.61	17.4	19	12.6	788
328	1625	9.28	54.3	0.63	23.7	17	14	795
329	1625	9.28	54.3	0.664	31.6	17	10.5	780
330	1635	9.34	54.3	0.679	38.7	19	14.2	795
331	1635	9.34	54.3	0.68	48.2	14	14.5	750

TABLE XXVI

ENGINE TEST RESULTS - SERIES III

Runs at: P.F. Injection begins at 5° B.T.C.(exh.)
P.F. Injection pressure = 1200 lb/in^2

Run No.	N R.P.M.	B.H.P.	B.M.E.P. lb./in.^{2}	B.S.F.C. $\frac{\text{lb.}}{\text{B.H.P.hr.}}$	$\frac{\text{R.F.}\%}{\text{T.F.}}$	μ deg. crank angle	τ	T_{exh} °F
332	1605	9.16	54.3	0.594	6.75	19	12.35	750
333	1610	9.2	54.3	0.556	3.78	24	12.42	730
334	1605	9.16	54.3	0.614	10.2	19	10	792
335	1605	9.16	54.3	0.606	11.2	17	13.15	802
336	1620	9.25	54.3	0.646	19.4	14	9.28	802
337	1620	9.25	54.3	0.647	23.4	13	11.55	790
338	1630	9.32	54.3	0.605	32.9	14	11	732
339	1640	9.37	54.3	0.587	39.7	14	11	705
340	1635	9.34	54.3	0.605	46	14	12.2	720
341	1635	9.34	54.3	0.614	55.5	19	13.55	705

TABLE XXVII

ENGINE TEST RESULTS - SERIES III

Runs at: P.F. Injection begins at 5° B.T.C.(exh.)
P.F. Injection Pressure = 1000 lb/in^2

Run No.	N R.P.M.	B.H.P.	B.M.E.P. lb/in^2	B.S.F.C. $\frac{\text{lb.}}{\text{B.H.P.hr.}}$	$\frac{\text{P.F.}}{\text{T.F.}}$ %	μ deg. crank angle	τ	T_{exh} °F
342	1603	9.15	54.3	0.585	8.15	21	6.8	775
343	1612	9.21	54.3	0.58	6.75	21	7.5	758
344	1621	9.25	54.3	0.551	5.95	23	9.85	742
345	1615	9.24	54.3	0.552	5.25	24	9.35	720
346	1612	9.21	54.3	0.555	5.15	24	8.12	735
347	1615	9.24	54.3	0.556	3.87	27	11.42	720
348	1600	9.14	54.3	0.614	11.2	19	8.75	791
349	1619	9.25	54.3	0.615	16	17	12.25	788
350	1635	9.34	54.3	0.595	26.8	15	12	755
351	1638	9.35	54.3	0.603	37.4	14	11	692
352	1638	9.35	54.3	0.599	53.2	17	11	675

TABLE XXVIII

ENGINE TEST RESULTS - SERIES III

Runs at: P.F. Injection begins at 5° B.T.C.(exh.)
P.F. Injection Pressure = 600 lb/in^2

Run No.	N R.P.M.	B.H.P.	B.M.E.P. lb/in^2	B.S.F.C. $\frac{\text{lb.}}{\text{B.H.P.hr.}}$	$\frac{\text{P.F.}\%}{\text{T.F.}}$	μ deg. crank angle	τ	T_{exh} °F
353	1618	9.25	54.3	0.56	6.75	23	15	758
354	1615	9.24	54.3	0.555	4.15	27	14	755
355	1608	9.19	54.3	0.56	5.05	27	11.65	750
356	1605	9.16	54.3	0.621	13.65	21	15	810
357	1602	9.14	54.3	0.58	9.25	19	13.15	800
358	1598	9.13	54.3	0.61	8.82	19	10.5	815
359	1610	9.2	54.3	0.609	12.9	17	14	812
360	1610	9.2	54.3	0.607	12.55	17	11.7	805
361	1635	9.34	54.3	0.585	18.5	15	11.45	765
362	1632	9.33	54.3	0.583	23.8	19	12	732
363	1635	9.34	54.3	0.583	29	19	12.42	722

TABLE XXIX

ENGINE TEST RESULTS - SERIES IV

Runs at: Variable cooling water temperature
P.F. Injection begins at 5° B.T.C.(exh.)

Run No.	N R.P.M.	B.H.P.	B.M.E.P. lb/in^{-2}	B.S.F.C. $\frac{lb.}{B.H.P.hr.}$	$\frac{P.F.}{T.F.}\%$	μ deg crank angle	τ	T_{exh} °F	$T_{C.W.}$ °F
364	1615	9.24	54.3	0.56	5.5	23	10.1	763	180
365	1608	9.19	54.3	0.556	5.15	27	15	763	170
366	1625	9.28	54.3	0.552	5.26	23	14	758	158
367	1618	9.25	54.3	0.54	4.92	23	14	735	140
368	1620	9.25	54.3	0.55	4.32	29	24	720	128
369	1603	9.15	54.3	0.556	4.9	29	33	718	115

TABLE XXX

ENGINE TEST RESULTS - SERIES V

Runs at: Variable Speed
Constant Racks Positions for both pumps
P.F./T.F. = 15.8%
F/A = 0.0396

Run No.	N R.P.M.	B.M.E.P. lb/in^2	$\frac{\text{P.F.}}{\text{T.F.}}$%	μ milli-seconds	μ deg. crank angle	$T_{exh.}$ °F
370	1775	60.5	15.8	1.595	17	955
371	1915	59.6	15.8	1.48	17	1005
372	2000	59.6	15.8	1.339	16.08	1005
373	1700	56	15.8	1.665	17	828
374	1390	50.6	15.8	2.28	19	715
375	1150	52.45	15.8	2.75	19	610
376	950	56	15.8	3.0	17.1	585
377	1640	52.45	15.8	1.86	18	790

TABLE XXXI

ENGINE TEST RESULTS - SERIES V

Runs at: Variable Speed
Constant Main Fuel Pump Rack Position
F/A = 0.0329

Run No.	N R.P.M.	B.M.E.P. lb/in^2	$\frac{P.F.}{T.F.}$ %	μ milli-seconds	μ deg. crank angle	$T_{exh.}$ °F
378	1625	54.3	0	3.18	31	690
379	1760	51.6	0	2.92	30.8	750
380	1860	51.6	0	2.78	31	770
381	1940	47.9	0	2.51	29.3	830
382	2040	45.2	0	2.45	29.9	950
383	1480	56	0	3.15	28	680
384	1180	54.3	0	3.81	27	590
385	850	54.3	0	3.93	20	510

TABLE XXXII

ENGINE TEST RESULTS - SERIES VI

Runs at: M.F. Injection begins at 9° B.T.C.
P.F. Injection begins at 5° B.T.C.(exh.)

Run No.	N R.P.M.	B.H.P.	B.M.E.P. lb/in^2	B.S.F.C. $\frac{\text{lb.}}{\text{B.H.P.hr.}}$	$\frac{\text{P.F.}}{\text{T.F.}}$ %	μ deg crank angle	τ	T_{exh} °F
386	1625	9.28	54.3	0.606	22.4	0	0	752
387	1615	9.24	54.3	0.6	17.15	0	0	725
388	1611	9.21	54.3	0.589	15.9	0	0	756
389	1621	9.25	54.3	0.582	13	0	0	762
390	1621	9.25	54.3	0.592	12.65	0	0	772
391	1620	9.25	54.3	0.58	8.75	13.5	12.8	783
392	1615	9.24	54.3	0.699	3.34	23	24.3	958
393	1635	9.34	54.3	0.581	28.1	9	30.2	770
394	1635	9.34	54.3	0.607	30.4	9	26.9	765
395	1590	7.66	45.6	0.835	0	23	∞	1040*

* Max. load.

TABLE XXXIII

ENGINE TEST RESULTS - SERIES VI

Runs at: M.F. Injection begins at 14° B.T.C.
P.F. Injection begins at 5° B.T.C.(exh.)

Run No.	N R.P.M.	B.H.P.	B.M.E.P. lb/in^2	B.S.F.C. $\frac{\text{lb.}}{\text{B.H.P.hr.}}$	$\frac{\text{P.F.}}{\text{T.F.}}$ %	μ deg crank angle	τ	T_{exh} °F	F/A
396	1615	3.08	18.1	1.02	0	34	∞	548	0.021
397	1645	6.26	36.2	0.798	0	29	∞	782	0.0329
398	1620	9.25	54.3	0.641	0	29	∞	862	0.0402
399	1585	11.18	66.9	0.625	0	29	240	1045	0.0476

TABLE XXXIV

ENGINE TEST RESULTS - SERIES VI

Runs at: M.F. Injection begins at 14° B.T.C.
P.F. Injection begins at 5° B.T.C.

Run No.	N R.P.M.	B.H.P.	B.M.E.P. lb/in^2	B.S.F.C. $\frac{\text{lb.}}{\text{B.H.P.hr.}}$	$\frac{\text{P.F.}}{\text{T.F.}}$ %	μ deg. crank angle	τ	T_{exh} °F
400	1635	3.12	18.1	1.1	35.3	19	13.2	412
401	1635	3.12	18.1	0.979	35	12	19.35	420
402	1632	3.118	18.1	0.916	19.35	19	22.9	425
403	1625	3.09	18.1	0.899	13.85	27	20	418*
404	1620	3.08	18.1	0.935	10.1	29	62	458

* F/A = 0.01853

TABLE XXXV

ENGINE TEST RESULTS - SERIES VI

Runs at: M.F. Injection begins at 14° B.T.C.
P.F. Injection begins at 5° B.T.C. (exh.)

Run No.	N R.P.M.	B.H.P.	B.M.E.P. lb/in^2	B.S.F.C. $\frac{\text{lb}}{\text{B.H.P. hr}}$	$\frac{\text{P.F.}}{\text{T.F.}}$ %	μ deg. crank angle	τ	T_{exh} °F
405	1655	6.3	36.2	0.634	14.25	22	11.42	560
406	1660	6.32	36.2	0.619	9.99	26	11.42	585*
407	1650	6.29	36.2	0.665	6.45	24	36.3	642
408	1662	6.34	36.2	0.654	16	16	22.7	580
409	1655	6.3	36.2	0.665	21.5	14	26.9	580
410	1650	6.29	36.2	0.66	27.9	14	20.6	558

* F/A = 0.0255

TABLE XXXVI

ENGINE TEST RESULTS - SERIES VI

Runs at: M.F. Injection begins at 14° B.T.C.
P.F. Injection begins at 5° B.T.C. (exh.)

Run No.	N R.P.M.	B.H.P.	B.M.E.P. lb/in^2	B.S.F.C. $\frac{\text{lb}}{\text{B.H.P. hr}}$	$\frac{\text{P.F.}}{\text{T.F.}}$ %	μ deg. crank angle	τ	T_{exh} °F
411	1605	9.16	54.3	0.584	11.7	22	18.6	750
412	1615	9.24	54.3	0.631	6.45	24	18.8	802
413	1620	9.25	54.3	0.589	8.92	22	16.5	772
414	1605	9.16	54.3	0.56	13.45	22	20.3	738*
415	1635	9.34	54.3	0.567	15.65	14	18.25	725
416	1650	9.42	54.3	0.575	21.8	12	16.2	745
417	1645	9.4	54.3	0.562	15.3	14	20	730
418	1655	9.45	54.3	0.576	24.58	14	22.5	735
419	1665	9.52	54.3	0.572	30.1	14	24.4	750

* F/A = 0.0346

TABLE XXXVII

ENGINE TEST RESULTS - SERIES VI

Runs at: M.F. Injection begins at 14° B.T.C.
P.F. Injection begins at 5° B.T.C.(exh.)

Run No.	N R.P.M.	B.H.P.	B.M.E.P.** lb/in^2	B.S.F.C. $\frac{lb.}{B.H.P.hr.}$	$\frac{P.F.}{T.F.}$ %	μ deg. crank angle	τ	T_{exh} °F
420	1608	12.55	74.2	0.55	7.89	0	0	955
421	1595	11.7	69.6	0.815	3.87	26	18	1165
422	1600	12.19	72.4	0.549	8.13	19	31.6	942
423	1601	12.82	76	0.552	11.85	0	0	960
424	1600	13.1	77.7	0.55	16.25	0	0	972
425	1600	13.41	79.6	0.565	18.6	0	0	1005
426	1605	13.45	79.6	0.577	19.8	14	13.35	1028*

* F/A = 0.05

** Max. Loading

TABLE XXXVIII

ENGINE TEST RESULTS - SERIES VI

Runs at: M.F. Injection begins at 19° B.T.C.
P.F. Injection begins at 5° B.T.C.(exh.)

Run No.	N R.P.M.	B.H.P.	B.M.E.P. lb/in^2	B.S.F.C. $\frac{\text{lb.}}{\text{B.H.P.hr.}}$	$\frac{\text{P.F.}\%}{\text{T.F.}}$	μ deg. crank angle	τ	T_{exh} °F
427	1615	3.08	18.1	0.98	37.3	25	8.4	425
428	1605	3.059	18.1	0.974	31.9	25	13.05	412
429	1595	3.02	18.1	0.956	24.41	21	18.2	412
430	1605	3.059	18.1	0.935	17.6	29	17.6	420
431	1598	3.022	18.1	0.922	13.5	29	13.32	420
432	1591	3.015	18.1	0.882	10.55	31	-	420*
433	1605	3.059	18.1	0.93	8.2	31	-	

* F/A = 0.0185

TABLE XXXIX

ENGINE TEST RESULTS - SERIES VI

Runs at: M.F. Injection begins at 19° B.T.C.
P.F. Injection begins at 5° B.T.C.(exh)

Run No.	N R.P.M.	B.H.P.	B.M.E.P. lb/in^2	B.S.F.C. $\frac{lb.}{B.H.P.hr.}$	$\frac{P.F.}{T.F.}$ %	μ deg. crank angle	τ	T_{exh} °F
434	1602	6.1	36.2	0.67	14.31	29	14.2	575
435	1632	6.22	36.2	0.618	9.25	29	13.32	570*
436	1610	6.13	36.2	0.638	7.74	31	75	588
437	1600	6.09	36.2	0.664	13.9	24	17.6	575
438	1618	6.15	36.2	0.648	19.6	23	12.8	560
439	1620	6.16	36.2	0.657	27.8	21	11.72	545

*F/A = 0.0255

TABLE XL

ENGINE TEST RESULTS - SERIES VI

Runs at: M.F. Injection begins at 19° B.T.C.
P.F. Injection begins at 5° B.T.C.(exh.)

Run No.	N R.P.M.	B.H.P.	B.M.E.P. lb/in^2	B.S.F.C. $\frac{\text{lb.}}{\text{B.H.P.hr.}}$	$\frac{\text{P.F.}}{\text{T.F.}}$ %	μ deg. crank angle	τ	T_{exh} °F
440	1605	12.83	76	0.626	15	19	16.8	1020
441	1590	13.2	78.6	0.706	17.85	19	17.5	1155
442	1610	13.95	82.2	0.66	7.55	21	32	1165*
443	1615	13.09	76.9	0.65	5.15	29	32	1180
444	1580	12.05	72.4	0.777	3.5	26	21.66	1230

* F/A = 0.0585

TABLE XLI

ENGINE TEST RESULTS - SERIES VII

Runs at: Fuel is a mixture of 1% by volume of cumene hydroperoxide in Diesel fuel

Run No.	N R.P.M.	B.H.P.	B.M.E.P. lb/in^2	B.S.F.C. $\frac{lb.}{B.H.P.hr.}$	$\frac{P.F.}{T.F.}$ %	μ deg. crank angle	τ	T_{exh} °F	P.F.	M.F.
445	1625	9.28	54.3	0.571	0	34	∞	760	-	no
446	1645	9.4	54.3	0.587	13.1	29	19.7	800	no	no
447	1615	9.24	54.3	0.608	12.7	24	12	770	yes	no
448	1620	9.25	54.3	0.607	13.2	19	17.7	765	yes	yes
449	1605	9.16	54.3	0.577	0	24	48	760	-	yes
450	1615	9.24	54.3	0.642	12.1	24	43.4	860	no	yes

no = no additive was added to the fuel.

yes = additive was added to the fuel.

TABLE XLII

ENGINE TEST RESULTS - SERIES VIII

Runs at: Throat diameter = 0.196 inch

Run No.	N R.P.M.	B.H.P.	B.M.E.P. lb/in^2	B.S.F.C. $\frac{\text{lb.}}{\text{B.H.P.hr.}}$	P.F.% T.F.	μ deg. crank angle	τ	T_{exh} °F
451	1632	9.33	54.3	0.601	13.45	19	15.55	680
452	1625	9.28	54.3	0.6218	10.1	29	35.2	742
453	1615	9.24	54.3	0.6216	6.25	29	58	725
454	1628	9.3	54.3	0.599	11.3	19	21	685
455	1618	9.248	54.3	0.604	16.6	16	18.92	610
456	1625	9.28	54.3	0.58	18.65	14	17	600
457	1623	9.278	54.3	0.582	25.6	16	18	590
458	1616.5	9.238	54.3	0.568	28.9	16	18	600
459	1640	9.37	54.3	0.594	37	19	15.65	620
460	1650	9.42	54.3	0.607	44	19	10.85	622
461	1638	9.35	54.3	0.645	50.4	19	14.2	622
462	1620	9.25	54.3	0.585	0	31	64	635
463	1575	9.0	54.3	0.59	7.28			930
464	1575	9.0	54.3	0.654	0			1050

TABLE XLIII

ENGINE LOG SHEET

Eng. Mfg. Nordberg Serial No. 1-AH-900
Model UFS1-AH, (diesel), 4-stroke No. Cyl. 1
Bore 4-1/2, Stroke 5-1/4 in., Pist. Disp. 83.48 cu. in.
Comp. Ratio 14.5

Date: September 30, 1959

Dynamometer D-C cradle, Type TLC, GE,
Link Unibeam
Prim. Fuel Diesel — Main Fuel Diesel
P. Inj. begins 5° B.T.C.(Exh.) — Main Inj. begins 19° B.T.C.
Barometer 28.93 in. hg. — Room Temp. 72 °F
Cooling Water Temp. 140 °F — Oil Sump Temp. 160 °F

Run No.	Torque lb. ft.	Total Revs. N_m	Time t_m	Avg. R.P.M. N	Obs. B.H.P.	B.M.E.P. lb/in^2	Main-Fuel lb/b.h.p.-hr.	Prim. Fuel 1/16 lb. Time t_p	Prim. Fuel 1/16 lb. lb/b.h.p.-hr.	Prim. Fuel 1/16 lb. P.F.% T.F.%	B.S.F.C. lb/b.h.p.-hr.	Comp. Press. Div.	Max. Press θ_{max} deg. A.T.C.	Max. Press P_{max} Div.	Ign. St. θ_i	Ing. Delay μ deg.	τ	Exh. Temp.
145	30	2562	1.58	1621	9.26	54.3	0.511	3.93	0.103	16.65	0.615	14.5	10	28	T.C.	19	11.55	695
146	30	2551	1.565	1628	9.3	54.3	0.515	6.10	0.066	11.42	0.581	14	12	26	5°A*	24	9.8	710
147	30	2682	1.645	1630	9.32	54.3	0.49	6.94	0.058	10.8	0.548	18	12	31	5°A	24	9	675
148	30	2674	1.64	1630	9.32	54.3	0.491	9.8	.041	7.88	0.532	17.5	15	29	8°A	27	10.65	670
149	30	2541	1.555	1635	9.34	54.3	0.517	11.8	0.034	6.2	0.551	15	18	24	10°A	29	13.32	702
150	30	3043	1.86	1638	9.35	54.3	0.432	3.19	0.126	22.6	0.558	16	5	30	2°B**	17	8	672
151	30	3106	1.895	1638	9.35	54.3	0.424	3.07	0.131	23.6	0.555	16	8	29	2°B	17	12.3	658
152	30	3554	2.165	1635	9.34	54.3	0.372	2.06	0.195	34.8	0.567	16	8	30	4°B	15	13.7	650
153	30	4351	2.64	1648	9.42	54.3	0.301	1.425	0.279	48.15	0.58	16	8	31	5°B	14	13.85	631
154	30	4937	2.99	1650	9.44	54.3	0.267	1.175	0.339	56	0.606	17.5	5	30	5°B	14	14	660
155	30	5633	3.405	1652	9.45	54.3	0.234	0.975	0.409	63.6	0.643	18	10	29	T.C.	19	16.35	662

* A = A.T.C.

** B = B.T.C.

REFERENCES

1. Rothrock, A. M. and Waldron, C. D. "Effects of Air-Fuel Ratio on Fuel Spray and Flame Formation In a Compression-Ignition Engine," NACA, Report No. 545, 1935.

2. Schmidt, F. A. F. Verbrennungsmotoren, Springer, Berlin, 1945.

3. Lewis, B. and Von Elbe, G. Combustion Flames and Explosions of Gases, New York: Academic Press, 1951.

4. Granger, F. H., Grigg, G. H., Morton, F. and Reid, W. D. "Pre-Flame Reactions in Diesel Engines," Inst. of Petroleum Journal, 42, N. 387, March 1956.

5. Mason, J. M. and Hesselberg, H. E. "Engine Knock as Inlfuenced by Precombustion Reactions," S.A.E. Trans., 62, 1954.

6. Granger, F. H., Morton, F., Nissan, A. H. and Wright, E. P. "Pre-Flame Reactions in Diesel Engines," Inst. of Petroleum Journal, 38, N. 341, May 1952.

7. Lyn, W. T. "An Experimental Investigation Into the Effect of Fuel Addition to Intake Air on the Performance of a Compression-Ignition Engine," Proc. Inst. M. E. 168, No. 9, 1954.

8. Derry, L. D., Dodds, E. M., Evans, E. B. and Rolye, D. "The Effect of Auxiliary Fuels on the Smoke-Limited Power Output of Diesel Engines," Proc. Inst. M.E. 168, No. 9, 1954.

9. Alperstein, M., Swim, W.D. and Schweitzer, P. H. "Fumigation Kills Smoke," S.A.E. Trans. 66, 1958

10. Schweitzer, P. H. Combustion Problems in Diesel Engines, Fifth Symposium on Combustion, New York: Reinhold Publishing Company, 1955.

11. Corzilius, M. W., Diggs, D. R. and Pastell, D. L. "Some Factors Affecting Precombustion Reactions in Engines," S.A.E. Trans. 61, 1953.

12. Arnold, W. C., Beadle, R. H., Logelin, R. L. and Young, H. D. "Bifuel Approach to Burning Residual Fuels in Diesel Engines," S.A.E. Trans. 66, 1958.

13. Boerlage, G. D., Broeze, J. J. "Combustion Quality of Diesel Fuel," Industrial and Engineering Chemistry, 28 (1936) 1229.

14. El Wakil, M., Uyehara, D. A. and Myers, P. S. "A Theoretical Investigation on the Heating up Period of Injected Fuel Droplets Vaporizing in Air," NACA, T.N. 3179, 1954.

15. Semenov, N. N. Some Problems in Chemical Kinetics and Reactivity. Vol. I, II, Princeton University Press, 1959.

16. Bone, W. A. and Gardner, J. B. "Comparative Studies of the Slow Combustion of Methane, Methyl Alcohol, Formaldehyde and Formic Acid," Proc. Roy. Soc. (London), A, 154, (1936) 297.

17. Todes, O. M. "Acta Physiocochimica," U.R.S.S. 5, 785 (1936).

18. Gydon, A. G. Spectroscopy and Combustion Theory, London: Chapman and Hall Ltd, (1942) 49.

19. Townend, D. T. A. "Ignition Regions of Hydrocarbons," Chem. Rev. 21, (1937) 259: Townend, D. T. A. and Maccormac, M. "The Spontaneous Ignition Under Pressure of Typical Knocking and Non-Knocking Fuels," J. Chem. Soc., London (1938) 238.

20. Walsh, A. D. "Processes in the Oxidation of Hydrocarbon Fuels," Trans. Faraday Soc., 34 (1947), 297, 305.

21. Bateman, L., Hughes, H. and Morris, A. L. "Hydroperoxide Decomposition in Relation to the Initiation of Radical Chain Reactions," Disc., Faraday Soc., No. 14, (1953) 190.

22. Dixon, H. B. "Ignition Temperature of Gases," Ibid (1934) 1382.

23. Mullins, B. P. "Combustion in Vitiated Air," Selected Combustion Problems, Agard, London: Butterworth Sc. Publ. (1954).

24. Miller, R. E. "Some Factors Governing the Ignition Delays of a Gaseous Fuel," Seventh Symposium on Combustion, London: Butterworth Sc. Publ. (1958).

25. Gray, P. and Harper, M. J. "The Thermal Theory of Induction Periods and Ignition Delays, Seventh Symposium on Combustion, London: Butterworth Sc. Publ. (1959) 425.

26. Vicent, E. T. Supercharging the Internal Combustion Engine, New York: McGraw-Hill Company, 1948.

27. Rögener, H. "Z. Elektrochem," 53 (1949), 389.

28. Kamentskii, F. D. A. Zhur. Fiz. Khim. 13 (1939) 738, Kamentskii, F. Acta Physicochim. U.R.S.S. 20 (1945) 729.

29. Todes, D. M. Acta Physicochim U.R.S.S. (1936) 789.

30. Keenan, J. H., and Kaye, J. Gas Tables New York: Wiley and Sons, Inc. (1956).